Metabolic engineering *of Corynebacterium glutamicum* towards methanol-dependent growth

DISSERTATION

To obtain the degree of

Doctor of Science

Bielefeld University,

Department of Biology

<u>Submitted by:</u>

Guido Hennig

-Bielefeld, May 2019-

The practical work of this thesis has been performed at University Bielefeld at the Chair of Genetics of Prokaryotes from January 2016 until January 2019 under the supervision of Prof. Dr. Volker F. Wendisch.

Examiner: Prof. Dr. Volker F. Wendisch

Chair of Genetics of Prokaryotes

Faculty of Biology & CeBiTec, Bielefeld University

Parts of the introduction of this thesis have been published before in:

Wendisch, V. F., Brito, L. F., Lopez, M. G., Hennig, G., Pfeifenschneider, J., Sgobba, E., & Veldmann, K. H. (2016). The flexible feedstock concept in industrial biotechnology: metabolic engineering of *Escherichia coli*, *Corynebacterium glutamicum*, *Pseudomonas, Bacillus* and yeast strains for access to alternative carbon sources. *Journal of biotechnology*, *234*, 139-157.

Results presented in Chapter 3.6 have been published before in the master's thesis of Carsten Haupka:

"Methanol-dependent complementation of an engineered metabolic cut-off in the Pentose Phosphate Pathway of *Corynebacterium glutamicum* "

Erklärung

Die hier vorgelegte Dissertation habe ich eigenständig und ohne unerlaubte Hilfe angefertigt. Ich versichere, dass ich keine anderen als die angegebenen Quellen und Hilfsmittel benutzt, sowie Zitate kenntlich gemacht habe. Die Dissertation wurde in der vorgelegten oder in ähnlicher Form noch bei keiner anderen Institution eingereicht. Ich habe bisher keine erfolglosen Promotionsversuche unternommen

_____   _____

Ort, Datum   Guido Hennig

Abstract

Methanol is one of the most promising renewable feedstocks for the replacement of fossil fuels in the 21st century, due to its high energy density and the prospect of million-ton scale methanol production from environmental CO_2 in the future. Furthermore, increased methanol availability and high chemical purity make it an interesting non-food substrate alternative to commonly used sugars in biotechnological processes. Natural methylotrophs like the Gram-positive bacterium *Bacillus methanolicus* utilize methanol as sole carbon and energy source for growth and production of L-glutamate and L-lysine. However, lacking tools for genomic modifications in natural methylotrophs sparked the interest in recent years to engineer synthetic methylotroph organisms. First attempts to establish methylotrophy in *Escherichia coli* and *Corynebacterium glutamicum* remained unsuccessful and revealed the complexity of engineering the central metabolism of non-methylotrophs towards profitable methanol utilization.

In this work, methanol-dependent growth of *C. glutamicum* with ribose, xylose and gluconate was achieved through different metabolic cut-offs in the pentose phosphate pathway (PPP) by *rpe* (ribulose-5-phosphate epimerase) or *rpi* (ribose-5-phosphate isomerase) deletion and introduction of *mdh* (methanol dehydrogenase) from *B. methanolicus* and *hxlA* (3-hexulose-6-phosphate synthase) as well as *hxlB* (6-phospho-3-hexulose isomerase) from *Bacillus subtilis* encoding essential methanol utilization enzymes of the ribulose monophosphate (RuMP) pathway, which is naturally used for methanol utilization in *B. methanolicus*.

Maximum methanol-dependent biomass formation of *C. glutamicum* Δ*ald* Δ*fadH* Δ*rpe* (pEKEx3-*mdh-hxlAB*) (Evo 1) on ribose was increased 2.5-fold with a 3-fold improved specific growth rate through adaptive laboratory evolution (ALE). The evolved *C. glutamicum* strain Evo 14 showed full complementation of Δ*rpe* through methanol supplementation and formed the same biomass dependent on methanol as *C. glutamicum* wildtype (WT) with equal amounts of ribose.

Genome sequencing of the evolved methanol-dependent *C. glutamicum* strains Evo 8 and Evo 14 revealed a 15 bp deletion in the genomic sequence of cg3104 (putative ATPase involved in DNA repair) and a single nucleotide polymorphism

(SNP) in the gene *metK* (S-adenosylmethionine synthetase) leading to amino acid substitution S288N in the translated protein. Additional integration of an insertion sequence (IS) upstream of the riboflavin synthesis operon (*ribGCAH*) was uniquely found in Evo 14 and provided an alternative transcription start site (TSS) and ribosome binding site (RBS) for operon expression. Following cultivations with glucose revealed riboflavin deficiencies for *C. glutamicum* strains Evo 1 and Evo 8 but not Evo 14.

Deletion of cg3104 in strain Evo 1 resulted in a 60% increased plasmid copy number (PCN), and 60% higher HxlAB activity, without affecting methanol-dependent growth on ribose. Transferring *metK*_S288N into the genome of Evo 1 did also not influence final biomass formation from methanol and ribose, whereas reversion to the *metK* WT gene sequence in *C. glutamicum* Evo 14 led to significant impairment of methanol-dependent growth, reducing the final biomass by 70%. Combination of Δcg3104 and *metK*_S288N in strain Evo 1, in medium supplemented with riboflavin, finally elevated methanol-dependent growth to the level of *C. glutamicum* strain Evo 14 and *C. glutamicum* WT.

C. glutamicum strain Evo 8 was additionally used for methanol-dependent production of the non-natural product cadaverine with the co-substrate gluconate resulting in a final titer of 1.5 mM. Measurements of ^{13}C-methanol-derived carbon incorporation in cadaverine revealed approximately 60% isotopic labelling of the total cadaverine pool with 44% of molecules labelled at positions associated with RuMP pathway utilization of ^{13}C-methanol and 16% labelled from $^{13}CO_2$ fixation.

Knowledge about synthetic methylotrophy in *C. glutamicum* gained in this work will contribute to the potential engineering of the first synthetic methylotroph organism that will be capable of methanol-based growth and production of value-added compounds.

Abbreviations

All abbreviations are written-out once before used in the text. Commonly used biological abbreviations, as well as chemical formulas and units are not included here. Abbreviations only used in figures are explained in the figure description but not listed here. Enzyme/gene names only used once in the text are not included here as well.

General

ALE	Adaptive laboratory evolution
BLAST	Basic local alignment search tool
C1	One-carbon
CBB cycle	Calvin-Benson-Bassham cycle
CDW	Cell dry weight
EMCP	Ethyl-malonyl-CoA-pathway
GCS	Glycine-cleavage system
IS	Insertion sequence
Km^R	Kanamycin resistance
OD_{600}	Optical density at 600 nm
ORF	Open reading frame
PCN	Plasmid copy number
RBS	Ribosome binding site
RuMP	Ribulose monophosphate pathway
$Spec^R$	Spectinomycin resistance
TCA	Tricarboxylic-acid
Tet^R	Tetracycline resistance
TSS	Transcription start site
WT	Wildtype

Metabolites

CO_2	Carbon dioxide
DHA	Dihydroxyacetone
DHAP	Dihydroxyacetone phosphate
F6-P	Fructose-6-phosphate
FAD	Flavin adenine nucleotide
FMN	Flavin mononucleotide
GABA	γ-aminobutyric acid
GAP	Glyceraldehyde-3-phosphate
H_4F	Tetrahydrofolate
OMH	O-methyl-homoserine
Ru5-P	Ribulose-5-phosphate

Enzymes/Genes

Act	Methanol dehydrogenase activator protein
AdhA	Alcohol dehydrogenase
Ald	Acetaldehyde dehydrogenase
Edd	Phosphogluconate dehydratase
FadH	mycothiol-dependent formaldehyde dehydrogenase
Fba	Fructose-1,6-bisphosphate aldolase
FrmA	Formaldehyde dehydrogenase
GlpX	Fructose-1,6-bisphosphatase
GlyA	Serine hydroxymethyltransferase
GntK	Gluconate kinase
Gpm/GpmM	Phosphoglycerate mutase
Hps/HxlA	3-hexulose-6-phosphate synthase
LdcC	Lysine decarboxylase
Ldh	Lactate dehydrogenase
LysC	Aspartokinase
Maldh	Malate dehydrogenase
Mdh/Mdh2/Mdh3	Methanol dehydrogenase

MetK	S-adenosylmethionine synthetase
MetY	O-acetylhomoserine sulfhydrolase
MMO	Methane monooxygenase
Pfk	Phosphofructokinase
Pgi	Phosphoglucoisomerase
Phi/HxlB	6-phospho-3-hexulose isomerase
POS5	Peroxide sensitive NADH-Kinase
Ppc	Phosphoenolpyruvate carboxylase
Prk/PrkA	Phosphoribulokinase
Pyc	Pyruvate carboxylase
Rpe	Ribulose-5-phosphate epimerase
Rpi	Ribose-5-phosphate isomerase
RuBisCO	1,5-bisphosphate carboxylase
Tkt	Transketolase
XylA	Xylose isomerase
XylB	Xylulose kinase

VI

Index

x

1. <u>Introduction</u>

1.1 Methanol as sustainable alternative energy source

One of the major challenges in the 21st century will be the substitution of fossil fuels with renewable energy systems (Räuchle et al., 2016). Although energy generation from wind turbines and solar panels showed great potential in the past few years, one significant problem remained: the storage of generated electric power from renewable sources (Goeppert et al., 2018; Räuchle et al., 2016). A promising way to overcome this issue, is the storage of energy in chemicals such as hydrogen or methanol that can be combusted on demand (Bertau et al., 2010; Goeppert et al., 2018; Olah et al., 2009; Räuchle et al., 2016). In direct comparison to hydrogen, methanol has some crucial advantages as it has a higher energy density, is easier to store and transport due to its liquid form and is therefore safer to handle than gaseous hydrogen (Dalena et al., 2017; Gumber and Gurumoorthy, 2017).

Methanol has gained attention as alternative energy source recently and the feasibility of a "methanol economy" was proposed before (Goeppert et al., 2018; Olah, 2013; Olah et al., 2009). It is the most abundant organic non-methane gas in the atmosphere with an estimated annual emission of 123 to 343 Tg (teragram) (Millet et al., 2008). Natural methanol emissions emerge from e.g. ripening fruits (Frenkel et al., 1998), rotting plant material (Warneke et al., 1999) or growing plant leaves (Nemecek-Marshal et al., 1995). The latter is estimated to account for 40-80% of total atmospheric methanol emission (Millet et al., 2008).

Despite being a feasible industrial energy carrier for storage, methanol is used as raw material in the chemical industry for the production of chemicals such as acetic acid needed for paints, adhesives or polyethylene terephthalate PET) (Iaquaniello et al., 2017). The direct oxidation product of methanol, formaldehyde, is furthermore needed for plastics and fibres or in the production of fuels like gasoline and kerosene (Iaquaniello et al., 2017). The overall demand for methanol has increased 14-fold from 5 megatons (Mt) in 2005 to 70 Mt in 2015

and is expected to rise in the future, giving rise to new mega methanol production plants to satisfy the demand for increased methanol availability (Dalena et al., 2017; Olah et al., 2009; Schrader et al., 2009).

Nowadays, approximately 90% of industrially produced methanol is produced from natural gas (Blug et al., 2014) through the production of synthesis gas (syngas), subsequent conversion into crude methanol and concluding distillation to enhance the purity (Dalena et al., 2017). Moreover, methanol can be directly produced from syngas, gained from gasification of biomass, such as plant wastes (Barbato et al., 2014; Dalena et al., 2017; Pellegrini et al., 2011; Pirola et al., 2017). The most promising and environmentally friendly source for methanol production in the future will be the utilization of atmospheric CO_2, together with H_2 from hydrolyzed water (Aresta and Dibenedetto, 2007; Barbato et al., 2014). Geothermal CO_2 is already successfully used by a methanol production plant in Iceland, for an annual methanol production of up to 3.5 tonnes (t), with the prospect of further improvement to 35.000 t (Olah, 2013). With improving technologies in the future, an estimated 40 – 70 Mt methanol will be produced from CO_2 and H_2 by 2050 (Iaquaniello et al., 2017).

Since methanol can also be used as carbon source in biotechnological processes, interest to produce valuable products from methanol using naturally methylotroph bacteria has risen in the past decade (Brautaset et al., 2007; Fei et al., 2014; Marx et al., 2012; Naerdal et al., 2015; Pfeifenschneider et al., 2017; Sonntag et al., 2015). Due to its natural abundance and the prospect of mega production facilities, methanol will be an interesting candidate for future replacement of commonly used sugars in bacterial fermentations (Millet et al., 2008; Pfeifenschneider et al., 2017; Schrader et al., 2009). Although the current methanol price of 0.45 $/kg (Bertau et al., 2014) is not competitive to recent sugar prices (0.28 $/kg (Macrotrends.net, 2019)), the advantages of methanol are its chemical purity (Linton and Niekus, 1987), high degree of reduction for increased energy yield during utilization (Whitaker et al., 2015) and production from waste materials and environmental CO_2 (Barbato et al., 2014; Dalena et al., 2017; Iaquaniello et al., 2017).

Introduction

The biotechnological application of sugar substrates competes with the food industry that heavily relies on crop productivity and environmental conditions (Schrader et al., 2009), resulting in unpredictable price fluctuations of sugar-based feedstocks (Maitah and Smutka, 2019). Methanol on the other hand is not used as food or animal feedstock and can therefore be produced and applied independently, with constantly improving production plants that are predicted to steadily decrease the methanol price in the future (Goeppert et al., 2018; Olah, 2013; Schrader et al., 2009).

1.2 Natural methylotrophy

Methanol was shown to be toxic when fed to primates, due to emerging formate during its metabolization process (Clay et al., 1975; Tephly, 1991). Formate toxicity is caused by inhibition of the terminal cytochrome oxidase complex in the respiratory chain located in the mitochondria, leading to "histotoxic hypoxia", the inability to utilize blood-oxygen, and results in failure of organs with a high rate of oxygen consumption (eyes, brain, heart, kidneys) (Liesivuori and Savolainen, 1991). Methanol toxicity in prokaryotes is mainly caused by the direct oxidation product formaldehyde reacting with free thiol and amine groups to damage DNA and proteins of the cell by forming irreversible formaldehyde adducts (Chen et al., 2016). However, some microorganisms developed strategies to overcome methanol toxicity and naturally evolved towards the utilization of methanol as sole carbon and energy source for growth and production of value-added products (Anthony, 1983; Brautaset et al., 2007; Ochsner et al., 2014b).

Metabolism of methanol and other one-carbon compounds in nature developed in various different ways (Figure 1) (Anthony, 1983). During utilization by methylotrophic organisms, methanol is first oxidized to formaldehyde, which can then be further oxidized to formate and eventually to CO_2 through linear or cyclic detoxification pathways (Anthony, 1983).

Autotrophic bacteria such as *Paracoccus denitrificans* can assimilate CO_2 using the ribulose bisphosphate pathway (RuBP) to generate two molecules of 3-phosphoglycerate (3-PG) from one molecule of RuBP and CO_2, catalysed by ribulose-1,5-bisphosphate carboxylase (RuBisCO) (Dijkhuizen and Harder, 1984). Subsequent cyclic regeneration of ribulose-1,5-bisphosphate (RuBP) allows continuous CO_2 assimilation and the formation of energy and biomass for growth (Anthony, 1983; Dijkhuizen and Harder, 1984).

4
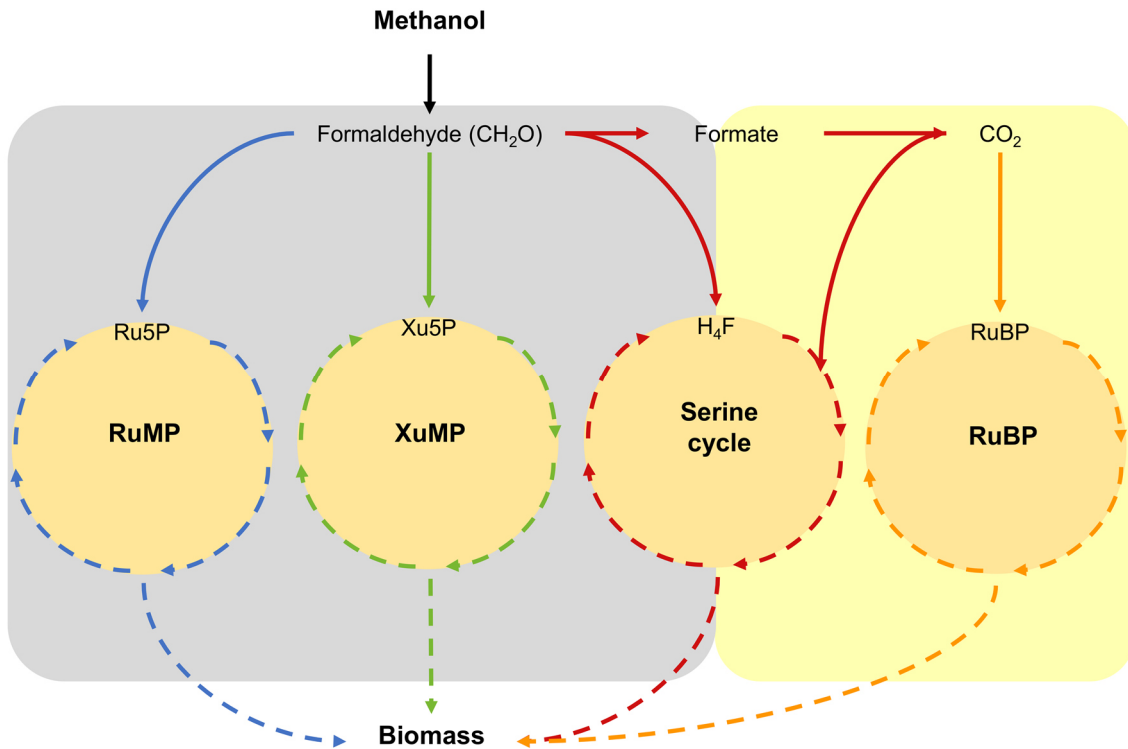
Figure 1: Schematic overview of natural C1 utilization pathways. Formaldehyde is either assimilated or further oxidized to CO_2 in methylotrophic organisms. Biomass can be obtained through formaldehyde (grey) or CO_2 assimilation (yellow). Bacterial formaldehyde fixation pathways include the ribulose monophosphate pathway (RuMP) (blue) and the serine cycle (red). Xylulose-5-phosphate pathway (green) naturally exists in yeasts. CO_2 fixation occurs in autotrophic bacteria using the ribulose-bisphosphate pathway (RuBP) (orange) and during the serine cycle (red). Dotted arrows indicate multiple reactions. Central metabolites for C1 assimilation are given for each pathway: Ru5-P (ribulose-5-phosphate), Xu5-P (xylulose-5-phosphate), H_4F (Tetrahydrofolate), RuBP (ribulose-bisphosphate).

In methylotrophic organisms, the direct methanol oxidation product formaldehyde can be assimilated into the central carbon metabolism in three different ways: (i) the ribulose monophosphate pathway (RuMP) or (ii) serine cycle in bacteria, or (iii) the xylulose monophosphate pathway (XuMP) occurring exclusively in yeasts. (Anthony, 1983; Arfman et al., 1989; Papoutsakis et al., 1978; Tani et al., 1978)(Figure 1).

Methylotrophic yeasts like *Pichia pastoris* fix formaldehyde to xylulose-5-phosphate (Xu5-P) catalysed by dihydroxyacetone synthase (DAS) to form glyceraldehyde-3-phosphate (GAP) and dihydroxyacetone (DHA) for biomass formation and regeneration of Xu5-P through several rearrangement reactions (Couderc and Baratti, 1980; Tani et al., 1978; Yurimoto et al., 2011).

Methanol oxidation and formaldehyde fixation in methylotrophic yeasts are carried out in distinct cell compartments, the peroxisomes, to protect the rest of the cell from formaldehyde toxicity (van der Klei et al., 2006; Yurimoto et al., 2011).

In the last few decades, new insights were obtained about how natural methylotrophic pathways operate in bacteria (Chistoserdova, 2015; Chistoserdova et al., 2009; Lidstrom, 1990; Lidstrom and Stirling, 1990; McTaggart et al., 2015; Šmejkalová et al., 2010; Vorholt, 2002) e.g. in the Gram-negative serine cycle- and EMCP (ethyl-malonyl-CoA-pathway)-utilizing *Methylobacterium extorquens* (Erb et al., 2007; Ochsner et al., 2014b; Vuilleumier et al., 2009) or the Gram-positive RuMP-utilizing model organism *Bacillus methanolicus* (Brautaset et al., 2007; Müller et al., 2015a).

In the serine cycle, formaldehyde can either directly react with tetrahydrofolate (H_4F) to form methylene-H_4F or is first enzymatically oxidized to formate and subsequently converted to methylene-H_4F (Šmejkalová et al., 2010). Methylene-H_4F is then used for a condensation reaction with glycine to yield serine, catalysed by serine hydroxymethyltransferase (*glyA*) (Ochsner et al., 2014b). Additional CO_2 fixation in the serine cycle occurs in a carboxylation reaction from phosphoenolpyruvate to oxaloacetate, catalysed by phosphoenolpyruvate carboxylase (*ppc*) (Ochsner et al., 2014b; Šmejkalová et al., 2010). In order to regenerate glycine, *M. extorquens* operates the additional EMCP to allow continuous formaldehyde assimilation and biomass formation (Erb et al., 2007; Ochsner et al., 2014b; Sonntag et al., 2014).

Bioenergetically, the RuMP pathway of *B. methanolicus* is the most efficient of the natural methanol utilization pathways in bacteria (Whitaker et al., 2015). Generation of one C3 molecule pyruvate from two formaldehyde and one CO_2 in the serine cycle requires the investment of two NADH and ATP, whereas the RuMP pathway yields one NADH and ATP for each pyruvate produced from three molecules of formaldehyde (Anthony, 1983; Whitaker et al., 2015). The preferred C3 product in the RuBP pathway is glyceraldehyde-3-phosphate (GAP), which is solely generated from CO_2 fixation in autotrophic bacteria, but requires an investment of 6 NAD(P)H and 9 ATP for each molecule produced (Anthony,

1983). Because of its favorable bioenergetics, RuMP pathway utilization of methanol offers the greatest potential for the engineering of synthetic methylotrophy and was therefore focused on in the present study.

1.3 The natural methylotroph *B. methanolicus*

The Gram-positive, thermophile and facultative methylotrophic *B. methanolicus* was first isolated and characterized towards the end of the 1980s (Arfman et al., 1989; Dijkhuizen et al., 1988; Schendel et al., 1990). It has since been developed into a model organism for natural methylotrophy (Brautaset et al., 2007; Müller et al., 2015) and was successfully used for methanol-based production of valuable compounds, such as L-lysine (Brautaset et al., 2003; Jakobsen et al., 2008; Nærdal et al., 2017), L-glutamate (Brautaset et al., 2010; Krog et al., 2013a), cadaverine (Naerdal et al., 2015) or γ-aminobutyric acid (GABA) (Irla et al., 2017). Plasmid dependent methylotrophic growth of *B. methanolicus* has been extensively studied in the past years (Brautaset et al., 2004; Heggeset et al., 2012; Irla et al., 2015, 2014; Müller et al., 2015c), leading to important insights on how the organism builds biomass solely from methanol.

Methylotrophic growth of *B. methanolicus* starts with the oxidation of methanol to formaldehyde, catalysed by NAD-dependent alcohol dehydrogenases, encoded by one of three distinct genes located in the genome (*mdh2*, *mdh3*) or the natural occurring plasmid pBM19 (*mdh*) (Arfman et al., 1989; Dijkhuizen et al., 1988; Heggeset et al., 2012). Formaldehyde can then be further oxidized to CO_2 in a linear dissimilation pathway or assimilated in RuMP pathway reactions (Kato et al., 2006; Müller et al., 2015a)(Figure 2). In the RuMP pathway, ribulose-5-phosphate (Ru5-P) is the central metabolite used for formaldehyde fixation by 3-hexulose-6-phosphate synthase (*hps/hxlA*) to yield a C6 hexulose-6-phosphate (H6-P) that is subsequently isomerized to fructose-6-phosphate (F6-P) by 6-phospho-3-hexuloisomerase (*phi/hxlB*). F6-P can then be further metabolized through glycolysis to generate pyruvate or be used to regenerate Ru5-P for continuous formaldehyde fixation in non-oxidative rearrangement reactions or following oxidative cyclic dissimilation yielding Ru5-P and CO_2 (Brautaset et al., 2004; Heggeset et al., 2012; Kato et al., 2006)(Figure 2).

Rearrangement of F6-P to Ru5-P is achieved by various non-oxidative reactions in the RuMP pathway (Figure 2). Phosphorylation of F6-P by phosphofructokinase (*pfk*) (Le et al., 2017) and subsequent cleavage by fructose-1,6-bisphosphate aldolase (*fba*) yields GAP and dihydroxyacetone phosphate (DHAP) (Stolzenberger et al., 2013b). DHAP can then be used in an aldol condensation with erythrose-4-phosphate (E4-P) to generate sedoheptulose-1,7-bisphosphate (S-1,7-bP), catalyzed by fructose-1,6-bisphosphate aldolase (*fba*) that also acts as sedoheptulose-1,7-bisphosphate aldolase (Stolzenberger et al., 2013b). The following dephosphorylation reaction catalysed by fructose-1,6-bisphosphatase/sedoheptulose-1,7-bisphosphatase (*glpX*) yields sedoheptulose-7-phosphate (S7-P) (Stolzenberger et al., 2013a). Through further reactions catalyzed by transketolase (*tkt*) (Markert et al., 2014), ribose-5-phosphate isomerase (*rpiB*) and ribulose-5-phosphate epimerase (*rpe*) (Le et al., 2017), Ru5-P is regenerated for further formaldehyde assimilation (Figure 2).

Cyclic dissimilation follows the oxidative branch of the pentose phosphate pathway (PPP) and regenerates Ru5-P through isomerization of F6-P to glucose-6-phosphate (G6-P) and subsequent oxidation reactions, including the decarboxylation of 6-phosphogluconate (6-PG) catalysed by 6-phosphogluconate dehydrogenase (*gnd*) (Figure 2) (Heggeset et al., 2012; Müller et al., 2015c).
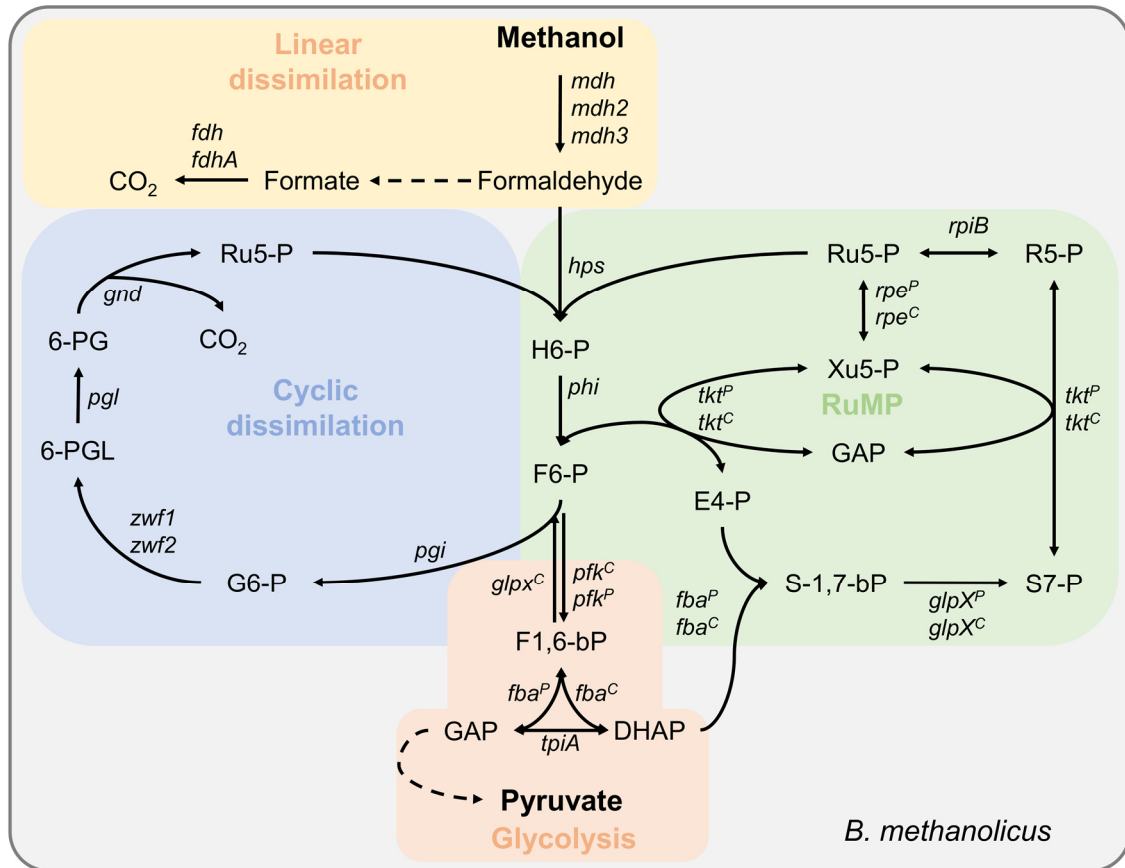
Figure 2: **Schematic overview of the central carbon metabolism in *B. methanolicus*.** Different pathways important for methylotrophy are depicted, including linear dissimilation (orange), cyclic dissimilation (blue) glycolysis (red) and ribulose-monophosphate pathway (RuMP) (green). In cases where two copies of a gene exist on the chromosome and the naturally occurring plasmid pBM19, genes are marked with ^{C} (chromosomal) or ^{P} (plasmid). Unlabelled genes are expressed from the chromosome. Dashed arrows indicate several reactions. Involved genes: *mdh/mdh2/mdh3* (methanol dehydrogenase) *fdh/fdhA* (formate dehydrogenase), *hps* (3-hexulose-6-phosphate synthase), *phi* (6-phospho-3-hexuloisomerase), *pfk* (phosphofructokinase), *glpX* (fructose-1,6-bisphosphatase), *fba* (fructose-1,6-bisphosphate aldolase), *tpi* (triosephosphate isomerase) *tkt* (transketolase), *rpe* (ribulose-5-phosphate epimerase), *rpiB* (ribose-5-phosphate isomerase) *pgi* (phosphoglucoisomerase), *zwf1/zwf2* (glucose-6-phosphate dehydrogenase), *pgl* (6-phosphoglucolactonase), *gnd* (6-phosphogluconate dehydrogenase). Abbreviations of metabolites: H6-P (hexulose-6-phosphate), F6-P (fructose-6-phosphate), F1,6-bP (fructose-1,6-bisphosphate), GAP (glyceraldehyde-3-phosphate), DHAP (dihydroxyacetone phosphate), G6-P (glucose-6-phosphate), 6-PGL (6-phosphogluconolactone), 6-PG (6-phosphogluconate), Ru5-P (ribulose-5-phosphate), R5-P (ribose-5-phosphate), S7-P (sedoheptulose-7-phosphate), E4-P (erythrose-4-phosphate), Xu5-P (xylulose-5-phosphate).

Introduction

Although *B. methanolicus* is well researched by now and genome sequences (Heggeset et al., 2012; Irla et al., 2014), as well as genome-wide transcriptomic data (Irla et al., 2015) are available, the development of a genetic toolbox is still a challenge and chromosomal modifications are not possible until now (Irla et al., 2016). Because of that and given the increasing importance of methanol utilization in industrial biotechnology, there is a huge interest to transfer the trait of methylotrophy, or one-carbon (C1) metabolism in general, to current industrially established microorganisms, in order to allow genomic modifications for the production of value-added chemicals from methanol or other C1 carbon sources (Chistoserdova, 2018, 2011; Whitaker et al., 2015).

Among industrially relevant and well-established microorganisms, *Corynebacterium glutamicum* is an interesting candidate to access methanol as feedstock in industrial production of value-added products.

1.4 The non-methylotroph biotechnological workhorse *Corynebacterium glutamicum*

Since the 1950s, when it was first isolated in Japan (Kinoshita et al., 1957), the Gram-positive, rod-shaped soil bacterium *C. glutamicum* has become a major workhorse for the industrial production of amino acids, especially L-lysine and L-glutamate (Becker et al., 2011; Kelle et al., 2005; Kimura, 2005; Wendisch et al., 2016b; Wittmann and Becker, 2007). Moreover, it was engineered for the production of other valuable chemicals, such as the alcohol 1,2-propanediol (Siebert and Wendisch, 2015), the dicarboxylic acid glutarate (Pérez-garcía et al., 2018), the methylated amino acid N-methyl-L-alanine (Mindt et al., 2018) or diamines like GABA (Jorge et al., 2016), putrescine (Nguyen et al., 2015) and cadaverine (Mimitsuka et al., 2007).

Cadaverine (1,5-diaminopentane) is an industrial relevant platform chemical for the production of bio-polyamides, such as nylon 6,6 (Kind et al., 2014; Kind and Wittmann, 2011). Previous efforts have already been made to optimize the biotechnological production of cadaverine with *C. glutamicum* from renewable resources like starch (Tsuchidate et al., 2008), xylose (Buschke et al., 2013) or glucose (Mimitsuka et al., 2007).

The generally recognized as safe (GRAS) organism is naturally capable of utilizing a wide spectrum of carbon sources, including hexoses (glucose, fructose), organic acids (acetate, lactate) or disaccharides (maltose, sucrose) (Blombach and Seibold, 2010; Gerstmeir et al., 2003; Stansen et al., 2005). Since the whole genome of *C. glutamicum* was sequenced in 2003 (Kalinowski et al., 2003), many metabolic engineering approaches focused on broadening the substrate spectrum of the organism even further, resulting in engineered *C. glutamicum* strains that acquired the ability to utilize a variety of different substrates through the heterologous expression of different utilization pathways (Becker and Wittmann, 2015; Wendisch et al., 2016a; Zahoor et al., 2012; Zhao et al., 2018).

Non-native carbon sources such as xylose (Kawaguchi et al., 2006; Meiswinkel et al., 2013), glycerol (Litsanov et al., 2013; Rittmann et al., 2008), starch (Tateno et al., 2007; Tsuge et al., 2013), glucosamine and N-acetyl glucosamine (Matano

et al., 2014; Uhde et al., 2013), dicarboxylic acids (Youn et al., 2008), lactose and galactose (Barrett et al., 2004), hexuronic acids (Hadiati et al., 2014), arabinose (Kawaguchi et al., 2008; Meiswinkel et al., 2013; Schneider et al., 2011) or methyl-acetate (Choo et al., 2016) were successfully established as sole carbon and energy source for *C. glutamicum*.

Therefore, the industrial workhorse *C. glutamicum* is a promising host for the synthetic utilization of C1 substrates through heterologous expression of utilization pathways to further expand the substrate spectrum for growth and production of valuable compounds from renewable non-food substrates, such as formate, CO_2 or methanol.

1.5 The current state of synthetic C1 utilization

1.5.1 <u>Formate and CO_2</u>

Besides methanol, recent work has been focused on the engineering of synthetic formate and CO_2 utilizing organisms (Bar-Even, 2016; Erb et al., 2017; Schwander and Erb, 2016; Yishai et al., 2018). Formate can be obtained by the reduction of CO_2, which makes it an ecologically, as well as biotechnologically relevant carbon source that can theoretically be assimilated in various different ways (Bar-Even, 2016). The first synthetic biological pathway for formate utilization through reduction to formaldehyde and subsequent fixation of three formaldehyde molecules to DHA by the computationally designed enzyme formolase was proposed a few years ago (Siegel et al., 2015; Tai and Zhang, 2015). The functionality of the proposed pathway could be confirmed *in vitro*, by conversion of formate to DHAP when acetyl-CoA synthase from *Escherichia coli*, acetaldehyde dehydrogenase from *Listeria monocytogenes* and DHA kinase from *Saccharomyces cerevisiae* were additionally supplemented (Siegel et al., 2015). However, formolase activity did not support growth of *E. coli* and the preferred product at low formaldehyde concentrations was revealed to be glycolaldehyde, which additionally reduced the carbon yield of the designed pathway (Poust et al., 2015).

Recent work focused on simultaneous formate and CO_2 fixation by re-routing the naturally occurring glycine cleavage system (GCS) in *E. coli* to establish the reductive glycine pathway (Bang et al., 2018; Döring et al., 2018; Yishai et al., 2018). Engineered auxotrophies for serine and glycine, created through genomic deletions of *glyA* (serine hydroxymethyltransferase), *kbl* (2-amino-3-ketobutyrate CoA ligase), *ltaE* (threonine aldolase) and *aceA* (isocitrate lyase) were successfully complemented by formate utilization through heterologously expressed formate-H_4F ligase from *M. extorquens* and additional CO_2 assimilation by the endogenous reductive glycine route. Successful assimilation of both C1 carbon sources was validated by isotopic labelling experiments with $^{13}CO_2$ and ^{13}C-formate, revealing incorporation of labelled carbon at all positions in the amino acids serine and glycine (Bang et al., 2018; Döring et al., 2018; Yishai et al., 2018).

Introduction

Interest to directly assimilate environmental CO_2 with engineered organisms, for the production of valuable compounds and fuels has risen in the last decade (Claassens et al., 2018; Fast and Papoutsakis, 2012; Nybo et al., 2015). Although natural autotrophs exist in nature and can be engineered (Nybo et al., 2015), the demand for synthetic autotrophs has spawned a variety of possibilities to assimilate CO_2 (Bar-even et al., 2011; Fast and Papoutsakis, 2012). An early approach was the transfer of the 3-hydroxypropionate (3-HPA) carbon fixation bicycle from *Chloroflexus aurantiacus,* containing 19 reactions catalyzed by 13 different enzymes*,* to *E. coli* (Mattozzi et al., 2013)*.* To achieve this, the pathway was first divided into four different sub-pathways: 1) CO_2 addition to acetyl-CoA and further conversion to propionyl-CoA, 2) Assimilation of another CO_2 molecule to propionyl-CoA and subsequent conversion to succinyl-CoA, 3) Acetyl-CoA regeneration from succinyl-CoA to yield glyoxylate 4) Coupling of glyoxylate and propionyl-CoA for further utilization to gain pyruvate and acetyl-CoA (Mattozzi et al., 2013). The functionality of the separate sub-pathways was confirmed through complementation of different host mutations, however, heterologous expression of the whole pathway did not support autotrophic growth of the engineered *E. coli* strain (Mattozzi et al., 2013).

In an attempt to decouple biomass formation from energy metabolism in *E. coli* through deletion of genes encoding phosphoglycerate mutases (*gpm*, *gpmM*) to diminish gluconeogenesis, a fully functional Calvin-Benson-Bassham cycle (CBB) was established by plasmid-based heterologous expression of *prkA* (phosphoribulokinase) from *Synechococcus elongatus* PCC 7942 as well as RuBisCO from *Rhodospirillum rubrum* ATCC 11170 and subsequent laboratory evolution (Antonovsky et al., 2016). The evolved strain exhibited triose, pentose and hexose sugar synthesis for biomass solely from CO_2 assimilation, while being fed with pyruvate to generate energy in form of reducing equivalents and ATP in lower glycolysis and TCA cycle reactions (Antonovsky et al., 2016).

Recent work was focused on the creation of synthetic pathways for CO_2 fixation, in contrast to the transfer of naturally existing pathways (Bouzon et al., 2017; Schwander et al., 2016; Schwander and Erb, 2016). A fully synthetic pathway for *in vitro* CO_2 fixation was established by a combination of 17 enzymes from 9 different organisms and improved by several iterations of metabolic proofreading

and enzyme engineering (Schwander et al., 2016; Schwander and Erb, 2016). The crotonyl–CoA/ethylmalonyl-CoA/hydroxybutyryl-CoA (CETCH) cycle exhibited *in vitro* CO_2 fixation with rates comparable to CO_2 fixation measured from plant crude extracts (Schwander et al., 2016).

Additional work reported about the 4-hydroxy-2-oxobutanoic acid (HOB) cycle in *E. coli* that introduced HOB as a novel artificial metabolite to substitute serine and glycine as natural C1 donors (Bouzon et al., 2017). The pathway was established in *E. coli* lacking enzymes for the C1 transfer from glycine/serine to H_4F by two subsequent stages of adaptive laboratory evolution (ALE) to first establish HOB as new intermediate metabolite and secondly improve endogenous HOB production, yielding a strain dependent on CO_2 fixation for anabolic reactions (Bouzon et al., 2017).

1.5.2 <u>Methanol</u>

The transfer of dissimilatory oxidation of methanol is straightforward and often non-methylotrophs like *E. coli* or *C. glutamicum* possess the respective enzymes (Gonzalez et al., 2006; Gutheil et al., 1992; Herring and Blattner, 2004; Leßmeier et al., 2013; Witthoff et al., 2013, 2012). Currently, transfer of methylotrophy to non-methylotrophs is of great interest (Whitaker et al., 2015), but has not resulted in full synthetic methylotrophy until now (Chen et al., 2018; Leßmeier et al., 2015; Meyer et al., 2018; Müller et al., 2015b; Tuyishime et al., 2018).

Although only a few reactions of the RuMP pathway are missing in non-methylotroph organisms, heterologous expression of suitable enzymes has not been not sufficient for a full transfer of methylotrophy (Bennett et al., 2018; Leßmeier et al., 2015; Müller et al., 2015b; Witthoff et al., 2015). Natural methylotrophy in *B. methanolicus* requires a constant flux towards Ru5-P regeneration for formaldehyde fixation, in order to allow continuous growth on methanol, and is subject to complex regulatory mechanisms that are still not fully understood until now (Chistoserdova, 2011; Heggeset et al., 2012; Irla et al., 2015; Müller et al., 2015c, 2015a). Since the central carbon metabolism of non-methylotrophs is naturally not adapted to formaldehyde assimilation, a rewiring of carbon fluxes is necessary to guarantee sufficient and continuous regeneration of Ru5-P for formaldehyde fixation and a functional transfer of the RuMP pathway (Whitaker et al., 2015).

In early work, biomass yields of *Pseudomonas putida* S12 in glucose chemostat cultures were increased from 35% (C-mol biomass/C-mol glucose) to 91% through expression of *hps* and *phi* from *Bacillus brevis* and an additional feed of formaldehyde to glucose (Koopman et al., 2009).

However, current work on synthetic methylotrophy mainly focused on the transfer and optimization of RuMP pathway reactions to the model organisms *E. coli* and *C. glutamicum* (Bennett et al., 2018; Leßmeier et al., 2015; Meyer et al., 2018; Müller et al., 2015b; Price et al., 2016; Tuyishime et al., 2018).

1.5.2.1 <u>Synthetic methylotrophy in *E. coli*</u>

In *E. coli*, *mdh2* (methanol dehydrogenase) and the gene encoding the Mdh activator protein *act* from *B. methanolicus* PB1 were expressed heterologously, together with *hps* and *phi* from *B. methanolicus* MGA3 (Müller et al., 2015). Isotopic labelling experiments with ^{13}C-methanol revealed up to 40% incorporation of methanol-carbon at multiple positions in hexoe-6-phosphates, indicating functional cyclic activity of the RuMP pathway. Carbon incorporation from ^{13}C-methanol could not be further increased by deletion of *frmA* (formaldehyde dehydrogenase), which is essential for the endogenous glutathione-dependent, linear formaldehyde detoxification pathway (Müller et al., 2015).

In another approach, *hps* and *phi* from *Mycobacterium gastri* MB19 were heterologously expressed as fusion protein. The purified *hps-phi* fusion showed approximately 2-fold activity during *in vitro* assays, compared to an equimolar mixture of both single enzymes. Strains expressing the fusion protein also exhibited improved formaldehyde consumption and better growth in comparison to the wild type, with formaldehyde present in the medium (Orita et al., 2007). Following work used *mdh3* (methanol dehydrogenase) from *B. methanolicus* MGA3 and the already established fusion of *M. gastri* genes *hps* and *phi* for a self-assembling, scaffoldless, supramolecular enzyme complex in an attempt to improve substrate channelling of formaldehyde (Price et al., 2016). Clustering improved *in vitro* utilization of methanol 50-fold in comparison to an equimolar mixture of the individual enzymes. The additional expression of *ldh* (lactate dehydrogenase) from *E. coli* as "NADH sink" further improved *in vitro* methanol consumption, resulting in an overall 97-fold improvement over the uncomplexed enzymes. However, *in vivo* methanol consumption of an *E. coli* strain expressing the enzyme complex was only improved 2.3-fold in comparison to singular expression of *mdh* and the *hps-phi* fusion (Price et al., 2016).

For methanol conversion to the value-added, non-natural product naringenin, *E. coli* was first engineered towards heterologous expression of *mdh* from *Bacillus stearothermophilus* and RuMP pathway enzymes (*hps* and *phi*) from *B. methanolicus* in a genomic Δ*frmA* background (Whitaker et al., 2017). Carbon incorporation from ^{13}C-methanol up to 53% at multiple positions in 3-PG demonstrated functional cyclic activity of the RuMP pathway (Whitaker et al.,

2017). Additional heterologous expression of 4-coumaroyl-CoA ligase from *Arabidopsis thaliana* and chalcone synthase from *Petunia hybria* led to naringenin production with approximately 18% of the total naringenin pool labelled from ^{13}C-methanol at at least one position (Whitaker et al., 2017).

Recent work reported improved carbon labeling of central metabolites (pyruvate, phosphoenolpyruvate) from ^{13}C-methanol up to 60% through deletion of *pgi* (phosphoglucoisomerase) and *frmA*, episomal heterologous expression of *mdh*, *hps* and *phi,* together with the genomic integration for heterologous expression of *rpe*, *tkt*, *fba*, *glpX* and *pfk* from *B. methanolicus* (Bennett et al., 2018).

To successfully couple growth to methanol utilization in *E. coli*, deletions of *edd* (phosphogluconate dehydratase), *rpiAB* (ribose-5-phosphate isomerase) and *maldh* (malate dehydrogenase) were performed to prevent growth on gluconate as sole carbon source and additionally reduce TCA cycle activity. Subsequent plasmid-based introduction of *mdh2* from *B. methanolicus* PB1 and *hps-phi* from *Methylobacillus flagellatus,* allowed the strain to grow on gluconate only when methanol was supplemented (Meyer et al., 2018). Growth was further improved through ALE, yielding strain MeSV2.2 that exhibited around 30% increased biomass formation with gluconate and methanol, compared to the *E. coli* WT cultivated with the same amount of gluconate (Meyer et al., 2018).

Distinct approaches following the same concept, were genomic deletions of *rpi* or *rpe* to create a methanol dependency with xylose or ribose as co-substrate in *E. coli.* The Δ*rpe* mutant exhibited weak methanol-independent growth on ribose after a lag-phase of 29 h, making it unsuitable for ALE (Chen et al., 2018). The *rpi* deletion strain, however, exhibited methanol-dependent growth on xylose which was further improved through ALE to yield a strain growing with a specific growth rate of with a specific growth rate of 0.17 ± 0.006 h^{-1}, which was twice as fast as the previously reported methanol-dependent strain MeSV2.2 (0.081 ± 0.002 h^{-1}) by Meyer et al. (Chen et al., 2018; Meyer et al., 2018).

1.5.2.2   Synthetic methylotrophy in *C. glutamicum*

Although natural methanol utilization in *C. glutamicum* was extensively studied in the past (Leßmeier et al., 2013; Leßmeier and Wendisch, 2015; Witthoff et al., 2013) (Figure 3A), attempts to establish a synthetic pathway for biomass formation from methanol has only been partially successful (Leßmeier et al., 2015; Witthoff et al., 2015)(Figure 3B).

For co-utilization of methanol in *C. glutamicum*, the linear detoxification pathway was first removed by deleting *ald* (aldehyde dehydrogenase) and *fadH* (mycothiol-dependent formaldehyde dehydrogenase) (Leßmeier et al., 2013). Then *hxlA and hxlB* from *B. subtilis,* as well as *mdh* from *B. methanolicus* MGA3 were heterologously expressed (Leßmeier et al., 2015). Enzymes encoded by *hxlAB* are homologues of *B. methanolicus hps* and *phi* (Yasueda et al., 1999) that exhibited faster *in vivo* formaldehyde assimilation in *C. glutamicum* (Leßmeier et al., 2015)*.* Carbon incorporation from ^{13}C-methanol up to 45% in F6-P and labelling at multiple positions indicated functional cyclic operation of the RuMP *in vivo* (Leßmeier et al., 2015). Applying this strategy to a cadaverine producing strain, additionally expressing *ldcC* (lysine decarboxylase) from *E. coli* and endogenous feedback-resistant aspartokinase (*lysC*)*,* resulted in ^{13}C-labelling of 16% of the total cadaverine pool from ^{13}C-methanol with a produced titer of 1.5 g/l from ribose and methanol. Therefore, the non-natural carbon source methanol was partially converted to the non-natural product cadaverine by recombinant *C. glutamicum*. However, net biomass formation from methanol was not observed (Leßmeier et al., 2015)(Figure 3B).

In another approach, *mdh* and *act* from *B. methanolicus* were heterologously expressed, together with *hxlAB* from *B. subtilis* for co-utilization of methanol and glucose in a Δ*ald* Δ*fadH* genomic background (Witthoff et al., 2015). The engineered *C. glutamicum* strain revealed up to 25% incorporation of ^{13}C-methanol-derived carbon in Fructose-1,6-bisphosphate with a threefold increased methanol consumption rate in comparison to the WT control strain (Witthoff et al., 2015)(Figure 3B).
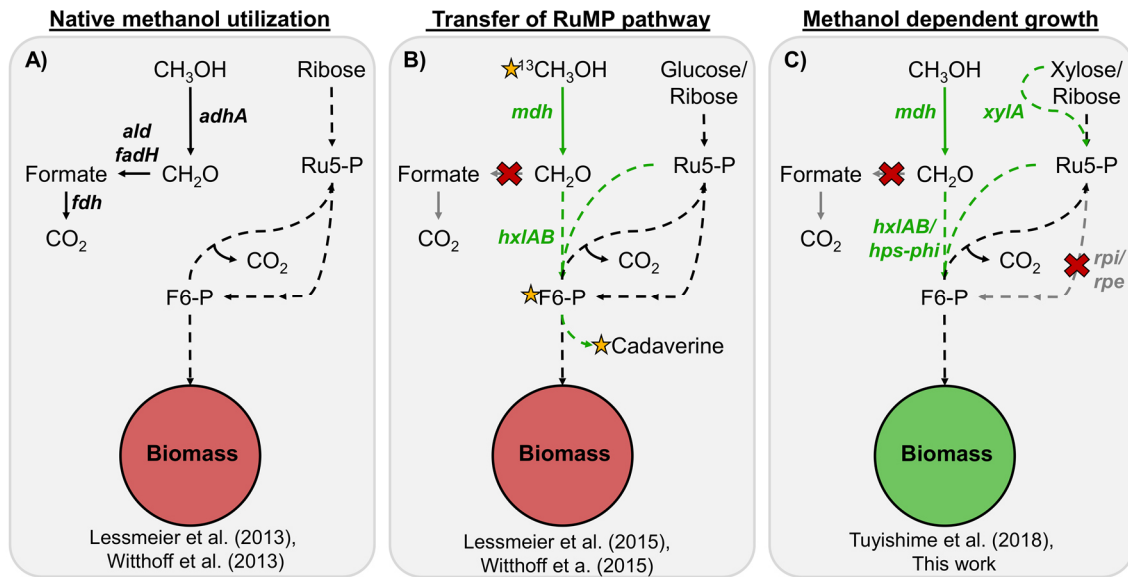
Figure 3: Schematic depiction of attempts to establish methanol utilization in *C. glutamicum*. Relevant pathways for methanol utilization are depicted in reduced form. Dotted arrows represent multiple reactions, green arrows represent heterologous pathways, grey arrows and red crosses show deleted pathways. A) Native methanol utilization in *C. glutamicum*. Methanol is first oxidized to formaldehyde by alcohol dehydrogenase (*adhA*) and subsequently and then further to formate by acetaldehyde dehydrogenase (*ald*) and mycothiol-dependent formaldehyde dehydrogenase (fadH), before final oxidation of formate to CO_2 by formate dehydrogenase (*fdh*). Methanol is not used to form biomass. B) Transfer of RuMP pathway to *C. glutamicum*. Methanol utilization genes methanol dehydrogenase (*mdh*) from *B. methanolicus* and 3-hexulose-6-phosphate synthase *(hxlA)* as well as 6-phospho-3-hexulose isomerase (*hxlB*) from *B. subtilis* were introduced to a Δ*ald* Δ*fadH* genetic background to prevent formaldehyde oxidation. Labelling experiments with ^{13}C-methanol revealed incorporation of methanol-derived carbon in central metabolites and the non-natural product cadaverine (yellow star), without net biomass formation from methanol. C) Methanol-dependent growth through metabolic cut- by deletion of ribose-5-phosphate isomerase (*rpi*) or ribulose-5-phosphate epimerase (*rpe*) in a Δ*ald* Δ*fadH* genetic background and expression of xylulose isomerase (*xylA*) from *E. coli* for xylose utilization as co-substrate to methanol. Additional expression of *hxlAB* or homologue genes *hps-ph*i from *B. methanolicus* led methanol-dependent biomass formation.

To couple methanol utilization and biomass formation, the linear formaldehyde detoxification pathway (Δ*ald* Δ*fadH*), as well as *rpi* (ribose-5-phosphate isomerase) were deleted and *xylA* (xylose isomerase) from *E. coli, hps* and *phi* from *B. methanolicus* and *mdh* from *Bacillus stearothermophilus* were introduced on plasmids for heterologous expression (Tuyishime et al., 2018). The engineered *C. glutamicum* strain exhibited methanol-dependent biomass formation with xylose, revealing up to 64% of average carbon incorporation from

[13]C-methanol into the amino acid histidine (Tuyishime et al., 2018)(Figure 3C). The specific growth rate on xylose and methanol was improved almost 3-fold from 0.012 h^{-1} to 0.03 h^{-1} through ALE (Tuyishime et al., 2018).

The work presented here followed a similar strategy with a distinct approach to further improve methanol-dependent biomass formation in *C. glutamicum*. Here, *rpe* was deleted in *C. glutamicum* Δ*ald* Δ*fadH*, to create a metabolic cut-off in the PPP for methanol-dependency with ribose as co-substrate. Additionally, *mdh* from *B. methanolicus* and *hxlAB* from *B. subtilis* were introduced on a plasmid for heterologous expression to allow methanol-dependent growth for further improvement through ALE (Figure 3C). As alternative approach, *rpi* was deleted and *xylA* from *E. coli* was additionally expressed for methanol-dependent growth of *C. glutamicum* on xylose and gluconate.

1.6 Objectives

Although intensive work has been done in the past to establish methanol as sole carbon source in the industrial workhorse *C. glutamicum*, synthetic methylotrophy was never achieved. The main objective of this work was to establish and improve biomass formation from methanol in *C. glutamicum* to increase knowledge for future engineering of synthetic methylotroph strains. This included:

1. Engineering of a methanol-dependent *C. glutamicum* strain
2. Improvement of methanol-dependent growth by ALE
3. Investigation of mutations in evolved *C. glutamicum* strains
4. Transfer of beneficial mutations to the unevolved parental strain
5. Production of the value-added non-natural product cadaverine from methanol

2. Materials and methods

2.1 Strains and plasmids

All strains and plasmids used in this work are listed in Table 1 and Table 2.

Table 1: Strains used in this work

Strain	Relevant characteristics	Source/reference
C. glutamicum strains		
WT	Wild type strain ATCC 13032	ATCC 13032
Δ*ald* Δ*fadH*	WT strain with deletions of *ald* and *fadH*	(Leßmeier et al., 2013)
Δ*ald* Δ*fadH* Δ*rpe*	WT strain with deletions of *ald*, *fadH* and *rpe*	This work
Δ*ald* Δ*fadH* Δ*rpi*	WT strain with deletions of *ald*, *fadH* and *rpe*	Carsten Haupka
Evo 1	WT strain with deletions of *ald*, *fadH* and *rpe*, harbouring the plasmid pEKEx3-*mdh-hxlAB*	This work
Evo 1 Δcg3104	Evo 1 with deletion of cg3104	This work
Evo 1 *metK*_S288N	Evo 1 with a point mutation in the *metK* gene, leading to amino acid substitution S288N	This work
Evo 1 Δcg3104 *metK*_S288N	Evo 1 with deletion of cg3104 and point mutation in the *metK* gene, leading to amino acid substitution S288N	This work
Evo 1 Δcg3104 Δ*metY*	Evo 1 with deletion of cg3104 and *metY*	This work
Evo 8	Improved methanol-utilizing strain derived from Evo 1 through adaptive laboratory evolution	This work
Evo 14	Improved methanol-utilizing strain derived from Evo 1 through adaptive laboratory evolution	This work
E. coli **Strains**		
DH5α	φ80d*lacZ*ΔM15, Δ(*lacZYA-argF*)U169, hsdR17, recA1, gyrA96, nupG, purB20, relA1, deoR, thi-1, glnV44, endA1	(Hanahan, 1985)
S17-1	Genomic integration of RP4 2-Tc::Mu Km::Tn7; recA, Tp^R, Sm^R, pro, res$^-$, mod$^+$	(Simon et al., 1983)

Table 2: Plasmids used in this work

Plasmid	Relevant characteristics	Source/reference
pEKEx3	Spec^R, shuttle vector for *E. coli*/*C. glutamicum*; IPTG-inducible gene expression (P$_{tac}$, lacI^Q, pBL1 oriV$_{Cg}$, pUC18 oriV$_{Ec}$)	(Stansen et al., 2005)
pEKEx3-*hxlAB*	Spec^R, pEKEx3 with *hxlAB* from *B. subtilis*	(Leßmeier et al., 2015)
pEKEx3-*mdh-hxlAB*	Spec^R, pEKEx3 with *mdh* from *B. methanolicus* and *hxlAB* from *B. subtilis*	(Leßmeier et al., 2015)
pEKEx3-*xylAB*	Spec^R, pEKEx3 with *xylA* from *X. campestris* and *xylB* from *C. glutamicum*	(Meiswinkel et al., 2013)
pVWEx1	Km^R, shuttle vector for *E. coli*/*C. glutamicum*; IPTG-inducible gene expression (P$_{tac}$, lacI^Q, pHM1519 OriV$_{Cg}$, pACYC177 OriV$_{Ec}$)	(Peters-Wendisch et al., 2001)
pVWEx1-*rpe*	Km^R, pVWEx1 with *rpe* from *C. glutamicum*	This work
pVWEx1-*rpi*	Km^R, pVWEx1 with *rpi* from *C. glutamicum*	Carsten Haupka
pVWEx1-*mdh-hxlAB*	Km^R, pVWEx1 with *mdh* from *B. methanolicus* and *hxlAB* from *B. subtilis*	Carsten Haupka
pVWEx1-*lysC*^{fbr}-*ldcC*	Km^R, pVWEx1 with feedback resistant *lysC*^{T311I} from *C. glutamicum* and *ldcC* from *E. coli*	(Leßmeier et al., 2015)
pECXT99A	Tet^R, shuttle vector for *E.coli*/*C.glutamicum*, IPTG-inducible gene expression (P$_{trc}$, lacI, pGA1 oriV$_{Cg}$, pUC18 oriV$_{Ec}$)	(Kirchner and Tauch, 2003)
pECXT99A-*mdh-hxlAB*	Tet^R, pECXT99A with *mdh* from *B. methanolicus* and *hxlAB* from *B. subtilis*	This work
pECXT99A-*xylAB*	Tet^R, pECXT99A with *xylA* from *X. campestris* and *xylB* from *C. glutamicum*	(Veldmann et al., 2019)
pECXT99A-*lysC*^{fbr}-*ldcC*	Tet^R, pECXT99A with feedback resistant *lysC*^{T311I} from *C. glutamicum* and *ldcC* from *E. coli*	Carsten Haupka

pK19*mobsacB*	Km^R, shuttle vector for *E. coli*/*C. glutamicum* to construct insertions/deletions in *C. glutamicum* (*p*K18 oriV~Ec~, *sacB, lacZα*)	(Schäfer et al., 1994)
pK19*mobsacB*-Δ*rpe*	Km^R, pK19*mobsacB* with up- and downstream flanking regions of the *C. glutamicum rpe* gene for deletion	(Leßmeier, unpublished)
pK19*mobsacB*-Δ*rpi*	Km^R, pK19*mobsacB* with up- and downstream flanking regions of the *C. glutamicum rpi* gene for deletion	This work
pK19*mobsacB*-Δcg3104	Km^R, pK19*mobsacB* with up- and downstream flanking regions of the *C. glutamicum* gene cg3104 for deletion	This work
pK19*mobsacB*-Δ*metY*	Km^R, pK19*mobsacB* with up- and downstream flanking regions of the *C. glutamicum metY* gene for deletion	This work
pK19*mobsacB*-*metK*_S288N	Km^R, pK19*mobsacB* derivative to introduce a base exchange from T to C, at position 863 in the *metK* gene, leading to amino acid change S288N	This work
pK19*mobsacB*-*metK*_N288S	Km^R, pK19*mobsacB* derivative to introduce a base exchange from C to T, at position 863 in the *metK* gene, leading to amino acid change N288S	This work
pK19*mobsacB*-SNP_*dxs-rnd*	Km^R, pK19*mobsacB* derivative to introduce a base exchange from C to T, in the intergenic region between the genes *dxs* and *rnd*	This work

2.2 Oligonucleotides

All oligonucleotides used for cloning throughout this work are listed in Table 3.

Table 3: Primers used in this work

Primer name	Sequence (5'-3')	Purpose
GH78_fw	CCTGCAGGTCGACTCTAGAGGAAAGGAGGCCCTTCAGATGGCACAACGTACTCCAC	Amplification of *rpe* to clone pVWEx1-*rpe*
GH79_rv	ATTCGAGCTCGGTACCCGGGTTACTGCGCGAGTGCTCG	
GH80_fw	ATTCGAGCTCGGTACCCGGGGATCCGAAAGGAGGCCCTTCAGATGACAACAAACTTTTTCATTCCACCAG	Amplification of *mdh* + *hxlAB* from pEKEx3-*mdh-hxlAB* to clone pECXT99A-*mdh-hxlAB*
GH81_rv	CCTGCAGGTCGACTCTAGAGGATCCTATTCAAGGTTTGCGTGGTGAG	
GH103_fw	GCATGCCTGCAGGTCGACTCTAGAGTTGGCGCACCGACTGTCACGTCG	Amplification of *metK* from Evo 1 or Evo 14 to clone pK19*mobsacB-metK*_S288N and pk19*mobsacB-metK*_N288S
GH104_rv	AGTGAATTCGAGCTCGGTACCCGGGGGGTTTTTGCCATGAATCCGAAGATACTACA	
GH107_fw	GCATGCCTGCAGGTCGACTCTAGAGCCATCAGTTCTCATCATTGCGGT	Amplification of up- and downstream region of the intergenic region between *dxs* and *rnd* for cloning of pK19*mobsacB*-SNP_*dxs-rnd*
GH108_rv	AGTGAATTCGAGCTCGGTACCCGGGAACGCTGGTTCCGCATCATCACC	
GH113_fw	CCTGCAGGTCGACTCTAGAGACAAAACTGAAGCGATGCCCAAAG	Amplification of upstream region of cg3104 to clone pK19*mobsacB*-Δcg3104
GH114_rv	AATTGCCCTGAGCTTGTTCGCTGGTCACTTCT	
GH115_fw	CGAACAAGCTCAGGGCAATTCCAGTTTCTCTAGGATCG	Amplification of downstream region of cg3104 to clone pK19*mobsacB*-Δcg3104
GH116_rv	ATTCGAGCTCGGTACCCGGGCGCCACCACCTCCGCTGTAAAAC	

GH125_fw	CCTGCAGGTCGACTCTAGAGTAGCGTT GCTGTACACCAAATCATCG	Amplification of upstream region of *metY* to clone pK19*mobsacB*-Δ*metY*
GH126_rv	TTCGAGGTCAGCGATATTGTCGTACTTT GGCATTTGGAGGTC	
GH127_fw	CAAATGCCAAAGTACGACAATATCGCTG ACCTCGAAGGCG	Amplification of downstream region of *metY* to clone pK19*mobsacB*-Δ*metY*
GH128_rv	AATTCGAGCTCGGTACCCGGGGATCGA AATTTCCATCTGGATGCATGGAGCC	
CH01_fw	TGCAGGTCGACTCTAGAGCGCACCTTTAG GGCGTATGG	Amplification of upstream region of *rpi* to clone pK19*mobsacB*-Δ*rpi*
CH02_rv	GGGTAGGTGATTTGAATTTGTTCCAAGGT ATACGCGCATGG	
CH03_fw	ACAAATTCAAATCACCTACCCCGCACTGG AATCGCACCT	Amplification of downstream region of *rpi* to clone pK19*mobsacB*-Δ*rpi*
CH04_rv	CGACGGCCAGTGAATTCCGAGCCTTGGT GGGCAAG	
CH29_fw	ATTACGCCAAGCTTGCATGCCTGCAGAAA GGAGGCCCTTCAGATGCGCGTATACCTT GGAGC	Amplification of *rpi* to clone pVWEx1-*rpi*
CH30_rv	AGTGAATTCGAGCTCGGTACCCGGGTTA TTCGTTAGGAACGACAGGTGC	
CH40_fw	ATTACGCCAAGCTTGCATGCCTGCAGAAA GGAGGCCCTTCAGATGACAACAAACTTTT TCATTCCACCAG	Amplification of *mdh* + *hxlAB* from pEKEx3-*mdh-hxlAB* to clone pVWEx1-*mdh-hxlAB*
CH41_rv	AGTGAATTCGAGCTCGGTACCCGGGGAT CCCTATTCAAGGTTTGCGTGGTGAG	

CH45_fw	TTCGAGCTCGGTACCCGGGGATCCTCTAG AGAAAGGAGGCCCTTCAGGTGGCCCTGG TCGTACAG	Amplification of *lysC*fbr + *ldcC* from pVWEx1- *lysC*fbr-*ldcC* to clone pECXT99A-*lysC*fbr-*ldcC*
CH46_rv	AAGCTTGCATGCCTGCAGGTCGACTCTAG ATTATCCCGCCATTTTTAGGACTCG	
196_fw	CGCCAGGGTTTTCCCAGTCACGAC	Verification primer for cloning in pK19*mobsacB*
197_rv	AGCGGATAACAATTTCACACAGGA	
581_fw	CATCATAACGGTTCTGGC	Verification primer for cloning in pEKEx3/pVWEx1
582_rv	ATCTTCTCTCATCCGCCA	
1127_fw	GCGCCGACATCATAACGG	Verification primer for cloning in pEKEx3/pVWEx1/pECXT99A
1128_rv	GGCGTTTCACTTCTGAGTTCGG	
VE09_fw	AAAGTCCGTGCGTGGTTTGC	Verification of *rpe* deletion
VE10_rv	CCACGGTGGACGCAAACTTC	
VE17_fw	GATGTTCGGCTACGCCACCAAC	Verification of *metK*_S288N/*metK*_N288S
VE18_rv	GTAACCCCAAAAGAGGTAAAACCCGC	
VE25_fw	GGTTCTTGATGAGGATGCGGGTG	Verification of cg3104 deletion
VE26_rv	GAGATCATCGTTAGACAGCGAACGC	
VE33_fw	GGGGACTTCTTCACGCCTACTGG	Verification of *metY* deletion
VE34_rv	GAATGGACGTGGCGGGGAAG	
CH27_fw	CTTGGCGGCGTCTACATTTC	Verification of *rpi* deletion
CH28_rv	ACTACTACCCTGGCGGTAAC	
GQ03_fw	ACCGTGCATGGTGGCTAGTC	qPCR primer targeting *gntK* on *C. glutamicum* genome
GQ04_rv	GCAAGGTGGATGGCATGAAG	
GQ13_fw	CGCGCTCATGATGTTTGTGG	qPCR primer targeting oriV$_{Cg}$ on pEKEx3-*mdh-hxlAB*
GQ14_rv	AGCATGTTGCGGTGCAAGTG	

2.3 Chemicals

All chemicals used throughout this study were purchased from Sigma-Aldrich GmbH (Taufkirchen, Germany), Merck AG (Darmstadt, Germany), Carl Roth (Karlsruhe, Germany) or VWR international GmbH (Darmstadt, Germany) if not stated otherwise.

2.4 Cultivation conditions

2.4.1 *E. coli*

E. coli strains were cultivated in lysogeny broth complex medium (LB)(Bertani, 1951) at 37°C. Strains were streaked on LB agar plates and incubated overnight. Liquid cultures were inoculated either from agar plates or frozen glycerol stocks and cultivated in 100 ml shake flasks overnight at 180 rpm shaking frequency. The medium was supplemented with 25 µg m/l kanamycin or 100 µg m/l spectinomycin when appropriate.

2.4.2 *C. glutamicum*

C. glutamicum strains were cultivated at 30°C. Strains were streaked from frozen glycerol stocks on brain-heart-infusion (BHI) agar plates and incubated for 1-2 days. Precultures for growth experiments were inoculated from single colonies and grown overnight in BHI medium at 120 rpm. Growth experiments were performed in CG XII minimal medium (Keilhauer et al., 1993). Cells of precultures were harvested by centrifugation (5 min, 4000 rpm) and washed twice with CG XII Buffer (pH 7), before inoculation of main cultures to a starting optical density at 600 nm (OD_{600}) of ~ 0.5. Growth was subsequently monitored through OD_{600} measurements. Biomass concentrations of *C. glutamicum* were calculated with the correlation $CDW = 0.353 \cdot OD_{600}$, as described previously (Bolten et al., 2007).

For cultivations including methanol, 100 ml flasks without baffles with a filling volume of 8 ml were used. Suitable antibiotics in appropriate concentrations were added for strains harbouring plasmids and their derivatives (pEKEx3, 100 µg m/l spectinomycin), (pVWEx1/pk19*mobsacB*, 25 µg m/l kanamycin), (pECXT99A, 5 µg m/l tetracycline). To induce plasmid-based gene expression, 1 mM isopropyl-β-D-1-thiogalactopyranoside (IPTG) was supplemented.

Growth experiments in the microbioreactor system BioLector (m2p labs; Baesweiler, Germany) were carried out using 48-well flower plates (MTP-48-B; m2p labs) with a filling volume of 1 ml, at 30°C and 1200 rpm shaking frequency. Humidity was set to 85% and online biomass measurements of scattered light were obtained along cell growth with backscatter gains of 20 or 50.

Statistical significance of growth differences between strains was determined by two-sample t-test analysis assuming equal variances, confirming significance at $p ≤ 0.05$.

2.4.3 Strain preservation

For long-term storage of *E. coli* and *C. glutamicum* strains, frozen glycerol stocks were prepared. 650 µl of liquid LB/BHI overnight cultures, inoculated from single colonies, were mixed with 350 µl of 87% glycerol in cryo-vials and stored at -80°C.

2.4.4 Adaptive laboratory evolution (ALE)

C. glutamicum Δ*ald* Δ*fadH* Δ*rpe* (pEKEx3-*mdh-hxlAB*) (Evo 1) was used for ALE in two phases, to improve methanol-dependent growth.

Phase 1 [Evo 1-8]: Strains were cultivated in CG XII minimal medium containing 20 mM ribose and 500 mM methanol, with a starting OD_{600} of ~0.5. Low biomass formation made it necessary to inoculate an intermediate LB overnight culture, to allow a starting OD_{600} of 0.5 for the next transfer to CG XII minimal medium.

Phase 2 [Evo 8-14]: Strains were cultivated in CG XII minimal medium containing 20 mM ribose, 500 mM methanol and 0.5 g/l yeast extract, with a starting OD_{600} of 0.5 and subsequently transferred to fresh CG XII medium, after maximal biomass formation was reached, to start the next cultivation.

All cultivations were carried out in technical triplicates, using the culture with the highest final OD_{600} of the triplicate for further transfers to fresh medium. Before each transfer, a glycerol stock of the chosen culture was prepared for long-term storage at -80°C. Re-inoculations were done after 24-72h, dependent on when the maximal OD_{600} was reached.

To assure the genetical identity of evolved strains, cultures after 8, 12 and 14 transfers were plated on BHI to get single colonies. Those were then used to inoculate 12 separate BHI overnight precultures for cultivation in CG XII with 20 mM ribose and 500 mM methanol. The strain reaching the highest methanol-dependent biomass formation was chosen for long-term preservation at -80°C.

2.5 DNA isolation, manipulation, and transformation

2.5.1 Molecular work

Primers and plasmid maps were designed *in silico* before cloning, using Clone Manager 9 (Sci-Ed Software, Denver, USA) or SnapGene software v.4.3 (GSL Biotech, Chicago, USA). All primers used in this work were purchased from Metabion (Steinkirchen, Germany). Colony PCRs to verify cloning and genomic modifications were done with Taq polymerase (New England Biolabs, Ipswich, USA) and PCR to amplify DNA-fragments for cloning was performed with Allin HiFi polymerase (HighQu, Kraichtal, Germany) according to the manufacturer's protocol. Restriction enzymes BamHI and EcoRI to cut vectors pEKEx3, pVWEx1, pK19mob*sacB* and pECXT99A and DpnI for degradation of methylated template DNA were obtained from Thermo Fisher Scientific (Waltham, USA). Antarctic phosphatase for dephosphorylation of cut DNA fragments was purchased from New England Biolabs (Massachusetts, USA). Cloning of plasmids was performed by Gibson assembly (Gibson et al., 2009), with homologous overhangs of 20-30 bp and a molar ratio of insert to vector of 5:1.

Plasmids from *E. coli* were isolated using GeneJET Plasmid Miniprep Kit from Thermo Fisher Scientific (Waltham, USA), following the manufacturer's manual. Plasmid isolations from *C. glutamicum* were carried out using the same kit with a modified protocol. Before cell lysis, cells were treated with 15 mg/ml lysozyme in resuspension buffer of the kit for 3 h at 30°C.

Genomic deletions or base exchanges in *C. glutamicum* were performed as previously described (Eggeling and Bott, 2004; Schäfer et al., 1994). Flanking regions (400 bp) of the target gene were cloned into the mobilizable suicide vector pK19*mobsacB* and conjugation with *E. coli* S-17 was used for transformation (Schafer et al., 1990). Cloned plasmids and performed deletions or base exchanges were confirmed by sequencing at CeBiTeC sequencing core facility center (Bielefeld, Germany).

2.5.2 Transformation

Competent cells of *E. coli* strains were prepared by $CaCl_2$-method and transformed by heat shock method as described before (Sambrook and Russell, 2001). Transformations were carried out with 200 ng DNA and cells were subsequently transferred to 500 µl liquid LB-medium, regenerated for 1 h at 37°C and plated on LB plates containing an appropriate antibiotic.

Electrocompetent *C. glutamicum* cells were prepared and transformed by electroporation as previously described (Eggeling and Bott, 2004). Electroporation was performed at 2.5 kV, 25 µF and 200 Ω in a GenePulser Xcell by Bio-Rad (Hercules, California). Transformed cells were kept in BHIS medium at 46°C for 6 minutes and regenerated for 1 h at 30°C before plating them on BHI plates containing an appropriate antibiotic.

2.5.3 gDNA isolation

Isolation of genomic DNA from *E. coli* and *C. glutamicum* WT for further use in PCR reactions was performed as described previously (Eikmanns et al., 1994).

Genomic DNA of the different artificially evolved *C. glutamicum* strains, for DNA library preparation and subsequent whole-genome sequencing, was isolated using NucleoSpin® Microbial DNA kit from Macherey-Nagel (Düren, Germany). Cells were cultivated overnight in BHI complex medium, harvested through centrifugation (5 min, 4000 rpm) and kept on ice afterwards. Disruption of cells was carried out using a Silamat S6 swing mill (Ivoclar Vivadent, Ellwangen, Germany) with glass beads in a 1.5 ml Eppendorf tube in three steps of 1 min, with intermediate cooling on ice to prevent denaturation. The remaining procedure was carried out as stated in the manufacturer's protocol. The quality of the purified genomic DNA was verified by gel electrophoresis and DNA concentration determination using DropSense™ 16 spectrophotometry (Trinean, Ghent, Belgium; software version 2.1.0.18).

2.6 Enzymatic assays

Enzymatic activity measurements were performed with crude extracts of *C. glutamicum.* Cells grown overnight in BHI medium containing 1 mM IPTG and appropriate antibiotics were harvested by centrifugation (5 min, 4000 rpm), washed in 50 mM phosphate buffer and subsequently disrupted by sonication. Sonication was carried out with an amplitude of 50% and a duty circle of 0.5 for 9 min. Afterwards, total protein concentrations were determined using the Bradford method (Bradford, 1976) with bovine serum albumin as standard. Bradford measurements and enzyme activity assays were all performed with a Shimadzu UV-1800 spectrophotometer (Duisburg, Germany) in 1.5 ml cuvettes (Sarstedt, Germany). Activities were calculated from linear slopes, according to the law of Lambert-Beer (ε_{NADH} = 6.22 M^{-1} cm^{-1}), defining one unit (U) as the amount of enzyme necessary for conversion of 1 µM substrate per minute. For calculations of specific activities (U/mg), the total protein concentration of crude extracts was used. Statistical significance of measured activities was determined

by two-sample t-test analysis assuming equal variances, confirming significance at $p \leq 0.05$.

2.6.1 <u>Methanol dehydrogenase</u>

To measure activities of heterologously expressed methanol dehydrogenase from *B. methanolicus*, a previously described method for *E. coli* was modified (Müller et al., 2015). Measurements were carried out at 30°C in a total volume of 1 ml, containing 25 mM phosphate buffer pH 7.4, 5 mM MgSO$_4$, 5 mM NAD$^+$ and 50 µl crude extract in varying dilutions. The reaction was started by addition of 2 M methanol and formation of NADH was continuously measured at 340 nm for 3 min.

2.6.2 <u>Coupled activity of HxlA and HxlB</u>

Activities of HxlA and HxlB in crude extracts were measured in a coupled assay, different from a previously described method (Leßmeier et al., 2015). Measurements were carried out in a total volume of 1 ml, containing 25 mM phosphate buffer pH 7.4, 5 mM MgCl$_2$, 5 mM ribose-5-phosphate, 0.5 mM NAD$^+$, 2 U phosphoriboisomerase from spinach (Sigma), 2 U phosphoglucoisomerase from yeast (Sigma), 2 U Glucose-6-P dehydrogenase from *Leuconostoc mesenteroides* (Sigma) and 50 µl crude extract in varying dilutions. The reaction was started by addition of 5 mM formaldehyde. Formation of NADH was continuously measured at 340 nm and 30°C for 6 min.

2.7 Whole genome sequencing

In the present study, a hybrid genome assembly approach combining long and short sequencing reads (Pechtl et al., 2018) was applied as basis for mutational analysis in the artificially evolved *C. glutamicum* strains Evo 8 and Evo 14 in comparison with first generation strain Evo 1. First, genomic DNA purified from each analysed strain was used to prepare mate-pair shotgun sequencing libraries using Nextera Mate Pair Sample Preparation Kit (Illumina, San Diego, USA). The whole-genome sequencing run was carried out applying mate-pair protocol on an

Illumina MiSeq system. De novo DNA sequence assembly was performed using Newbler software v.2.8 (Roche Diagnostics, Rotkreuz, Switzerland), resulting in 33, 32 and 35 scaffolds containing 493, 285 and 630 contigs for Evo 1, Evo 8 and Evo 14 data, respectively. Furthermore, to obtain long sequencing reads from genomic DNA samples, whole genome sequencing shotgun library was sequenced using Nanopore MinION sequencing technologies (Oxford Nanopore Technologies, Oxford, UK). Barcoded DNA fragments (up to 50 kb) from each DNA sample were pooled and used to prepare sequencing library with 1D Square Sequencing Kit (R9.5; Oxford Nanopore Technologies) and the generated library was loaded to a Nanopore R9.5 flow cell for subsequent sequencing on USB MinION sequencer. Nanopore output reads were base called using Albacore software v.1.2.4 (https://github.com/albacore). Sequence data was assembled with Canu assembler v.1.5 (Koren et al., 2017), resulting in 11 contigs for Evo 1 data, 6 contigs for Evo 8 and 2 contigs for Evo 14. Long Nanopore-derived contigs were polished with short Illumina-drived reads using Pylon tool (Walker et al., 2014). Finally, genome sequences were finalized using Consed genome finishing tool (Gordon et al., 1998).

Moreover, complete genome sequences of Evo 8 and Evo 14 were aligned with the Evo 1 genome sequence using SnapGene software v.4.3 (GSL Biotech, Chicago, USA) for single nucleotide polymorphisms (SNPs) and small insertions and deletions (indels) visualization. Variant calling was performed manually, identifying SNPs and indels by verification of the mismatches observed in alignment of complete genome sequences of Evo 8 and Evo 14 against the parental strain Evo 1 genome sequence reference.

2.8 Quantitative PCR

Plasmid copy numbers of different *C. glutamicum* strains were determined using quantitative PCR (qPCR). Experiments were carried out in 96-well plates, sealed with a transparent adhesive cover in a CFX Connect™ Real-Time PCR Detection System (Biorad, Hercules, USA). In a total volume of 20 µl for each reaction, 10 µl of SensiFAST™ SYBR® No-ROX Kit from Bioline (Heidelberg, Germany) were used together with 100 nmol/l forward/reverse primer and 4 µl of diluted template

DNA. Template DNA, including chromosomal and plasmid DNA, was isolated beforehand from BHI overnight cultures (with appropriate antibiotics) of different *C. glutamicum* strains (see Chapter 2.5.3). Primers were designed for amplification of fragments around 250 bp, targeting *C. glutamicum* chromosomal gene *gntK* encoding gluconate kinase and oriV$_{Cg}$ on pEKEx3. Relative standard curves for both chromosomal and plasmid targets were constructed with serial dilutions of DNA, ranging from 100 to 0.1 ng/µl. Chromosomal and plasmid specific amplicons were then detected in separate reactions, each in technical triplicates with a concentration of 10 ng/µl. Calculations to determine plasmid copy numbers were done as described previously (Škulj et al., 2008). Statistical significance of PCN differences was determined by two-sample t-test analysis assuming equal variances, confirming significance at $p \leq 0.05$.

2.9 Quantification of metabolites using HPLC

For metabolite quantification in supernatants, samples from cultivations were taken at different time points and centrifuged twice for 10 min at 10.000 rpm. Supernatants were subsequently stored at -20°C until use. To measure ribose and gluconate concentrations, supernatants were diluted 1:5, whereas 1:20 dilutions were applied for cadaverine measurements.

Metabolites were detected and quantified using the Agilent 1200 series High-Performance Liquid Chromatography (HPLC) from Agilent Technologies Sales & Services GmbH & Co. KG (Waldbronn, Germany).

Ribose and gluconate concentrations were measured using 5 mM H_2SO_4 as mobile phase, at a flow rate of 0.8 ml/min. For sample separation, a column (300 x 80 mm, particle size 10 µm, 25 Å from CS-Chromatographie Service GmbH (Langerwehe, Germany)) was applied, before metabolites were detected with a refractive index detector (RID G1362A, 1200 series, Agilent Technologies Sales & Services, (Waldbronn, Germany)). External calibration was done with ribose and gluconate in concentrations of 5, 10, 15 or 20 mM.

Cadaverine was quantified using a mobile phase of 0.25% sodium acetate (pH 6) and methanol in a ratio of 7:3 and a flow rate of 1 ml/min. Amino groups were

derivatized with ortho-phthaldialdehyde (OPA) in a pre-column (LiChrospher 100 RP8 EC-5 µ (40 x 4 mm) (CS Chromatographie Service GmbH, Langerwehe, Germany)) as described before (Georgi et al., 2005). Analytes were separated using a reversed-phase main column (LiChrospher 100 RP8 EC-5µ (125 x 4 mm), CS Chromatographie Service GmbH) and subsequently excited at 230 nm to detect emissions at 450 nm with a fluorescence detector (FLD G1321A, 1200 series, Agilent Technologies). For each sample, an internal standard of 100 µM L-asparagine was added for normalization. External calibration was done with cadaverine in concentrations of 5, 10, 15 and 20 µM.

2.10 Determination of labelled carbon in cadaverine from ^{13}C-methanol

Overnight cultures of *C. glutamicum* Evo 8 (pECXT99A-*lysC-ldcC*) in BHI medium with 1 mM IPTG and antibiotics were used to inoculate modified M9 minimal medium with 20 mM gluconate and 500 mM ^{13}C-methanol as sole carbon sources, to a starting OD_{600} of 0.5. Modified M9 medium contained 7.5 g/l Na_2HPO_4, 3 g/l KH_2PO_4, 0.5 g/l NaCl, 0.25 g/l $MgSO_4 \cdot 7 H_2O$, 0.003 g/l $CaCl_2$, 0.5 g/l NH_4Cl and trace elements from the composition of CG XII minimal medium (Keilhauer et al., 1993).

Samples of 1 ml were taken after 24, 48 and 72 h and centrifuged for 10 min at 10.000 rpm. Supernatants were subsequently frozen at -20°C for measurements of ^{13}C enrichment at different carbon positions in cadaverine as described before (Leßmeier et al., 2015), at Institut National des Sciences Appliquées (INSA, Tolouse). Cadaverine was quantified with a Bruker Ascend 800 MHz magnet using a 1D-^{1}H-NMR (nuclear magnetic resonance) approach with a ^{13}C-decoupled DANTE-Z pulse sequence for isotopic quantification of ^{13}C-enrichments in cadaverine.

3. <u>Results</u>

3.1 Engineering of a methanol-dependent
C. glutamicum strain

3.1.1 <u>Deletion of *rpe* prevents growth of *C. glutamicum* on ribose</u>

To engineer a metabolic cut-off in the PPP for methanol-dependency in *C. glutamicum*, first the *rpe* gene, encoding ribulose-5-phosphate epimerase was deleted in a strain already lacking the linear formaldehyde detoxification pathway (Δ*ald* Δ*fadH*) (Leßmeier et al., 2013) (Figure 3). The resulting strain *C. glutamicum* Δ*ald* Δ*fadH* Δ*rpe* was then examined regarding its capability to utilize ribose as sole carbon source.

Deletion of the *rpe* gene resulted in a growth deficiency on ribose as sole carbon source (Figure 4). After reintroduction of *rpe* on the pVWEx1-*rpe* plasmid, the Δ*rpe* strain was able to grow on ribose again, whereas the same knockout strain harbouring the empty vector did not show any growth (Figure 4). However, growth rate and biomass formation after 28 h were slightly decreased when *rpe* was overexpressed ($\mu = 0.15 \pm 0.01$, OD_{600} of 3.40 ± 0.36, corresponding to 1.20 ± 0.12 gCDW/l), in comparison to the WT strain carrying the empty vector pVWEx1 ($\mu = 0.19 \pm 0.01$, OD_{600} of 4.47 ± 0.09, corresponding to 1.58 ± 0.03 gCDW/l)(Figure 4).
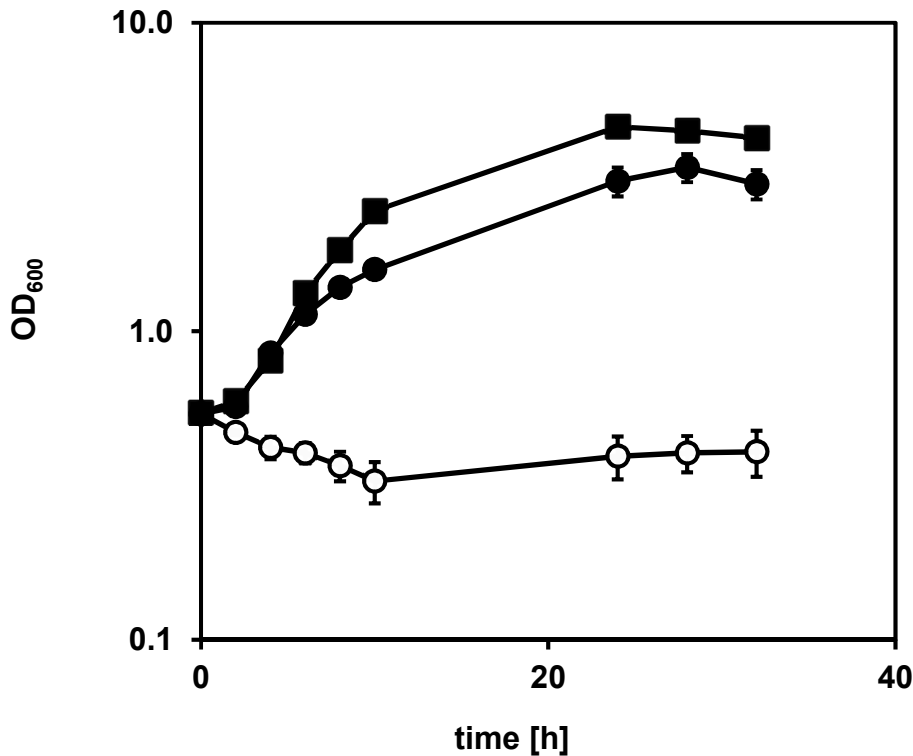
Figure 4: Complementation of *C. glutamicum* deletion strain Δ*rpe* with a plasmid borne *rpe* gene.

Growth of *C. glutamicum* WT (pVWEx1) (squares), Δ*ald* Δ*fadH* Δ*rpe* (pVWEx1) (open circles) and Δ*ald* Δ*fadH* Δ*rpe* (pVWEx1-*rpe*) (closed circles) in a shake flasks cultivation with CG XII minimal medium and 20 mM ribose as sole carbon source. Cultures were inoculated to a starting OD_{600} of 0.5. Error bars depict standard deviations of biological triplicates.

As deletion of the *rpe* gene was successfully complemented through xylose supplementation in *E. coli* before (Chen et al., 2018), it was hypothesized that the deletion of *rpe* could also be complemented through xylose supplementation and introduction of xylose utilizing enzymes in *C. glutamicum*.

The vector, pECXT99A-*xylAB* was introduced to enable xylose utilization for *C. glutamicum* Δ*ald* Δ*fadH* Δ*rpe*. Xylose utilization through overexpression of xylose isomerase (*xlyA*) from *Xanthomonas campestris* and endogenous xylulose kinase (*xylB*) has been established for *C. glutamicum* before (Meiswinkel et al., 2013). The resulting strain *C. glutamicum* Δ*ald* Δ*fadH* Δ*rpe* (pECXT99A-*xylAB*) was cultivated with 20 mM xylose or 20 mM ribose as sole carbon sources, or with a combination of both, to investigate whether Δ*rpe* could be complemented by additional supply of xylose to ribose.

No growth of *C. glutamicum* Δ*ald* Δ*fadH* Δ*rpe* (pECXT99A-*xylAB*) was observed on ribose or xylose as sole carbon source (Figure 5). In comparison to the WT strain harbouring the pECXT99A-*xylAB* plasmid, with ribose as the sole carbon source ($\mu = 0.24 \pm 0.00$), the Δ*rpe* strain was hampered in its growth, when ribose and xylose together were provided to complement the cut-off in the PPP ($\mu = 0.06 \pm 0.01$). Biomass formed by the Δ*rpe* strain after 30 h on ribose and xylose was reduced by roughly 75% (OD_{600}: 1.54 ± 0.11 corresponding to 0.54 ± 0.05 gCDW/l), compared to the WT growing only on ribose (OD_{600}: 4.87 ± 0.45 corresponding to 1.72 ± 0.16 gCDW/l)(Figure 5).
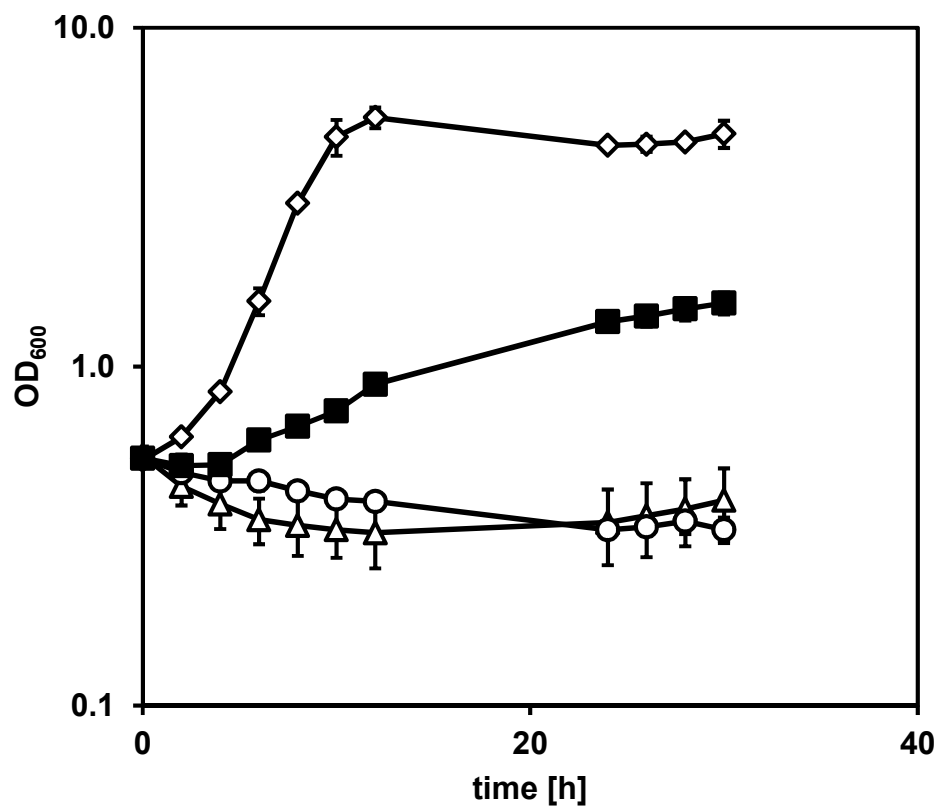
Figure 5: Partial complementation of *C. glutamicum* Δ*rpe* through expression of *xylAB* genes and simultaneous supply of ribose and xylose.

Strains were cultivated in shale flasks containing CG XII medium with either 20 mM ribose or 20 mM xylose (open symbols), or both (closed symbols). *C. glutamicum* WT (pECXT99A-*xylAB*) (diamonds) was cultivated with 20 mM ribose as control. *C. glutamicum* Δ*ald* Δ*fadH* Δ*rpe* (pECXT99A-*xylAB*) was cultivated with ribose (circles), xylose (triangles) or both (squares). Cultures were inoculated to a starting OD_{600} of 0.5. Error bars depict standard deviations of biological triplicates.

Nevertheless, in presence of both carbon sources, growth was restored to a certain degree, making the complementation partially successful (Figure 5). To further couple biomass formation to methanol utilization in *C. glutamicum*, additional investigation of suitable expression platforms for the heterologous genes *mdh* and *hxlAB* essential for methanol oxidation and formaldehyde fixation was performed.

3.1.2 Determination of a suitable expression system for methanol-utilizing enzymes

To determine which *C. glutamicum* expression plasmid is the most suitable for heterologous expression of genes encoding essential methanol utilization enzymes, first an activity assay for methanol dehydrogenase (Mdh) from *B. methanolicus* expressed from different vectors was performed (Figure 6).

Mdh enzymatic activity derived from expression vector pEKEx3 (2.44 ± 0.34 mU/mg) was significantly higher ($p < 0.05$) than that derived from pECXT99A (1.42 ± 0.26 mU/mg). Nevertheless, pEKEx3- or pVWEx1-derived Mdh activity (1.71 ± 0.22 mU/mg) were not significantly different ($p > 0.05$) (Figure 6).

3.1.2 Determination of a suitable expression system for methanol-utilizing enzymes
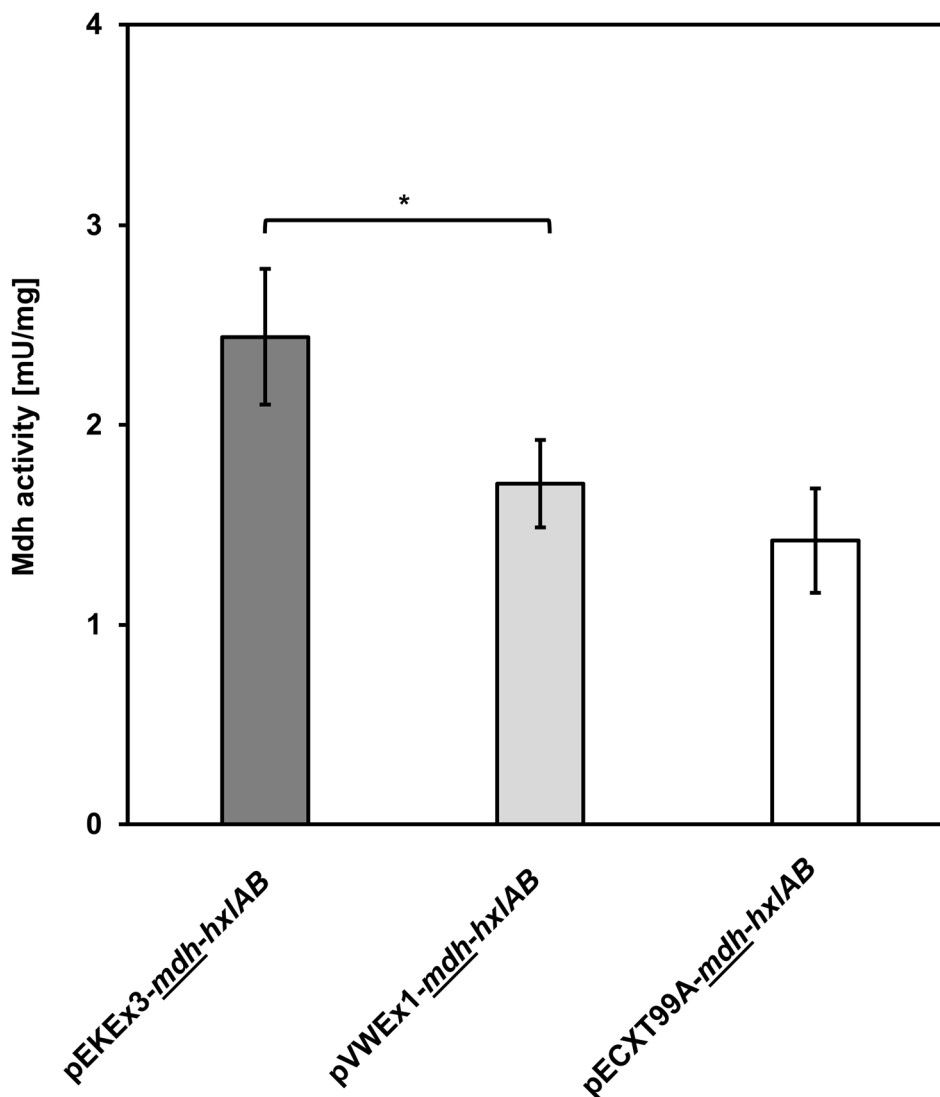
Figure 6: Enzymatic activity of heterologous Mdh in *C. glutamicum* based on different expression vectors.

Specific activity (mU/mg) of Mdh was determined from crude extracts of overnight cultures of *C. glutamicum* Δ*ald* Δ*fadH* Δ*rpe* (pEKEx3-*mdh-hxlAB*) (grey), (pVWEx1-*mdh-hxlAB*) (light grey) and (pECXT99A-*mdh-hxlAB*) (white). Error bars depict standard deviations of technical triplicates. Statistical significance was determined by students t-test analysis and is indicated (*) for $p \leq 0.05$.

Afterwards, the coupled enzymatic activity of 3-hexulose-6-phosphate synthase (HxlA) and 3-hexulose-6-phosphate isomerase (HxlB) from *B. subtilis*, expressed from different vectors was additionally determined (Figure 7). The coupled activity of HxlA and HxlB was highest when expressed from pEKEx3 (197 ± 18 mU/mg), compared to pVWEx1 (154 ± 11 mU/mg) and pECXT99A (92 ± 10 mU/mg) (Figure 7). Based on these results, pEKEx3 was chosen for the expression of *mdh* and *hxlAB* in following experiments.
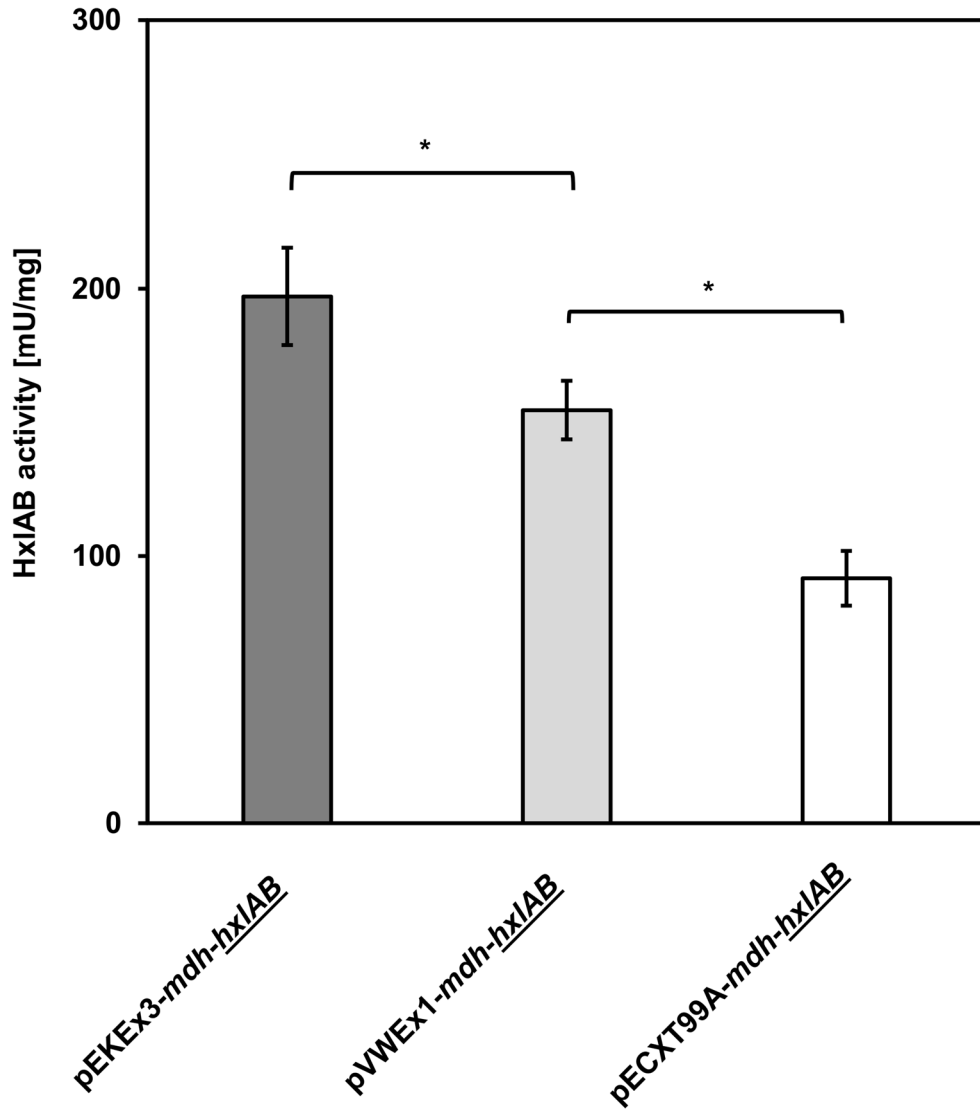
Figure 7: Combined enzymatic activity of HxlAB in *C. glutamicum* based on different expression vectors.

Coupled specific activities (mU/mg) of HxlAB were determined from crude extracts of overnight cultures of C. glutamicum Δ*ald* Δ*fadH* Δ*rpe* (pEKEx3-*mdh-hxlAB*) (grey), (pVWEx1-*mdh-hxlAB*) (light grey) and (pECXT99A-*mdh-hxlAB*) (white). Error bars depict standard deviations of three distinct measurements. Statistical significance was determined by students t-test analysis and is indicated (*) for $p \leq 0.05$.

3.1.3 Methanol-dependent growth of *C. glutamicum* on ribose

After the introduction of a metabolic cut-off in the pentose phosphate pathway through deletion of *rpe* in *C. glutamicum* Δ*ald* Δ*fadH,* genes encoding enzymes for methanol oxidation and formaldehyde fixation were introduced on the pEKEx3-*mdh-hxlAB* plasmid for heterologous expression. The resulting strain *C. glutamicum* Δ*ald* Δ*fadH* Δ*rpe* (pEKEx3-*mdh-hxlAB*) was cultivated in CG XII minimal medium with 20 mM ribose, with and without supplementation of 500 mM methanol to investigate the strains methanol dependency.

Indeed, the presence of methanol in the medium enabled the strain to grow, whereas there was no biomass formation observed in 120 h of cultivation without methanol supplementation. The strain reached a final OD_{600} of 1.95 ± 0.07, which translates to final biomass of 0.66 ± 0.03 gCDW/l with a specific growth rate of 0.03 ± 0.00 h^{-1} (Figure 8). In comparison to complementation through *rpe* overexpression (Figure 4), the growth of *C. glutamicum* Δ*ald* Δ*fadH* Δ*rpe* (pEKEx3-*mdh-hxlAB*) on 20 mM ribose and 500 mM methanol was approximately 80% slower than of strain Δ*ald* Δ*fadH* Δ*rpe (*pVWEx1-*rpe*) in CG XII minimal medium with 20 mM ribose as sole carbon source (μ = 0.15 ± 0.01 h^{-1}) (Figure 4), and final biomass was approximately halved. Despite of that, partial complementation of Δ*rpe* was achieved through heterologous expression of genes *mdh* and *hxlAB* encoding methanol utilizing enzymes and the addition of methanol to medium with ribose (Figure 8).
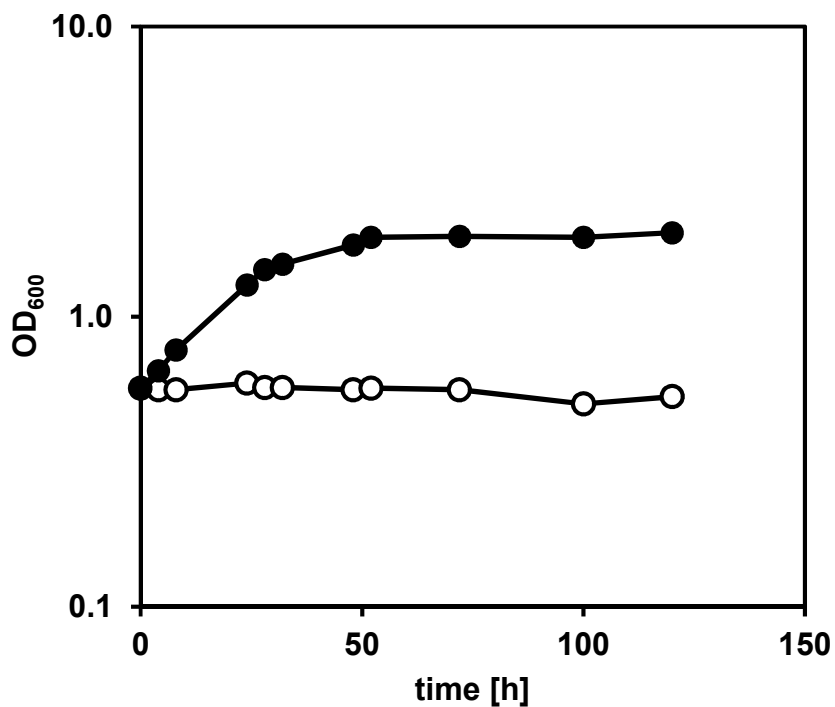
Figure 8: **Methanol-dependent** **growth** **of** *C. glutamicum Δald ΔfadH Δrpe* **(pEKEx3-*mdh-hxlAB*) on ribose*.*

C. glutamicum Δald ΔfadH Δrpe (pEKEx3-*mdh-hxlAB*) was cultivated in shake flasks containing CG XII minimal medium with 20 mM ribose as sole carbon source (open circles) or 20 mM ribose and 500 mM methanol (closed circles). Cultures were inoculated to a starting OD_{600} of 0.5. Error bars depict standard deviations from biological triplicates.

3.1.4 Influence of different ribose/methanol concentrations on growth of a methanol-dependent *C. glutamicum* strain

To examine the impact of varying ribose concentrations on biomass formation with methanol, *C. glutamicum* Δ*ald* Δ*fadH* Δ*rpe* (pEKEx3-*mdh-hxlAB*) was cultivated for 72 h with 5, 10, 20, 50 or 100 mM ribose and 500 mM methanol in CG XII minimal medium (Figure 9A).

The strain exhibited the weakest growth with the lowest (5 mM), as well as highest (100 mM) ribose concentrations in the medium with final ΔOD_{600} values of 0.67 ± 0.03 and 0.66 ± 0.07, respectively. Addition of 10 mM ribose led to a slightly increased ΔOD_{600} of 0.79 ± 0.06, similar to medium with 50 mM ribose (ΔOD_{600}: 0.82 ± 0.07). The highest biomass was reached with 20 mM ribose (ΔOD_{600}: 1.04 ± 0.08; $p < 0.05$) (Figure 9A). Based on this result, further experiments concerning methanol-dependent growth with ribose as co-substrate were carried out with 20 mM ribose.

Afterwards, supplementation of different methanol concentrations was applied to investigate the impact on biomass formation in a 72 h cultivation with 20 mM ribose as co-substrate. Growth was improved with increasing methanol concentrations in the medium (Figure 9B). The final ΔOD_{600} obtained with 100 mM methanol was 0.58 ± 0.06 and it further increased with 300 mM (0.98 ± 0.07), 500 mM (1.15 ± 0.06) and 700 mM (1.19 ± 0.05) (Figure 9B). However, final biomass formation did not significantly differ with 500- or 700 mM methanol in the medium ($p > 0.05$) (Figure 9B). Based on this result, the standard methanol concentration used in following cultivations was set to 500 mM.
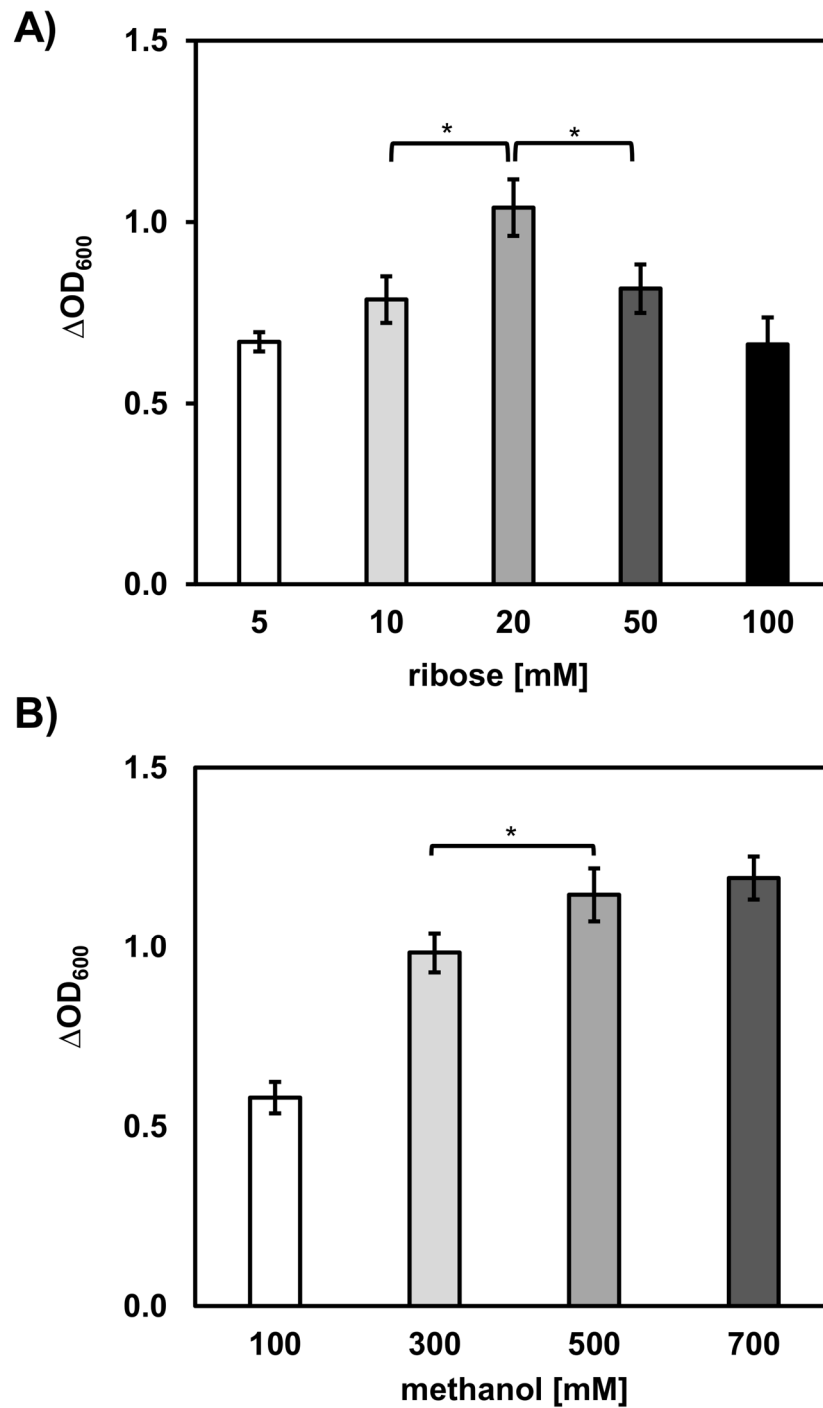
Figure 9: Influence of different ribose or methanol concentrations on growth of a methanol-dependent *C. glutamicum* strain.

C. glutamicum Δ*ald* Δ*fadH* Δ*rpe* (pEKEx3-*mdh-hxlAB*) was cultivated in shake flasks containing CG XII minimal medium with A) 500 mM methanol and 5 (white), 10 (light grey), 20 (grey), 50 (dark grey) or 100 mM (black) ribose. B) 20 mM ribose and 100 (white), 300 (light grey), 500 (grey) or 700 mM (dark grey) methanol. Cultures were inoculated to a starting OD_{600} of 0.5. Error bars depict standard deviations from three distinct cultures. Statistical significance was determined by students t-test analysis and is indicated (*) for $p \leq 0.05$.

3.1.5 Is methanol oxidation from *C. glutamicum* alcohol dehydrogenase (AdhA) sufficient to support growth?

It was known from previous work that *C. glutamicum* alcohol dehydrogenase AdhA accepts methanol as substrate (Witthoff et al., 2013). It was also shown in the present study that methanol-dependent growth can be achieved by strain *C. glutamicum* Δ*ald* Δ*fadH* Δ*rpe* (pEKEx3-*mdh-hxlAB*) with methanol oxidation promoted by heterologous expression of *mdh* from *B. methanolicus* (Figure 8). Hence, it was hypothesized that methanol oxidation from endogenous AdhA was sufficient to support growth in the methanol-dependent strain. In that case, expressing the essential formaldehyde fixation enzymes HxlA and HxlB would be enough for methanol-dependent growth of *C. glutamicum*. Therefore, to investigate whether additional expression of *B. methanolicus mdh* was necessary for methanol-dependent growth, *C. glutamicum* Δ*ald* Δ*fadH* Δ*rpe* was cultivated with pEKEx3-*hxlAB*, lacking the *mdh* gene. The cultivation was carried out in comparison to *C. glutamicum* Δ*ald* Δ*fadH* Δ*rpe* (pEKEx3-*mdh-hxlAB)* in CG XII minimal medium containing 20 mM ribose and 500 mM methanol as carbon sources.

It was revealed that the strain was not able to grow with ribose and methanol without co-expression of *mdh* to *hxlA*B (Figure 10). Whereas the *mdh* expressing strain showed similar growth to previous experiments (Figure 8), no growth was detected after 48 h for the strain without *mdh* expression (Figure 10). Therefore, the present study confirms that endogenous AdhA-based methanol oxidation of *C. glutamicum* was not enough to support growth on methanol and ribose and that heterologous *mdh* expression is required for methanol-dependent growth.
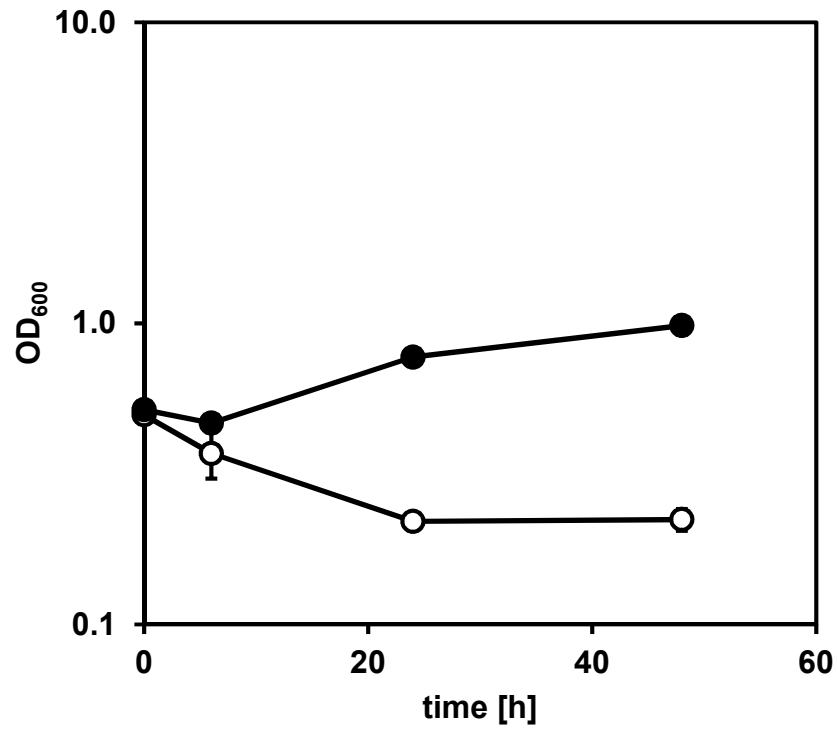
Figure 10: Methanol-dependent growth of *C. glutamicum* with or without expression of the *mdh* gene from *B. methanolicus*.

C. glutamicum Δ*ald* Δ*fadH* Δ*rpe* was cultivated in shake flasks containing CG XII minimal medium with 20 mM ribose and 500 mM methanol harbouring either the pEKEx3-*hxlAB* (open circles) or pEKEx3-*mdh-hxlAB* plasmid (closed circles). Cultures were inoculated to a starting OD_{600} of 0.5. Error bars depict standard deviations from biological triplicates.

3.2 ALE of a methanol-dependent *C. glutamicum* strain

Methanol-dependent growth with ribose was improved through ALE with *C. glutamicum Δald ΔfadH Δrpe* (pEKEx3-*mdh-hxlAB*), here named Evo 1. Serial transfers of cells to fresh CG XII medium containing methanol was previously applied to enhance methanol resistance in *C. glutamicum* WT (Leßmeier and Wendisch, 2015), as well as biomass formation of methanol-dependent *E. coli* and *C. glutamicum* strains (Chen et al., 2018; Meyer et al., 2018; Tuyishime et al., 2018).

Figure 11 shows the maximal ΔOD_{600} reached by evolved methanol-dependent *C. glutamicum* strains throughout 14 passages over the course of 52 days. From first generation strain Evo 1 to strain Evo 8 the maximal ΔOD_{600} increased from 1.34 to 2.95, which corresponds to a 2-fold biomass increase from 0.47 to 1.04 gCDW/l. Additional transfers resulted in increasing methanol-dependent biomass formation from strain Evo 8 to Evo 14, improving the maximal ΔOD_{600} to 4.59 (1.62 gCDW/l) (Figure 11). After 14 transfers, the biomass level of the strain dependent on methanol supplementation was similar to C. *glutamicum* WT with equal amounts of ribose and yeast extract.
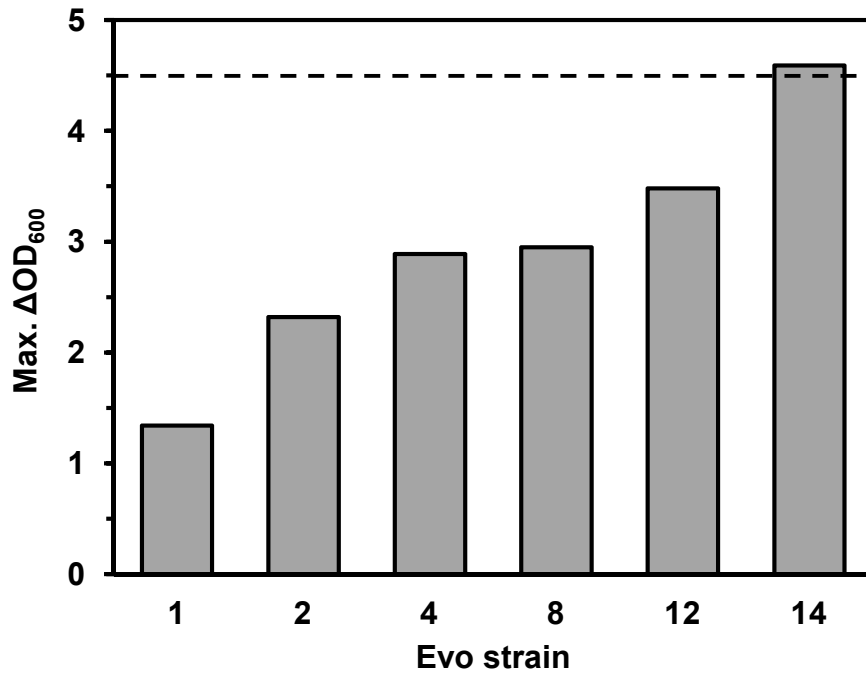
Figure 11*: Maximal ΔOD$_{600}$ reached by methanol-dependent *C. glutamicum* in adaptive laboratory evolution.**

C. glutamicum Δ*ald* Δ*fadH* Δ*rpe* (pEKEx3-*mdh-hxlAB*) was used for adaptive laboratory evolution towards methanol dependent growth in shake flasks. Serial transfers of grown cultures were done in two phases: **1. [Evo 1-8]:** Strains were cultivated in minimal medium containing 20 mM ribose + 500 mM methanol. Grown cultures were used to inoculate intermediate cultures of LB + 20 mM Ribose + 500 mM methanol, before starting the next cultivation in CG XII medium. **2. [Evo 8-14]:** Strains were cultivated in CG XII + 20 mM ribose + 500 mM methanol + 0,5 g/l yeast extract and subsequently transferred to fresh CG XII medium to start the next cultivation. Cultures were grown in triplicates but only data from the replicate with best growth characteristics, used for further reinoculation, is depicted. The dotted line represents the growth of *C. glutamicum* WT with equal amounts of ribose and yeast extract in CG XII medium.

3.3 Methanol-dependent growth of evolved *C. glutamicum* strains

For investigation and characterization of the improvements gained through ALE, the methanol-dependent *C. glutamicum* strains Evo 1, 8 and 14 were cultivated in CG XII medium with 20 mM ribose and 500 mM methanol to determine growth (Figure 12), as well as ribose consumption (Figure 13). None of the strains showed any growth without methanol after 48 h of cultivation (Figure 12).

After 24 h the methanol-dependent biomass formation of Evo 14 (OD_{600}: 2.45 ± 0.05, corresponding to 0.86 ± 0.02 gCDW/l) was twice as high as compared to Evo 8 (OD_{600}: 1.14 ± 0.08; 0.40 ± 0.03 gCDW/l) and approximately 2.7-fold higher than of Evo 1 (OD_{600}: 0.91 ± 0.01, corresponding to 0.32 ± 0.00 gCDW/l)(Figure 12).

Final biomass formation was determined after 48 h. All strains continued growth in presence of methanol, reaching final biomass of 0.39 ± 0.03 gCDW/l (OD_{600}: 1.10 ± 0.08) (Evo 1), 0.49 ± 0.04 gCDW/l (OD_{600}: 1.40 ± 0.11)(Evo 8) and 1.25 ± 0.05 gCDW/l (OD_{600}: 3.54 ± 0.16)(Evo 14) (Figure 12). Final biomass formation of *C. glutamicum* Evo 8 was slightly increased in comparison to Evo 1 (Figure 12). Evo 14 exhibited the best methanol-dependent growth characteristics of all strains, forming 2.5-fold more biomass in comparison to strain Evo 8 and more than 3-fold increased biomass compared to Evo 1 (Figure 12).
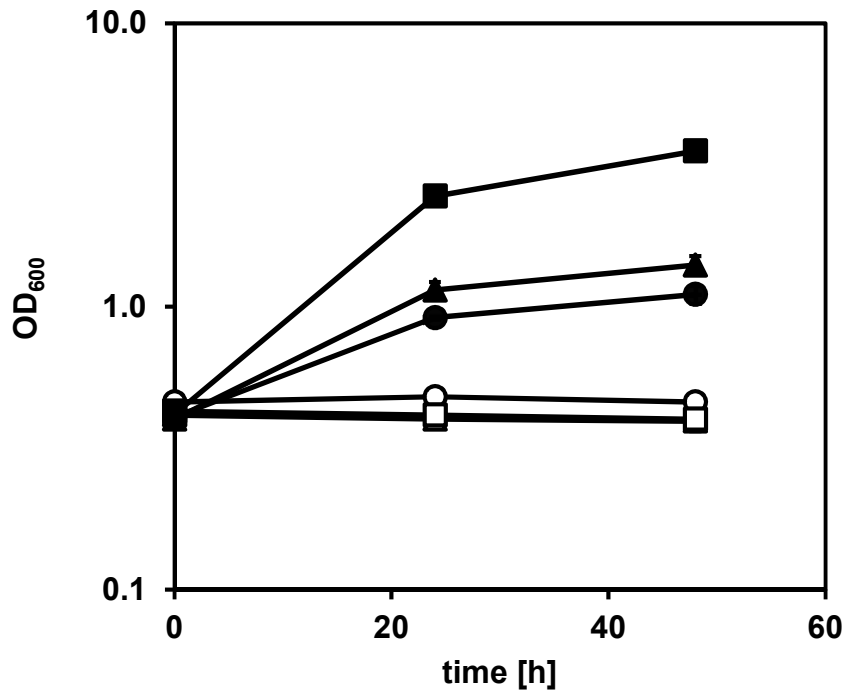
Figure 12: Growth of evolved methanol-dependent *C. glutamicum* strains with ribose and methanol.

Strains *C. glutamicum* Δ*ald* Δ*fadH* Δ*rpe* (pEKEx3-*mdh-hxlAB*) (Evo 1) (circles), Evo 8 (triangles) and Evo 14 (squares) were cultivated in shake flasks containing CG XII minimal medium with either 20 mM ribose as sole carbon source (open symbols) or 20 mM ribose and 500 mM methanol (closed symbols). Cultures were inoculated to a starting OD_{600} of 0.5. Error bars depict standard deviations from biological triplicates.

Furthermore, ribose consumption was monitored after 24 and 48 h to further investigate differences in growth between *C. glutamicum* Evo 1 the evolved strains Evo 8 and Evo 14 (Figure 13). No significant ribose consumption was observed in medium not containing methanol, regardless of the cultivated strain. Measurements revealed that Evo 8 cultures started with higher ribose concentrations compared to Evo 1 and Evo 14, respectively. Nevertheless, after 24 h, ribose concentrations in Evo 1 (11.70 ± 1.99 mM) and Evo 8 (13.39 ± 2.03 mM) cultures with methanol supplementation showed no significant difference anymore (Figure 13). Evo 8 consumed 9.82 ± 3.36 mM ribose with a consumption rate of 0.41 ± 0.29 mM/h in the first 24 h, which was not significantly different to Evo 1 that utilized 0.25 ± 14 mM/h up to a total amount of 6.08 ± 3.29 mM ribose. Evo 14 had a ribose consumption rate of 0.51 ± 0.12 mM/h, consuming 12.29 ± 2.79 mM ribose with 6.10 ± 1.8 mM

remaining in the medium after 24 h (Figure 13). Rate and total consumption of ribose in all strains cultivated with methanol did not significantly differ for the first 24 h.

After 48h, total ribose consumption in methanol supplemented cultures of Evo 1 and Evo 8 still did not differ significantly with 9.22 ± 2.89 mM (0.19 ± 0.06 mM/h) and 13.91 ± 1.48 mM (0.29 ± 0.03 mM/h) consumed, respectively. Both cultures did not exhibit complete ribose depletion after 48 h, leaving 8.56 ± 0.86 mM (Evo 1) and 9.30 ± 0.52 mM of ribose unutilized (Figure 13). Only Evo 14 cultures grown with methanol, showed complete ribose depletion with significantly higher and faster ribose consumption after 48 h compared to Evo 1 and Evo 8, with a total amount of 18.39 ± 1.76 mM ribose consumed with a consumption rate of 0.38 ± 0.04 mM/h (Figure 13).
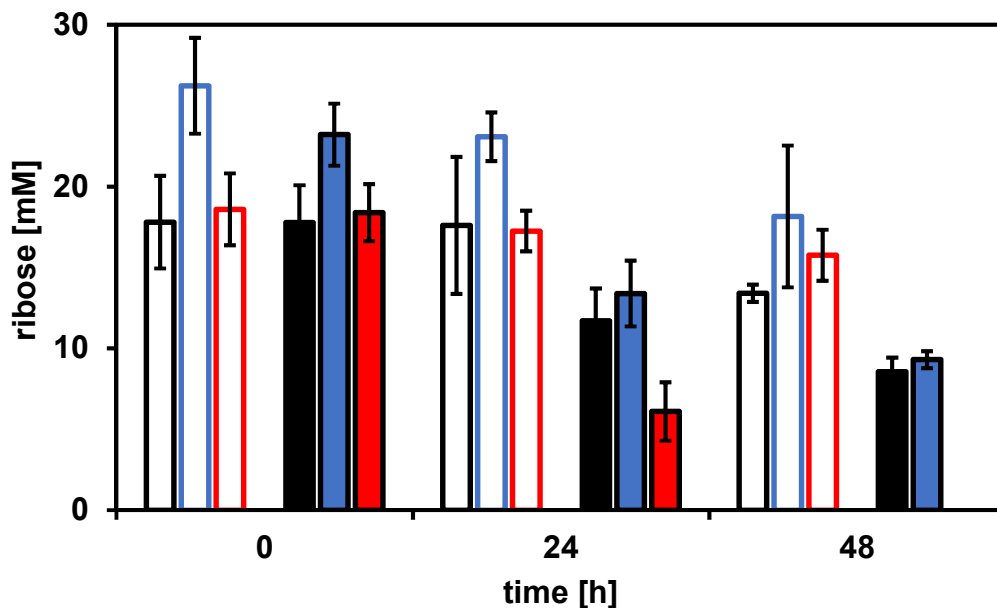
Figure 13: Ribose consumption of evolved *C. glutamicum* strains along methanol-dependent growth.

Strains *C. glutamicum* Δ*ald* Δ*fadH* Δ*rpe* (pEKEx3-*mdh-hxlAB*) (Evo 1) (black), Evo 8 (blue) and Evo 14 (red) were cultivated in shake flasks containing CG XII minimal medium with either 20 mM ribose as sole carbon source (empty bars) or 20 mM ribose and 500 mM methanol (filled bars). Ribose concentrations were measured by HLPC analysis for each culture after 0, 24 and 48 h. Error bars depict standard deviations from biological triplicates.

To investigate whether additional biomass formation could be achieved solely from methanol, the evolved methanol-dependent *C. glutamicum* strain Evo 14 was cultivated with 20 mM ribose and 500 mM methanol in comparison to *C. glutamicum* WT with 20 mM ribose as sole carbon source (Figure 14). No growth of Evo 14 was observed without methanol supplementation (Figure 14). The WT strain grew twice as fast on ribose as the methanol-dependent Evo 14 strain, reaching specific growth rates of 0.22 ± 0.00 h^{-1} compared to 0.10 ± 0.01 h^{-1} respectively. However, both strains ended forming the same biomass after 28 h (Figure 14). Evo 14 reached an OD_{600} of 4.80 ± 0.30, which translates to a biomass formation of 1.69 ± 0.10 gCDW/l from ribose and methanol, whereas the WT strain reached OD_{600} of 4.63 ± 0.31 (1.63 ± 0.01 gCDW/l). No significant difference in biomass between Evo 14 and the WT was observed, revealing that ALE did not result in extra biomass formation of Evo 14 solely from methanol (Figure 14). Nevertheless, ALE improved methanol-dependent growth, leading to full complementation of Δ*rpe* through methanol utilization in *C. glutamicum* strain Evo 14.
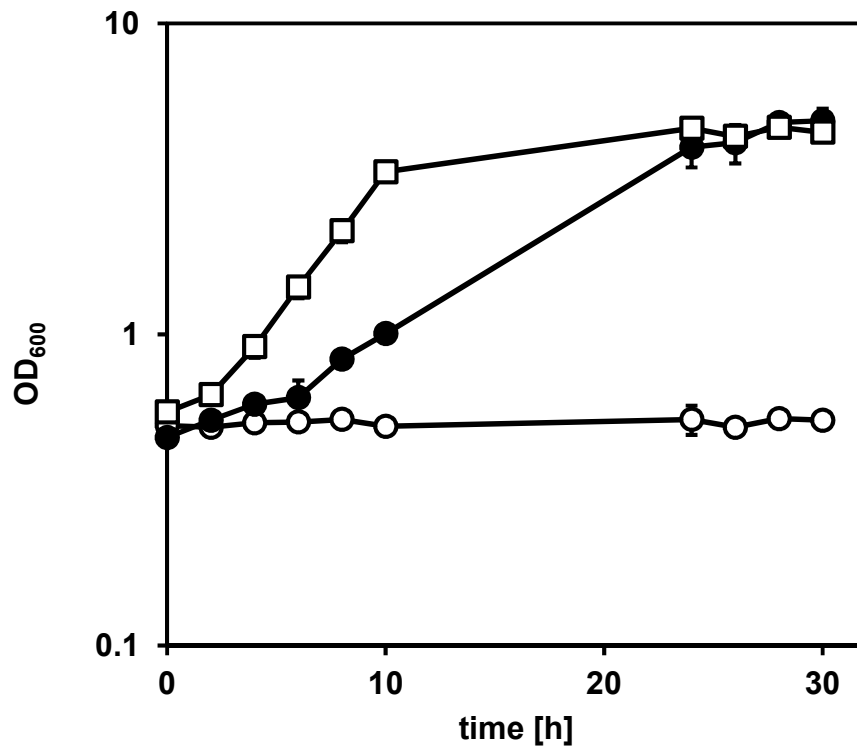
Figure 14: Methanol-dependent growth of Evo 14, in comparison to *C. glutamicum* WT with ribose.

Strains *C. glutamicum* Evo 14 (circles) and *C. glutamicum* WT (squares) were cultivated in shake flasks containing CG XII minimal medium with either 20 mM ribose as sole carbon source (open symbols) or 20 mM ribose and 500 mM methanol (closed symbols). Cultures were inoculated to a starting OD_{600} of 0.5. Error bars depict standard deviations from biological triplicates.

3.4 Sequencing and variant calling of evolved methanol-dependent *C. glutamicum* strains

3.4.1 Unique mutations revealed in evolved *C. glutamicum* strains

Whole genome sequencing followed by variant calling of *C. glutamicum* strains Evo 8 and Evo 14, and comparison to the parental Evo 1 strain, revealed unique mutations that emerged during ALE (Table 4). All mutations listed in Table 4 were present in both evolved strains.

Table 4: Unique mutations found for *C. glutamicum* strains Evo 8 and Evo 14 in comparison to Evo 1.

Gene	Mutation	Effect
cg3104	15 bp deletion	Partial deletion of CDS
metK (cg1806)	Single base exchange C → T at position 863	Amino acid substitution S288N
res (cg1929)	Single base exchange G → A at position 272	Amino acid substitution R91H
SNP_*dxs-rnd*	Single base exchange C → T in intergenic region between *dxs* (cg2081) and *rnd* (cg2083)	unknown

In cg3104, a gene that is annotated to encode an "ATPase involved in DNA repair" (Kalinowski et al., 2003), a 15 bp deletion was found (Table 4), deleting amino acids 1061 – 1065 in the translated protein and introducing a frame shift for the remaining amino acid sequence (1066 – 1111). Since the gene and its product have not been characterized yet, the impact of the partial deletion of the coding sequence on the functionality of the protein remains unknown.

The *metK* gene encoding S-adenosylmethionine synthetase (cg1806) in *C. glutamicum* (Grossmann et al., 2000), revealed to have a single base exchange at position 863 (C to T), leading to an amino acid substitution from serine to asparagine at position 288 (S288N) in the translated protein (Table 4). According to the universal protein database (UniProt Consortium, 2018), the amino acid exchange discovered in Evo 8 and Evo 14 was located right next to the enzyme's methionine binding lysine residue at position 289 (https://www.uniprot.org/uniprot/Q9K5E4).

Another single base exchange was discovered in the gene sequence of *res* (cg1929), coding for a site-specific recombinase, located in the prophage region CGP3 of the *C. glutamicum* genome (Frunzke et al., 2008a; Kalinowski et al., 2003). A single base exchange of guanine to adenine at position 272 in the gene resulted in a change of amino acid at position 91 from arginine to histidine (R91H)(Table 4). The *res* gene product in *C. glutamicum* has not been further characterized.

The last unique SNP was discovered in the intergenic region of *rnd* (cg2081), coding for ribonuclease D and *dxs* (cg2083), encoding 1-deoxyxylulose-5-phosphate synthase (Heider et al., 2014; Kalinowski et al., 2003). 20 base pairs downstream of the *dxs* gene, cytosine was exchanged with thymine in the evolved strains (Table 4).

Since the SNP_*dxs-rnd* mutation occurred in an intergenic region and the mutated *res* gene is part of the prophage CGP3 in the *C. glutamicum* genome, both mutations were not further investigated.

3.4.2 Impact of transposon insertion into *rpe*-deletion locus in Evo 14

In addition to the mutations listed in Table 4, an insertion sequence integration was detected in the remains of the deleted *rpe*-locus of *C. glutamicum* strain Evo 14. Figure 15 shows a comparison of gene arrangements surrounding the *rpe* gene of Evo 1 and Evo 14 to further illustrate the transposon integration site.
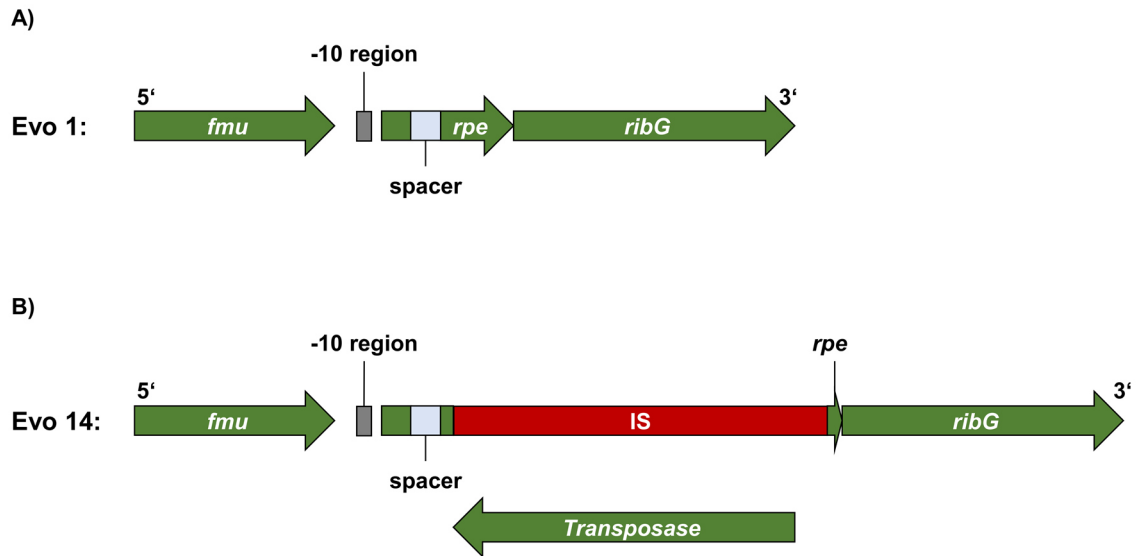
Figure 15: Schematic overview of the genomic organisation of *rpe* and *ribG* genes in methanol-dependent *C. glutamicum* strains Evo 1 and Evo 14.

A) Gene arrangements up- and downstream of *rpe* (ribulose-5-phosphate epimerase), after *rpe* deletion in *C. glutamicum* Δ*ald* Δ*fadH* Δ*rpe* (pEKEx3-*mdh-hxlAB*) (Evo 1). Depicted are coding regions of *fmu* (putative 16s rRNA methyltransferase) and *ribG* (putative bifunctional riboflavin-specific deaminase/reductase) (green), remaining base pairs of *rpe* (green), an artificial spacer sequence for crossover PCR integrated into the *rpe* locus (blue) and the promoter region (-10 region) shared by *rpe* and *ribG* (grey). B) Gene arrangements up- and downstream of *rpe* in Evo 14, after adaptive laboratory evolution. Integration of an insertion sequence (IS) into the *rpe* locus is shown in red, containing a coding region for a transposase (green).

During *rpe* deletion in *C. glutamicum* Δ*ald* Δ*fadH*, the first 18 and last 36 bp of the gene sequence remained untouched and were separated by an artificial spacer sequence that was built in for crossover PCR (Eggeling and Bott, 2004; Link and Phillips, 1997), when the pK19*mobsacB*-Δ*rpe* deletion vector was constructed prior to this work (Lennart Leßmeier, personal communication).

Genome sequencing of Evo 14 revealed a 1.461 bp insertion at bp position 654 of the WT *rpe*-gene, within the remaining *rpe* base pairs downstream of the artificial spacer sequence after *rpe*-deletion (Figure 15B). BLAST analysis (Altschul et al., 1990) showed that the sequence has been a transposable element/insertion sequence (IS), including a gene encoding a transposase for re-localization in the *C. glutamicum* genome (Mahillon and Chandler, 1998). The IS found between *rpe* (cg1801) and *ribG* (cg1800) in Evo 14 can be found at two other distinct locations in the *C. glutamicum* WT genome. First, between the genes cg1212 (coding for a permease) and cg1214 (coding for cysteine sulfinate desulfinase) and second between the genes cg2724 (coding for a conserved hypothetical protein) and cg2726 (coding for a putative membrane protein) (Altschul et al., 1990; Kalinowski et al., 2003). Those insertion sequences were still present in Evo 14, making the revealed insertion between *rpe* and *ribG* a unique third copy of the IS in the evolved strain.

The genes *rpe* and *ribG* are part of a bigger operon structure that further includes the genes *ribC*, *ribA* and *ribH* downstream of *ribG* (Pfeifer-Sancar et al., 2013). Analysis of the IS integration site and the downstream *ribG* gene uncovered features that might have had an impact on *ribGCAH* expression in *C. glutamicum* Evo 14 (Figure 16).
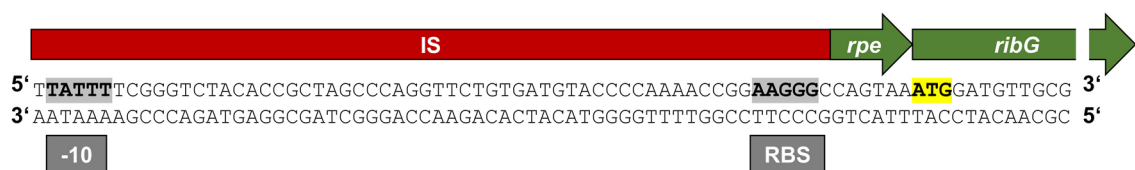
Figure 16: Alternative promoter and ribosome binding site for *ribG* transcription, provided by an insertion sequence in *C. glutamicum* strain Evo 14.

Segments of the nucleotide sequences of *ribG* (green), *rpe* (green) and the insertion sequence (IS) (red) are depicted. Motifs within the IS for a -10 region (TATTTT) and an RBS (AAGGG) shown in grey. The ATG start codon of *ribG* (yellow) is additionally highlighted.

According to a previously published transcriptome analysis of *C. glutamicum* (Pfeifer-Sancar et al., 2013), the IS provided an alternative -10 region (TATTTT), as well as ribosome binding site (AAGGG) 7 bp upstream of the *ribG* start-codon close to -10 region (TAxxxT) and RBS (xAGGA) consensus sequences. In the WT strain, *rpe* and *ribG* share the same promoter region (Figure 15A), being transcribed leaderless, without detectable ribosome binding site (Albersmeier et al., 2017; Pfeifer-Sancar et al., 2013). Alternative transcription of *ribGCAH* might have caused improved growth of strain Evo 14, in comparison to Evo 1.

3.5 Investigation of revealed mutations in evolved *C. glutamicum* strains

3.5.1 Impact of insertion sequence on riboflavin metabolism in *C. glutamicum* strain Evo 14

To further examine the impact of the IS integration in *C. glutamicum* strain Evo 14 on metabolism and growth, strains Evo 1, Evo 8 and Evo 14 were cultivated in minimal medium with 20 mM glucose as sole carbon source, with and without supplementation of 20 µM riboflavin.

C. glutamicum Evo 1 surprisingly exhibited weak growth on glucose after 52 h of cultivation. However, with riboflavin supplemented to the medium, growth could be restored, despite a lag-phase of 16 h (Figure 17A). Growth of the Evo 8 strain without riboflavin was also hampered and exponential growth was restored by riboflavin supplementation (Figure 17B).

Addition of riboflavin resulted in no difference concerning final biomass formation of the Evo 14 strain (Figure 17C). However, the specific growth rate was significantly increased when riboflavin was provided (μ = 0.12 ± 0.00 h^{-1}), in comparison to no riboflavin in the medium (μ= 0.09 ± 0.01 h^{-1}). Based on these results, following growth experiments with *C. glutamicum* Evo 1 in CG XII minimal medium were carried out with supplementation of 20 µM riboflavin.
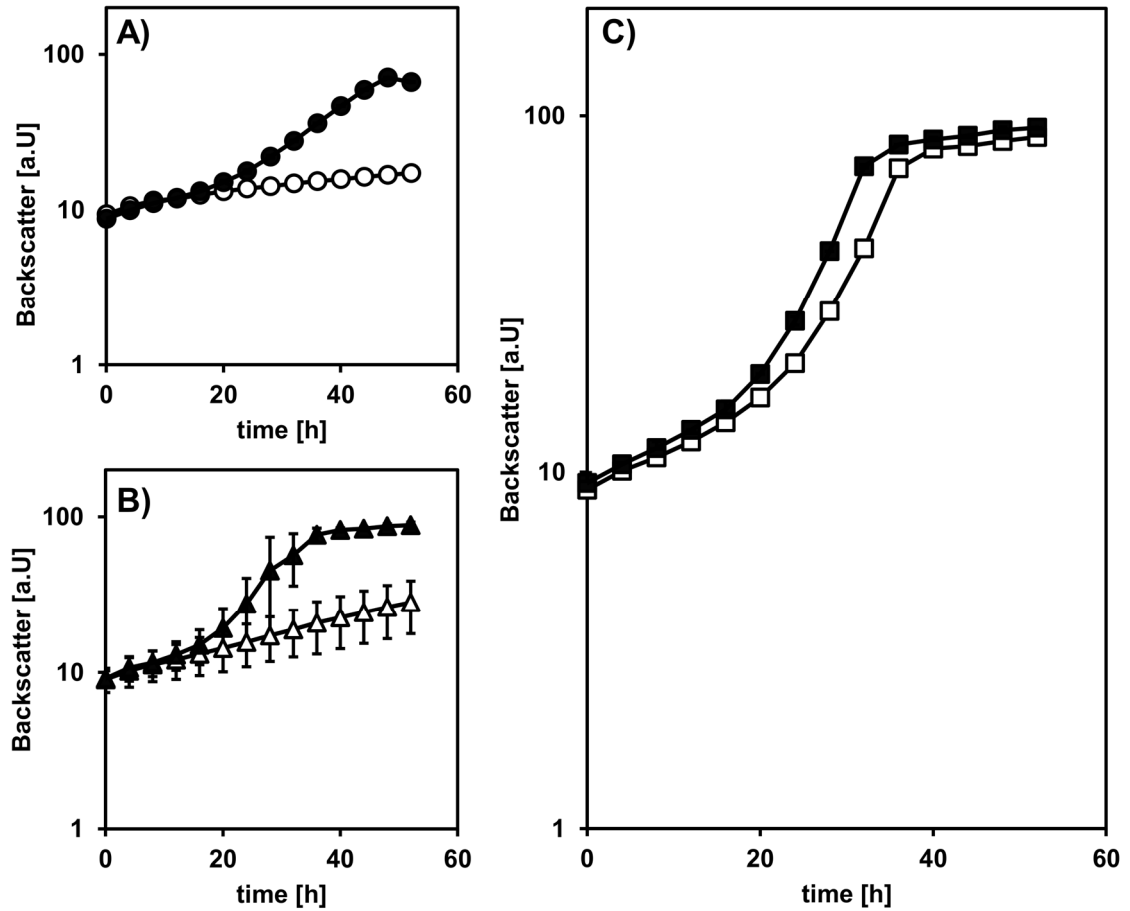
Figure 17: Growth of *C. glutamicum* strains Evo 1, Evo 8 and Evo 14 on glucose, with and without riboflavin supplementation.

A) *C. glutamicum Δald ΔfadH Δrpe* (pEKEx3-*mdh-hxlAB*) (Evo 1), B) *C. glutamicum* strain Evo 8, C) *C. glutamicum* strain Evo 14 were cultivated using the BioLector in FlowerPlates with 1 ml filling volume of CG XII minimal medium with 20 mM glucose as sole carbon source (open symbols) or supplemented with 20 µM riboflavin (closed symbols). Backscatter was detected in BioLector with a gain of 20. Error bars depict standard deviations from biological triplicates.

3.5.2 Transfer of mutations gained from ALE to first generation strain *C. glutamicum* Evo 1

In order to better understand the relevance of revealed mutations in the evolved methanol-dependent strains Evo 8 and Evo 14 (Table 4) in relation to the improved methanol-dependent growth, *C. glutamicum* strain Evo 1 was engineered accordingly.

Genomic deletion of cg3104 was performed, as well as introduction of the *metK*_S288N point mutation, to mimic the genetic condition of the evolved strains. Modifications were first introduced separately (Figure 18A and B), before combination of both mutations in the single strain *C. glutamicum* Evo 1 Δcg3104 *metK*_S288N (Figure 18C). All strains were examined for methanol-dependent growth with ribose to reveal which mutation had the most significant influence on the increased biomass formation from ribose and methanol gained through ALE.

Growth of Evo 1 *metK*_S288N and Evo 1 Δcg3104, compared to the not modified Evo 1 strain are depicted in Figure 18A and B, respectively.

In both cases, modification of a single gene did not result in a significant change of growth rate or final biomass formation of Evo 1 with ribose and methanol. However, the addition of riboflavin to the medium led to an overall higher biomass formation of Evo 1 compared to previous cultivations. Whereas 0.66 ± 0.02 gCDW/l had been the maximum biomass formation previously reached (Figure 8), Evo 1 reached 0.91 ± 0.15 gCDW/l (OD_{600}: 2.59 ± 0.42) with riboflavin supplementation in these experiments (Figure 18A and B).

Combining both mutations, Δcg3104 and *metK*_S288N, in one strain led to an increase in biomass formation (Figure 18C). The growth rate was doubled from 0.04 ± 0.00 h^{-1} of the unmodified Evo 1 parental strain to 0.08 ± 0.00 h^{-1} and the final OD_{600} reached after 30 h of cultivation (4.65 ± 0.48, corresponding to a biomass of 1.64 ± 0.17 gCDW/l), was in range of the previously measured biomass formation of Evo 14 (1.69 ± 0.10 gCDW/l)(Figure 14).
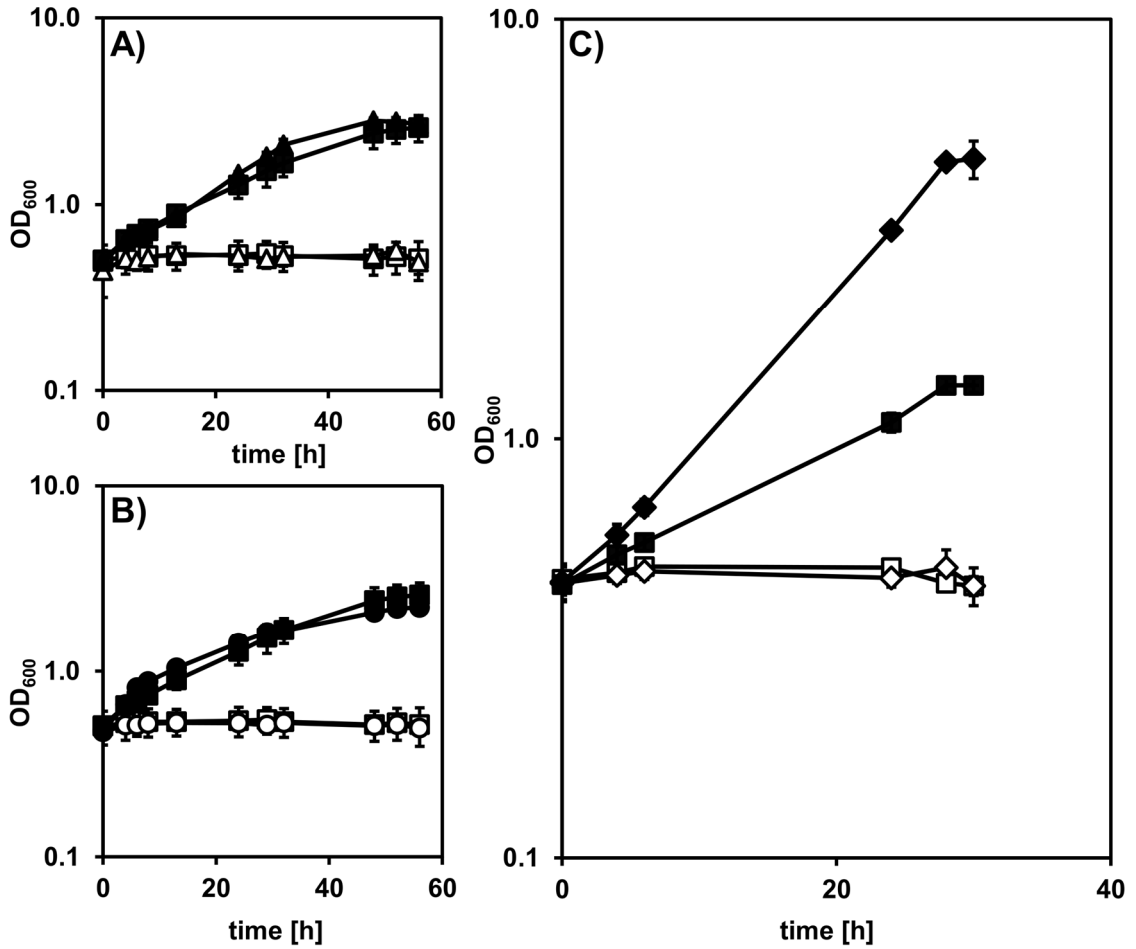
Figure 18: Methanol-dependent growth of *C. glutamicum* Evo 1 strains after transfer of ALE mutations.

C. glutamicum Δald ΔfadH Δrpe (pEKEx3-mdh-hxlAB) (Evo 1) (squares) and A) Evo 1 metK_S288N (triangles), B) Evo 1 Δcg3104 (circles), C) Evo 1 Δcg3104 metK_S288N (diamonds) were cultivated in shake flasks containing CG XII minimal medium with 20 mM ribose as sole carbon source (open symbols) or with 20 mM ribose and 500 mM methanol (closed symbols). All cultures were supplemented with 20 µM riboflavin. Cultures were inoculated to a starting OD_{600} of 0.5. Error bars depict standard deviations from biological triplicates.

3.5.3 The cg3104 gene and its influence on HxlAB activity and pEKEx3-*mdh-hxlAB* plasmid copy number

The cg3104 gene product was annotated as ATPase involved in DNA repair in *C. glutamicum* (Chapter 3.4.1) and ATPases are known to be involved in plasmid segregation in bacteria (Friehs, 2012; Kiekebusch and Thanbichler, 2014). Therefore, plasmid copy numbers (PCN) of pEKEx3-*mdh-hxlAB* were determined in *C. glutamicum* strains Evo 1, Evo 14 and Evo 1 Δcg3104.

Figure 19 shows the calculated relative PCN after qPCR using genomic and plasmid DNA of *C. glutamicum* strains Evo 14 and Evo 1 Δcg3104 as template, in comparison to the parental strain Evo 1 without modification. No significant difference between Evo 14 and Evo 1 Δcg3104 was detected (Figure 19). However, both strains showed a significantly increased relative PCN of approximately 60% compared to Evo 1 (Figure 19).
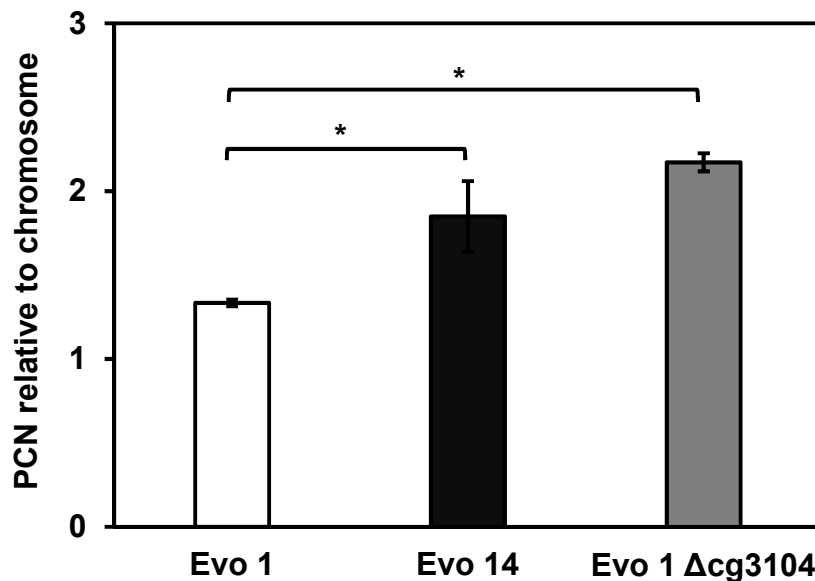
Figure 19: Calculated relative plasmid copy number of *C. glutamicum* strains Evo 1, Evo 14 and Evo 1 Δcg3104.

Quantitative PCR (qPCR) was performed on isolated genomic and plasmid DNA from overnight cultures of *C. glutamicum* Δ*ald* Δ*fadH* Δ*rpe* (pEKEx3-*mdh-hxlAB*) (Evo 1) (white), Evo 14 (black) and Evo 1 Δcg3104 (grey). Relative plasmid copy number (PCN) was calculated as previously described (Škulj et al., 2008), using serial dilutions from 100 to 0.1 ng/µl as standard curve for the chromosomal (*gntK*) and plasmid (oriV$_{Cg}$) targets. Error bars depict standard deviations of technical triplicates. Statistical significance was determined by students t-test analysis and is indicated (*) for $p \leq 0.05$.

In order to find out if increased PCN of pEKEx3-*mdh-hxlAB* by cg3104 deletion in strains Evo 1 and Evo 14 also resulted in higher activity of heterologously expressed enzymes, an enzymatic assay for combined HxlAB activities was performed (Figure 20). Comparison of activities from *C. glutamicum* strains Evo 1, Evo 14 and Evo 1 Δcg3104, revealed that both, Evo 14 and Evo 1 Δcg3104, exhibited around 60% higher HxlAB activity than the parental strain Evo 1 (Figure 20).

While HxlAB activity measured for Evo 1 (169 ± 22 mU/mg) was in the range of the previous experiment using pEKEx3 for *hxlAB* expression (197 ± 18 mU/mg) (Figure 7), activities of Evo 14 (268 ± 21 mU/mg) and Evo 1 Δcg3104 (268 ± 26 mU/mg) were significantly increased ($p < 0.05$) (Figure 20).
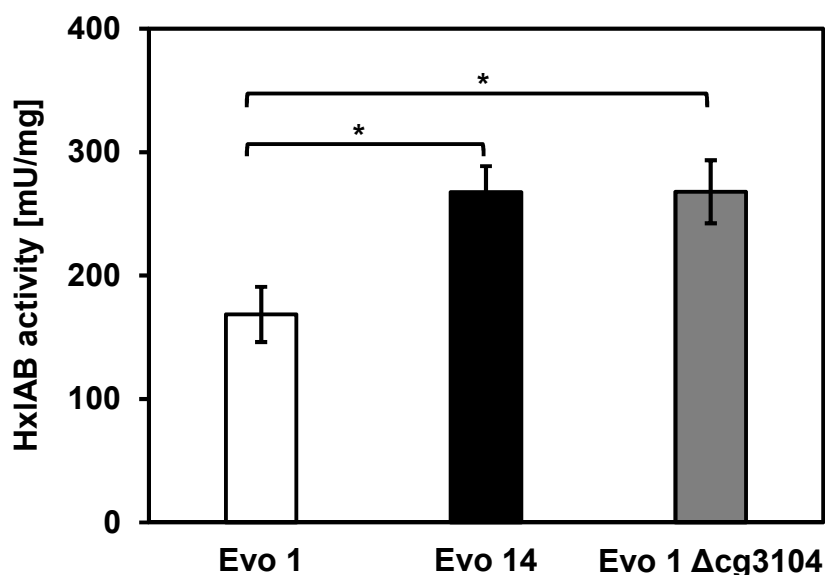
Figure 20: Combined enzymatic activity of HxlAB from *C. glutamicum* strains Evo 1, Evo 14 and Evo 1 Δcg3104.

Coupled specific activities (mU/mg) of HxlAB were determined from crude extracts of overnight cultures of *C. glutamicum* Δ*ald* Δ*fadH* Δ*rpe* (pEKEx3-*mdh-hxlAB*) (Evo 1) (white), Evo 14 (black) and Evo 1 Δcg3104 (grey). Error bars depict standard deviations of technical triplicates. Statistical significance was determined by students t-test analysis and is indicated by * for $p \leq 0.05$.

Deletion of cg3104 correlated with increased PCN in *C. glutamicum* Evo 1 (Figure 19) resulting in increased activity of heterologously expressed HxlAB, as observed in Evo 14 (Figure 20). Therefore, disruption of cg3104 influenced the PCN and expression of methanol utilizing enzymes during ALE, improving methanol-dependent growth of Evo 8 and Evo 14 (Figure 12).

3.5.4 The influence of *metK* and *metY* on methanol-dependent growth in *C. glutamicum.*

Since the deletion of cg3104 and the resulting increased HxlAB activity was not sufficient to elevate methanol-dependent growth of *C. glutamicum* Evo 1 (Figure **18**A), further investigation of the *metK* gene mutation was necessary to understand how a combination of Δcg3104 and *metK*_S288N improved methanol-dependent growth of *C. glutamicum* strains Evo 8 and Evo 14 (Figure **18**C).

In addition to the transfer of variant calling detected mutations to the first generation strain Evo 1 (Chapter 3.5.2), it was investigated whether a reversion of the *metK* mutation in Evo 14, from S288N to the WT sequence N288S, had an impact on methanol-dependent growth with ribose. Methanol-dependent growth of the Evo 14 *metK*_N288S reversion mutant strain in comparison to unchanged Evo 14 is depicted in Figure 21.

The Evo 14 *metK*_N288S reversion mutant strain exhibited less biomass formation on ribose and methanol compared to the not engineered *metK*_S288N strain (Figure 21). The final OD_{600} after 32 h dropped from 4.07 ± 0.24 to 1.21 ± 0.08, when *metK* in Evo 14 was reversed to the WT sequence, corresponding to a 70% reduction of biomass from 1.44 ± 0.08 to 0.43 ± 0.03 gCDW/l. *C. glutamicum* Evo 14 with WT *metK* sequence only reached growth levels on ribose and methanol comparable to those previously observed in Evo 1 (0.32 - 0.66 gCDW/l)(Figure 8 and Figure 12), despite mutations in cg3104 and the transposon integration at the *rpe* locus being present. This demonstrated that *metK* played a significant role in the improvement of methanol-dependent biomass formation, yet the function remained unknown.
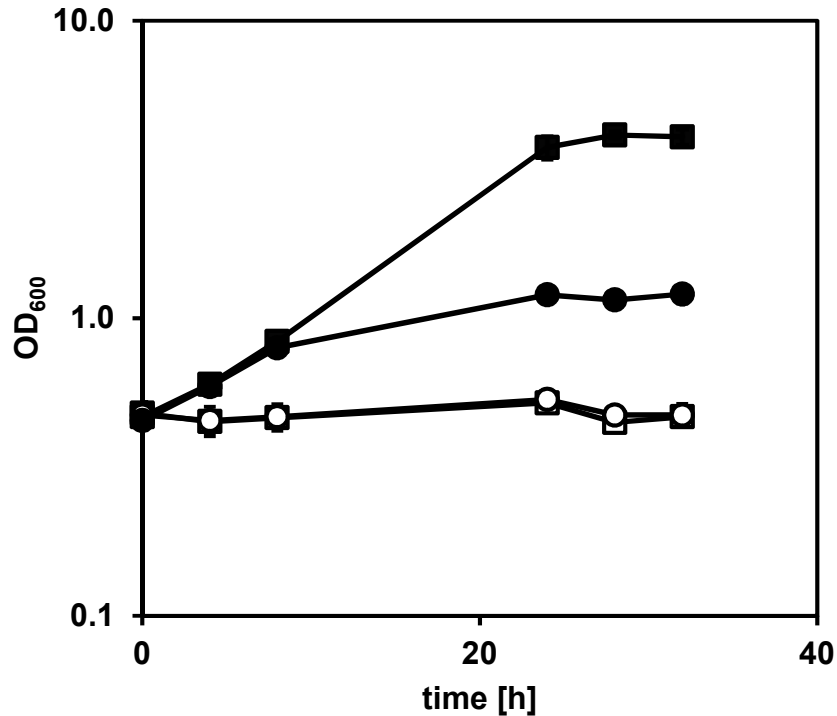
Figure 21: Influence of *metK* reversion to WT sequence on methanol-dependent growth of *C. glutamicum* strain Evo 14.

C. glutamicum Evo 14 (squares) and Evo 14 *metK*_N288S (circles) were cultivated in shake flasks containing CG XII minimal medium with 20 mM ribose as sole carbon source (open symbols) or with 20 mM ribose and 500 mM methanol (closed symbols). Cultures were inoculated to a starting OD_{600} of 0.5. Error bars depict standard deviations of biological triplicates.

It has already been reported that O-acetyl-homoserine sulfhydrolase (MetY) of *Corynebacterium acetophilum* catalyzes a side reaction with methanol that yields O-methyl-homoserine (OMH) (Murooka et al., 1977). OMH is structurally close to L-methionine (Grob et al., 2017), the natural substrate of MetK (Grossmann et al., 2000), but is also reported to inhibit the growth of various bacterial species (Roblin et al., 1945). Furthermore, a mutation in the *metY* gene, leading to amino acid substitution A165T, was previously shown to increase methanol tolerance of *C. glutamicum* WT (Leßmeier and Wendisch, 2015). To clarify whether MetY had

an influence on MetK and inhibited methanol-dependent growth, the *metY* gene was deleted in Evo 1 Δcg3104.

The resulting strain *C. glutamicum* Evo 1 cg3104 Δ*metY* was cultivated in CG XII minimal medium with 20 mM ribose and 500 mM methanol in comparison to Evo 14 (Figure 22).
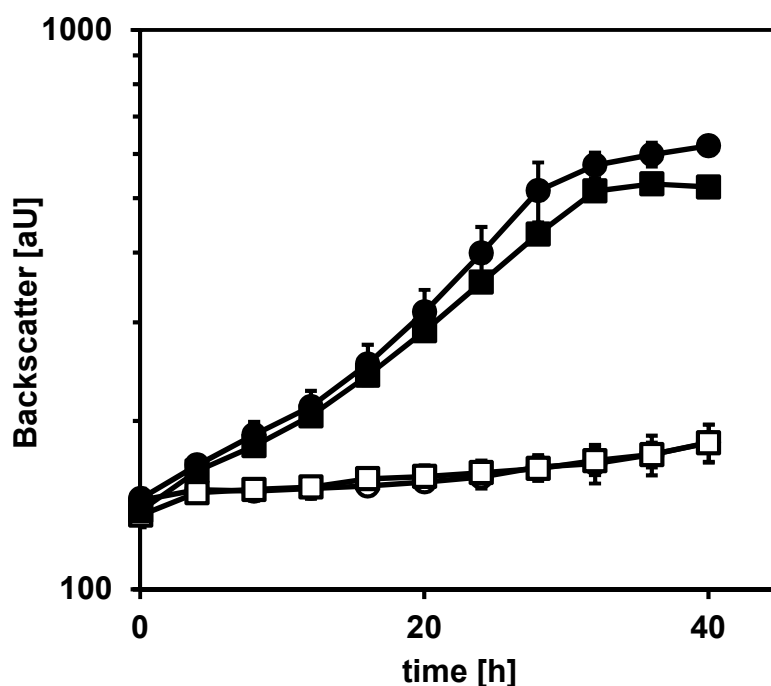
Figure 22: Methanol-dependent growth of *C. glutamicum* strain Evo 1 Δcg3104 Δ*metY* compared to strain Evo 14. *C. glutamicum* Δ*ald* Δ*fadH* Δ*rpe* (pEKEx3-*mdh-hxlAB*) (Evo 1) Δ*cg3104* Δ*metY* (circles) and Evo 14 (squares) were cultivated using the BioLector in FlowerPlates with 1 ml filling volume of CG XII minimal medium with 20 mM ribose as sole carbon source (open symbols) or with 20 mM ribose and 500 mM methanol (closed symbols). All cultures were supplemented with 20 µM riboflavin Error bars depict standard deviations of biological triplicates.

Despite the *metK* gene not being changed in Evo 1 Δcg3104 Δ*metY*, the strain showed equal growth to Evo 14 with ribose and methanol (Figure 22). This could previously only be achieved with Evo 1 Δcg3104 *metK*_S288N (Figure 18C) showing that *metY* deletion and *metK*_S288N mutation have the same effect on methanol-dependent growth of *C. glutamicum.* Therefore, both encoded enzymes significantly affect methanol-dependent biomass formation of *C. glutamicum* and presumably act on each other, when methanol is present.

3.6 Alternative approach towards methanol-dependency: Deletion of ribose-5-phosphate isomerase (*rpi*)

An alternative approach to create a methanol dependency through a metabolic cut-off was the deletion of the *rpi* gene, encoding ribose-5-phosphate isomerase, in *C. glutamicum Δald ΔfadH*, in combination with the supply of xylose or gluconate as alternative methanol co-substrates to ribose. This approach followed the same concept of disrupting the PPP by removal of a Ru5-P utilizing reaction (ribose-5-phosphate ↔ ribulose-5-phosphate), as it was successfully applied for *rpe* deletion before in the present study (Chapter 3.1.3). To allow xylose utilization, a previously established pathway was introduced through pEKEx3-*xylAB* for plasmid-based heterologous expression (Meiswinkel et al., 2013). Additionally, the strain was transformed with pVWEx1-*mdh-hxlAB* for heterologous expression of the methanol utilization pathway used before in this study.

In addition to xylose, gluconate was tested as alternative co-substrate for methanol-dependent growth of *C. glutamicum.* Gluconate gets metabolized through Ru5-P in the PPP of *C. glutamicum* (Blombach and Seibold, 2010) and was therefore hypothesized to be suitable co-substrate to couple growth and methanol utilization.

The resulting strain *C. glutamicum Δald ΔfadH Δrpi* (pEKEx3-*xylAB*) (pVWEx1-*mdh-hxlAB*) was neither able to grow on xylose nor gluconate as sole carbon source (Figure 23).

However, with methanol present in the medium, the strain exhibited growth on xylose with a growth rate of $\mu = 0.02 \pm 0.00$ h^{-1}, reaching 0.42 ± 0.11 gCDW/l (OD$_{600}$: 1.18 ± 0.16) after 48 h of cultivation (Figure 23A). Growth rate and final biomass formation with xylose and methanol were slightly decreased compared to previous experiments with the *C. glutamicum rpe* deletion strain growing with ribose and methanol ($\mu = 0.03 \pm 0.00$; 0.66 ± 0.03 gCDW/l) (Figure 8).

Nevertheless, it was possible to transfer the approach of methanol dependency towards the application xylose as alternative carbon source.

With gluconate as co-substrate to methanol (Figure 23B), the specific growth rate (μ= 0.03 ± 0.00 h^{-1}) was on par with previous experiments carried out with its Δ*rpe* counterpart (μ = 0.03 ± 0.00 h^{-1})(Figure 8), while final biomass formation with gluconate and methanol was slightly decreased (OD$_{600}$: 1.67 ± 0.01, corresponding to 0.59 ± 0.00 gCDW/l) compared to previous experiments with ribose (0.66 ± 0.03 gCDW/l)(Figure 8).

The concept of methanol dependency was successfully transferred to the deletion of *rpi* as alternative target gene for the creation of a metabolic cut-off and the application of the two alternative carbon sources xylose and gluconate for methanol-dependent growth in *C. glutamicum* (Figure 8). Therefore, methanol-dependent growth of *C. glutamicum* on three different carbon sources was reported in this study for the first time.
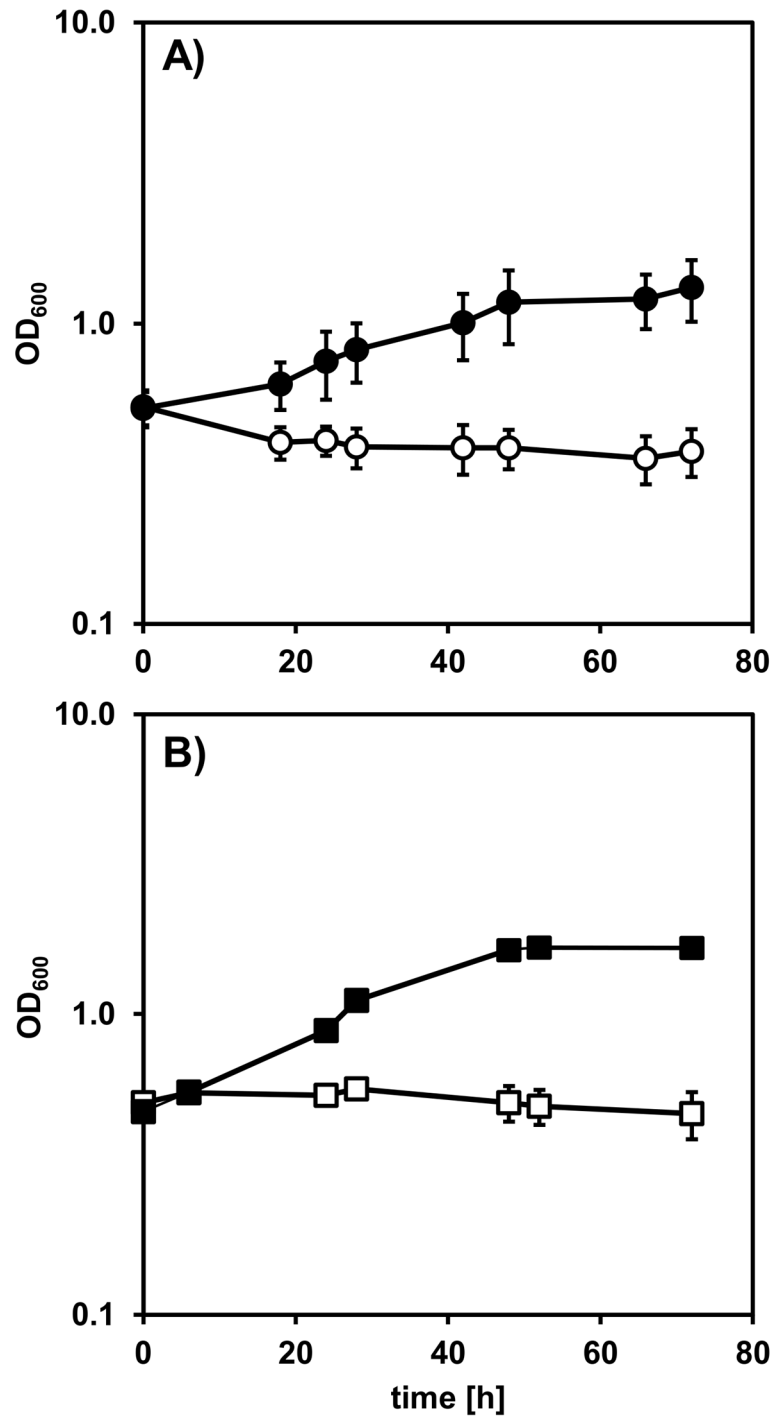
Figure 23: Methanol-dependent growth of an engineered *C. glutamicum* strain on xylose or gluconate after *rpi* deletion*.

C. glutamicum Δ*ald* Δ*fadH* Δ*rpi* (pEKEx3-*xylAB*) (pVWEx1-*mdh-hxlAB*) was cultivated in shake flasks containing CG XII minimal medium with A) 20 mM xylose as sole carbon source (open circles) or 20 mM xylose and 500 mM methanol (closed circles). B) 20 mM gluconate as sole carbon source (open squares) or 20 mM gluconate and 500 mM methanol (closed squares). Cultures were inoculated to a starting OD_{600} of 0.5. Error bars depict standard deviations of biological triplicates.

3.7 Methanol-dependent cadaverine production

3.7.1 Labelling of the non-natural product cadaverine from ^{13}C-methanol

In parallel with ALE (Figure 11), carbon labelling of the non-natural product cadaverine from ^{13}C-methanol was investigated, as in Leßmeier et al., 2015. At the time of experiment execution, *C. glutamicum* Evo 8 had been the most evolved methanol-dependent strain and was therefore chosen to be engineered for cadaverine production. To facilitate cadaverine production with Evo 8, the vector pECXT99A-*lysC-ldcC* was used for expression of endogenous, feedback resistant aspartokinase (*lysC*^{T311I}) (Kalinowski et al., 1991) and lysine decarboxylase (*ldcC*) from *E. coli* (Kind and Wittmann, 2011). Gluconate was chosen as secondary substrate to methanol, for provision of additional NADPH, benefitting the production of L-lysine (Lee and Lebeault, 1998), the direct precursor of cadaverine.

Previous work without methanol dependency reported production of up to 15 mM cadaverine from ribose in presence of methanol (Leßmeier et al., 2015). Here, Evo 8 was only capable to produce a fraction of the previously reported titer (1.5 mM)., dependent on methanol supplementation

Carbon labelling was revealed to be most prominent at carbon positions C2 and C4 in cadaverine with approximately 34% of molecules labelled (Figure 24). Approximately half as much ^{13}C enrichment could be observed at carbon position C3 (16%), whereas only 10% of carbons one or five were labelled. Previous work reported that labelling at the C1/C5 or C2/C4 positions indicate utilization of methanol through RuMP pathway reactions, whereas C3 labelled cadaverine results from anaplerotic carboxylation reactions fixing ^{13}CO$_2$ (Leßmeier et al., 2015). Therefore, Evo 8 was able to produce cadaverine dependent on methanol, using RuMP pathway reactions but also through ^{13}CO$_2$ fixation which has not been reported before.
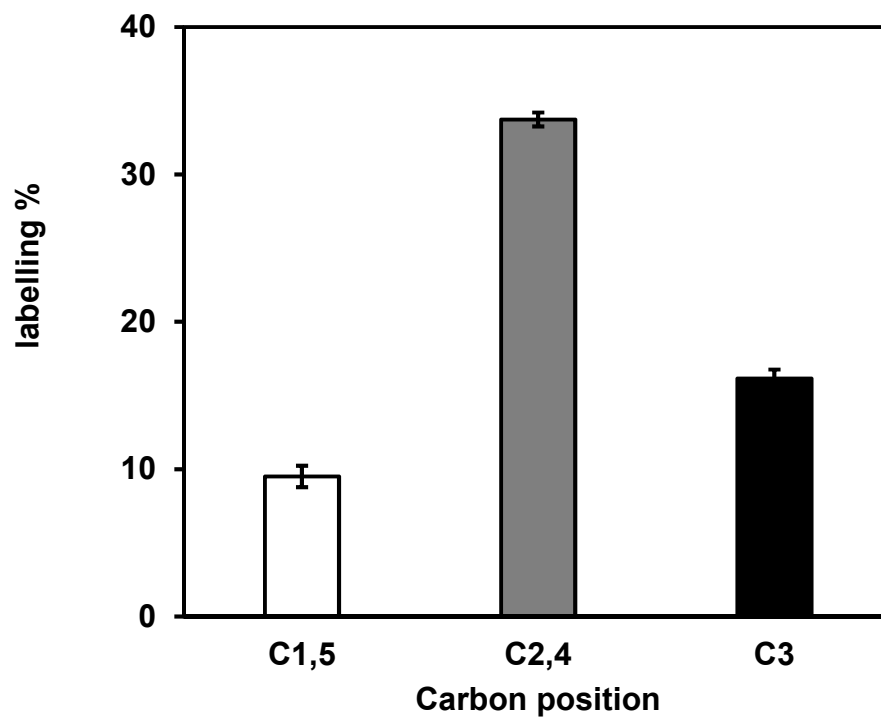
Figure 24: Labelled carbon positions in cadaverine from ¹³C- methanol in *C. glutamicum* strain Evo 8.

Cadaverine was produced by *C. glutamicum* Evo 8 (pECXT99A-*lysC*-*ldcC*) in shake flasks containing M9 minimal medium with 20 mM gluconate, 0.5 g/l yeast extract and 500 mM ¹³C-methanol for 72 h. Mean ¹³C enrichment in cadaverine was determined at carbon positions C1,C5 (white), C2,C4 (grey) and C3 (black). Error bars depict standard deviations of samples from biological triplicates.

4. <u>Discussion and Outlook</u>

4.1 Biotechnological potential of methanol using natural and synthetic methylotrophs

The present study attempted to establish synthetic methylotrophy in *C. glutamicum* through the artificial creation of a methanol dependency and subsequent ALE for improved methanol-dependent growth. Analysis of the gathered mutations in evolved strains that exhibited increased methanol-dependent biomass formation will elevate the existing knowledge of synthetic methylotrophy and lead a step closer to the first full synthetic methylotroph organism.

In Chapter 1.1, the potential of methanol as alternative carbon source in biotechnological processes was introduced. The methanol market price of 0.45 $/kg, which translates to 1.2 $/kg carbon substrate (Bertau et al., 2014; Ochsner et al., 2014b) is currently still higher compared to sugar (0.28 $/kg corresponding to 0.66 $/kg carbon substrate) (Macrotrends.net, 2019). However, sugar prices have shown significant price fluctuations in the past, ranging from 0.06 $/kg in 1960 up to 0.44$/kg in 2017 (Maitah and Smutka, 2019). In contrast, the price of methanol is expected to decrease steadily in the future, due to the construction of mega-methanol production facilities (Schrader et al., 2009) and the development of cheaper and more efficient methanol production technologies (Goeppert et al., 2018; Olah, 2013). Furthermore, methanol contains 50% more electrons per carbon as commonly used glucose, which makes it an appealing substrate for the production of reduced products, such as other alcohols and fatty- /carboxylic acids, or to enhance yields of products when fed as a co-substrate (Whitaker et al., 2015).

Methanol also has some significant advantages over the other industrially interesting C1 carbon sources methane (CH_4), formate (CH_2O_2) or CO_2. Although the gaseous methane (24.3 MJ/kg) has a higher energy density than methanol (22.7 MJ/kg) (Bertau et al., 2010), the volumetric energy density of methanol

remains favourable because of its liquid state of aggregation at room temperature (Bertau et al., 2014), which also makes methanol easier to store and cheaper to transport then methane (Bertau et al., 2014; Räuchle et al., 2016). The liquid state and high solubility of methanol in water (Bertau et al., 2014; Schendel et al., 1990) further makes it easier to handle in bacterial fermentations than gaseous substrates (CH_4, CO_2) (Linton and Niekus, 1987). In comparison to formate (6.2 MJ/kg), methanol has a higher energy density (Bertau et al., 2010; Celaje et al., 2016) and yields more energy in form of reducing equivalents during its utilization due to of its more reduced state (Müller et al., 2015a; Whitaker et al., 2015; Witthoff et al., 2013).

Scientific interest to use natural methylotroph organisms for the production of valuable products from methanol has risen in the past years (Pfeifenschneider et al., 2017; Zhang et al., 2018a). *B. methanolicus* strains have been reported to be suitable hosts for amino acid production, secreting up to 70 g/l of L-glutamate (Brautaset et al., 2010) and 35 g/l of L-lysine (Brautaset et al., 2003) in methanol fed-batch cultivations at 50°C. Furthermore, amino acid derived products such as cadaverine (11 g/l) (Naerdal et al., 2015) or GABA (9 g/l) (Irla et al., 2017) were successfully added to the product spectrum of *B. methanolicus*. Additionally, fine chemicals, such as mevalonate (2.65 g/l) (Liang et al., 2017) or α-humulene (1.65 g/l) (Sonntag et al., 2015), as well as organic acids like mesaconic acid (0.07 g/l) or methyl-succinic acid (0.06 g/l) (Sonntag et al., 2014) were reported products of natural methylotroph *M. extorquens* strains with methanol as sole carbon source.

Although knowledge about natural methylotrophs has increased (Heggeset et al., 2012; Irla et al., 2014; Ochsner et al., 2014b) genetic tools for natural methylotroph organisms are still scarce and limit the possibilities of engineering to further increase product titers and yields (Fei et al., 2014; Irla et al., 2016). Therefore, the development of synthetic methylotroph organisms will create the opportunity to overcome those limitations and exploit the full potential of methanol as biotechnological carbon source (Whitaker et al., 2015; Zhang et al., 2018a, 2017).

Discussion and Outlook

The application of methanol as co-substrate in cultivations of heterotroph organisms engineered towards synthetic methylotrophy already revealed the potential to increase product titers and yields (Litsanov et al., 2012; Wang et al., 2019; Zhang et al., 2018b). It was demonstrated in succinic acid production with *E. coli,* that yields could be improved from 0.91 ± 0.08 g/g to 0.98 ± 0.11 g/g, through co-supply of methanol to glucose and heterologous expression of *mdh*, *hps* and *phi* from *B. methanolicus* (Zhang et al., 2018b). Recently, L-lysine titers of an *E. coli* strain expressing RuMP pathway enzymes (Mdh, Hps, Phi) from *B. methanolicus* were doubled from 0.06 g/l with glucose as sole carbon source after additional expression of peroxide sensitive NADH kinase (POS5) from *Saccharomyces cerevisiae* and methanol supplementation to glucose for an enhanced NADH supply through methanol oxidation and its conversion to NADPH by POS5 (Wang et al., 2019).

Succinate yields in anaerobic fermentations with *C. glutamicum* were improved by 20% from 1.05 ± 0.02 mol/mol to 1.26 ± 0.02 mol/mol glucose in presence of formate and additional chromosomal integration and expression of *fdh (*formate dehydrogenase) from *Mycobacterium vaccae*, due to increased availability of reducing equivalents from formate oxidation (Litsanov et al., 2012). Formate could possibly be replaced by methanol in order to yield three times as much reducing equivalents in form of NADH since two additional NAD^+ dependent oxidation steps are required for the full oxidation from methanol to CO_2 (Leßmeier et al., 2013; Witthoff et al., 2013).

Furthermore, production of the non-natural product cadaverine from ribose and ^{13}C-methanol in *C. glutamicum* Δ*ald* Δ*fadH* expressing *mdh* from *B. methanolicus* and *hxlAB* from *B. subtilis*, as well as endogenous *lysC* and *ldcC* from *E. coli*, revealed integration of methanol-derived carbon in cadaverine with a maximal titer of approximately 15 mM (Leßmeier et al., 2015).

Here, before ALE conclusion (Chapter 3.2), the methanol-dependent *C. glutamicum* strain Evo 8 was chosen for cadaverine production from gluconate and ^{13}C-methanol to investigate the labelling patterns in the non-natural product (Figure 24). Gluconate was chosen as co-substrate, as it provides additional NADPH during its metabolization, which benefits lysine production in

C. glutamicum (Lee and Lebeault, 1998), and therefore increases the precursor supply for cadaverine production. Additionally, small amounts of yeast extract (0.5 g/l) were supplemented to the medium, since it was applied in ALE and was also known to promote growth with methanol (Whitaker et al., 2017). The final cadaverine titer produced by Evo 8 with 1.5 mM (Chapter 3.7.1) was approximately ten times less than previously reported titers of a methanol-utilizing *C. glutamicum* strain (~15 mM) (Leßmeier et al., 2015). However, cadaverine concentrations produced by the methanol-dependent *C. glutamicum* strain Evo 8 (Chapter 3.7.1) were not comparable to those reported for methanol-utilizing *C. glutamicum* before (Leßmeier et al., 2015), since the metabolic cut-off in the PPP of Evo 8 made growth and production of the strain dependent on methanol utilization (Chapter 3.3), whereas the previously reported *C. glutamicum* strain was still capable of using ribose as sole carbon source for growth and production, while co-utilizing methanol as additional substrate (Leßmeier et al., 2015). Therefore, methanol-dependent production of the non-natural product cadaverine with *C. glutamicum* was achieved here for the first time (Chapter 3.7.1).

4.2 Isotopic labelling of cadaverine from ^{13}C-methanol

Isotopic labelling of cadaverine produced from *C. glutamicum* strain Evo 8 (Chapter 3.7.1) was superior to a previous study about cadaverine production of a methanol-utilizing *C. glutamicum* (Leßmeier et al., 2015). Incorporation of ^{13}C-methanol-derived carbon in the total cadaverine pool was improved 3.75-fold from 16% in previous work (Leßmeier et al., 2015) to 60% (Figure 24). Carbon positions C1/C5 (10%) and C2/C4 (34%) (Figure 24) in the cadaverine molecule were considered to be connected to the assimilation of labelled formaldehyde through RuMP pathway reactions and show more than twice as much labelling as reported in previous work (C1/C5: 5%; C2/C4: 15%) (Leßmeier et al., 2015). Additionally, labelling at position C3 (16%), connected to the fixation of $^{13}CO_2$ was surprisingly revealed, as it had not been reported before (Leßmeier et al., 2015).

Generally higher incorporation of labelled carbon from ^{13}C-methanol at all carbon positions of cadaverine can be accounted to methanol-dependent growth and production of *C. glutamicum* strain Evo 8, in contrast to growth and cadaverine production on ribose, independently from additional supplied methanol in previous work (Leßmeier et al., 2015).

Labelled $^{13}CO_2$ could only emerge through cyclic dissimilation of F6-P in the oxidative branch of the PPP (Kruger and Von Schaewen, 2003; Leßmeier et al., 2015), since the linear formaldehyde oxidation pathway was deleted in *C. glutamicum* strain Evo 8 (Δ*ald* Δ*fadH*). Emerging $^{13}CO_2$ could then be re-assimilated to oxaloacetate through pyruvate carboxylase (*pyc*) (Eikmanns, 2005; Peters-Wendisch et al., 1998) or phosphoenolpyruvate carboxylase (*ppc*) reactions (Eikmanns, 2005; Eikmanns et al., 1989). Decarboxylation in the lysine synthesis pathway (Kelle et al., 2005), as well as the decarboxylation from lysine to cadaverine (Mimitsuka et al., 2007), yield unlabelled CO_2 (Leßmeier et al., 2015). No mutations in neither the *pyc*, nor the *ppc* gene were revealed in *C. glutamicum* strain Evo 8 (Table 4), indicating that increased assimilation of labelled CO_2 (Figure 24) had physiological or regulatory reasons.

Discussion and Outlook

Expression of *ppc* in *C. glutamicum* was previously found to be upregulated by sigma factor SigB (Ehira et al., 2008) at oxygen deprivation conditions (Inui et al., 2007). It is known that higher oxygen demands are characteristic for methanol utilization in natural methylotrophs, due to the high degree of reduction of methanol (Brautaset et al., 2007; Whitaker et al., 2015). Taking this into consideration, as growth of was coupled to methanol utilization in *C. glutamicum* strain Evo 8 (Chapter 3.3), it is possible that reduced oxygen availability in the medium might have led to increased *ppc* expression, resulting in higher CO_2 fixation than previously reported for methanol-utilizing and cadaverine producing *C. glutamicum* (Leßmeier et al., 2015). A recent study investigating the concentrations of cellular enzymes in *C. glutamicum* during growth on different carbon sources reported a 2.3-fold increase of Ppc with mannose as sole carbon source in comparison to glucose (Noack et al., 2017). Mannose is taken up and simultaneously phosphorylated to mannose-6-phosphate through a phosphotransferase system and subsequently converted to F6-P before entering glycolysis (Sasaki et al., 2011). Growth and mannose utilization were revealed to be very slow in *C. glutamicum*, since leftover substrate was still present after 80 h of cultivation (Noack et al., 2017). Since formaldehyde fixation with Ru5-P through RuMP pathway reactions also leads to F6-P formation (Figure 2), mannose and formaldehyde enter glycolysis at the same level and might have the same effect on *ppc* expression in *C. glutamicum*. However, further experiments are needed to confirm increased *ppc* expression during methanol-dependent cadaverine production.

Furthermore, increased *pyc* expression or activity could have possibly led to elevated $^{13}CO_2$ incorporation into cadaverine. The cellular concentration of Pyc enzyme in *C. glutamicum* was found to be increased 5-fold by growth on lactate in comparison to glucose (Noack et al., 2017). Lactate is the main by-product of *C. glutamicum* grown on sugar substrates under oxygen deprivation (Dominguez et al., 1998). Increased *pyc* expression might have been a result of de-repression from GlxR by lactate, a cyclic AMP (cAMP) dependent, global transcriptional regulator (Kim et al., 2004; Kohl et al., 2008) that was predicted to be responsible for *pyc* and *ppc* repression in *C. glutamicum* (Baumbach et al., 2011; Jungwirth et al., 2013). Further investigation of secreted metabolites and *pyc* expression

during methanol-dependent cadaverine production of *C. glutamicum* strain Evo 8 is needed to confirm this hypothesis.

In order to better understand whether increased *ppc* or *pyc* expression, as well as expression of genes from unknown processes, were decisive for increased incorporation of $^{13}CO_2$ into cadaverine, RNA isolation of methanol-grown cells and subsequent RNA-Seq analysis should be conducted to investigate gene expression levels. Once the responsible gene is detected, a clearer picture of the regulatory network during methanol-dependent growth and cadaverine production in *C. glutamicum* can be painted.

4.3 Engineering of methanol-dependent
C. glutamicum strains and methanol-dependent growth

In order to couple growth to methanol utilization in *C. glutamicum*, it was necessary to create a metabolic cut-off in the central carbon metabolism (Chapter 3.1). Since Ru5-P is the central metabolite needed for formaldehyde fixation in the RuMP pathway of *B. methanolicus* (Brautaset et al., 2007; Müller et al., 2015a)*, rpe* was chosen as main target for deletion in *C. glutamicum* (Chapter 3.1) to engineer methanol-dependency with the co-substrate ribose (Figure 25). As major parts of the practical work in the present study were conducted, three publications about synthetic methylotrophy through methanol-dependency in *E. coli* (Chen et al., 2018; Meyer et al., 2018) and *C. glutamicum* (Tuyishime et al., 2018) were released independently.

Although attempts in *E. coli* remained unsuccessful and resulted in methanol-independent growth on ribose after 29 h (Chen et al., 2018)*,* deletion of the *rpe* gene represented a promising starting point to achieve methanol-dependent biomass formation in *C glutamicum*, as no growth without methanol was observed for 120 h (Figure 8). When Rpe is not present in cells using ribose as sole carbon source, Ru5-P can no longer be converted to Xu5-P, leading to a dead-end in the PPP (Yokota and Lindley, 2004). Therefore, growth on ribose as sole carbon source could be diminished, favoring the accumulation of Ru5-P (Figure 25). The alternative route of *rpi* deletion (Chen et al., 2018; Meyer et al., 2018; Tuyishime et al., 2018) was established in *C. glutamicum* as well (Figure 25).(Chapter 3.6) and resulted in methanol-dependent growth on xylose and gluconate (Figure 23). However, the main focus was put on establishing methanol-dependency in *C. glutamicum* through *rpe* deletion and improvement of methanol-dependent growth through ALE (Chapter 3.1 – Chapter 3.3).

Previous work in *E. coli* reported successful complementation of Δ*rpe* through xylose supplementation (Chen et al., 2018). Here, introduction of additional xylose utilization enzymes was necessary to investigate whether this could be applied to *C. glutamicum* (Chapter 3.1.1), since the organism is not capable of natural xylose utilization (Kawaguchi et al., 2006). Heterologous expression of *xylA* from *X. campestris* and overexpression of endogenous *xylB* for xylose utilization were chosen for the Δ*rpe* (Chapter 3.1.1) and Δ*rpi* (Chapter 3.6) strains as it had been established for *C. glutamicum* before (Meiswinkel et al., 2013).

Since the conversion of Ru5-P to Xu5-P was disabled in the *rpe* deletion strain, additional supply of Xu5-P by xylose supplementation and XylAB reactions should have restored growth on ribose through subsequent transketolase and transaldolase reactions (Chen et al., 2018)(Figure 25). However, it was not possible to fully complement the *rpe* deletion through xylose supplementation and additional expression of xylose utilization enzymes in *C. glutamicum* (Figure 5), possibly due to insufficient transketolase activity, resulting in accumulated pentoses that were argued to be toxic before (Chen et al., 2018). Toxicity of pentoses was presumably also a cause of reduced biomass formation at ribose concentrations exceeding 20 mM in methanol-dependent growth of *C. glutamicum* (Figure 9).
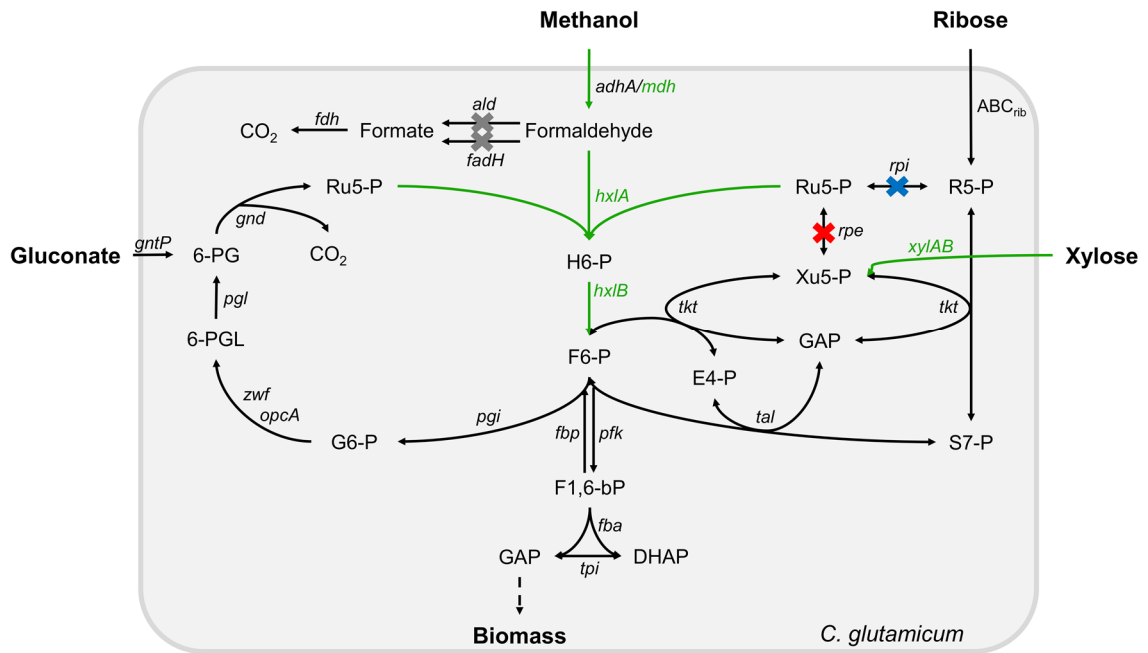
Figure 25: Overview of the central carbon metabolism in *C. glutamicum* engineered towards methanol dependency.

Synthetic pathways for methanol and xylose utilization are depicted in green and include methanol dehydrogenase (*mdh*), 3-hexulose-6-phosphate synthase (*hxlA*), 6-phospho-3-hexuloisomerase (*hxlB*), xylose isomerase (*xylA*) and xylulose kinase (*xylB*). Deletions performed prior to this work are shown in grey: aldehyde dehydrogenase (*ald*) and mycothiol dependent formaldehyde dehydrogenase. Deletions of ribulose-5-phosphate epimerase (*rpe*) (red) and ribose-5-phosphate isomerase (*rpi*) (blue) depict two distinct strategies of achieving methanol dependency. A dashed arrow indicates several reactions. Involved genes: ABC$_{rib}$ (ATP-binding cassette transporter for ribose import), *adhA* (alcohol dehydrogenase), *fdh* (formate dehydrogenase), *pfk* (phosphofructokinase), *fbp* (fructose-1,6-bisphosphatase), *tal* (transaldolase), *tkt* (transketolase), *pgi* (phosphoglucoisomerase), *zwf* and *opcA* (glucose-6-phosphate dehydrogenase), *pgl* (6-phosphoglucolactonase), *gnd* (6-phosphogluconate dehydrogenase, *fba* (fructose-1,6-bisphosphate aldolase), *tpi* (triosephosphate isomerase). Abbreviations of metabolites: H6-P (hexulose-6-phosphate), F6-P (fructose-6-phosphate), F1,6-bP (fructose-1,6-bisphosphate), GAP (glyceraldehyde-3-phosphate), DHAP (dihydroxyacetone phosphate), G6-P (glucose-6-phosphate), 6-PGL (6-phosphogluconolactone), 6-PG (6-phosphogluconate), Ru5-P (ribulose-5-phosphate), R5-P (ribose-5-phosphate), S7-P (sedoheptulose-7-phosphate), E4-P (erythrose-4-phosphate), Xu5-P (xylulose-5-phosphate).

Moreover, heterologous expression of *mdh* from *B. methanolicus*, as well as *hxlAB* from *B. subtilis* (homologues of *hps* and *phi* from *B. methanolicus*) introduced a new route for Ru5-P metabolization through methanol oxidation and fixation of formaldehyde to H6-P and subsequent isomerization to F6-P (Leßmeier et al., 2015; Yasueda et al., 1999)(Figure 25). With F6-P available in the central carbon metabolism, essential metabolites, such as E4-P needed for tryptophan production (Ikeda, 2005) or GAP to follow glycolysis (Yokota and Lindley, 2004) could be obtained through PPP reactions and further glycolytic F6-P utilization (Figure 25).

Therefore, biomass formation of the engineered *C. glutamicum* Δ*rpe* strain on ribose was successfully coupled to methanol utilization (Figure 8), being subsequently improved through ALE after 14 passages to CG XII minimal medium containing 20 mM ribose, 500 mM methanol and 0.5 g/l yeast extract over the course of 52 days (Figure 11)(Chapter 3.2). Furthermore, methanol consumption was successfully connected to biomass formation using xylose (Figure 23A) and gluconate (Figure 23B) as co-substrates through deletion of the *rpi* gene, achieving methanol-dependent growth of *C. glutamicum* on three different carbon sources for the first time (Chapter 3.1.3 and Chapter 3.6).

Methanol-dependent growth of the strain *C. glutamicum* Δ*ald* Δ*fadH* Δ*rpi* (pEKEx3-*xylAB*)(pVWEx1-*mdh-hxlAB*) from 20 mM xylose and 500 mM methanol (Chapter 3.6) reached final biomass of 0.42 ± 0.11 gCDW/l after 48 h of cultivation with a specific growth rate of 0.02 ± 0.00 h^{-1} (Figure 23A). It was shown before that *C. glutamicum* engineered towards xylose utilization grew up to 4.87 ± 0.54 gCDW/l with 100 mM xylose (Meiswinkel et al., 2013). Taking this into consideration, maximal biomass formation of a *C. glutamicum* strain heterologously expressing XylAB with 20 mM xylose can be estimated to approximately 1 gCDW/l. Therefore, only a partly complementation (42%) of the *rpi* deletion was achieved, leaving potential for future improvement through ALE.

Previously published work carried out ALE towards methanol-dependent growth on xylose of *C. glutamicum* Δ*ald* Δ*fadH* Δ*rpi* heterologously expressing *E. coli* *xylA* in two steps (Tuyishime et al., 2018). First, growth in CG XII minimal medium containing ribose and xylose as sole carbon sources was improved through 10

passages. Secondly, additional heterologous expression of *mdh* from *B. stearothermophilus* and *hps-phi* from *B. methanolicus* led to methanol-dependent growth of *C. glutamicum* strain MX 10 on xylose with a specific growth rate of 0.0006 h^{-1} that was subsequently improved by ALE through 14 passages (Tuyishime et al., 2018). The evolved *C. glutamicum* strain MX-11 reached methanol-dependent biomass formation of 1.17 ± 0.03 gCDW/l from 26.6 mM xylose and 125 mM methanol after 120 h of cultivation with a specific growth rate of 0.03 h^{-1} (Tuyishime et al., 2018). However, biomass data of the unevolved parental strain engineered for xylose utilization was not shown. According to the previous estimation based on the results from Meiswinkel et al., final biomass formation of a xylose utilizing *C. glutamicum* strain with 26.6 mM xylose can be estimated at approximately 1.30 gCDW/l, which is in range of the biomass reached by the evolved methanol-dependent *C. glutamicum* strain MX-11 published by Tuyishime et al. (2018), indicating full complementation of the Δ*rpi* metabolic cut-off.

Although no ALE experiment was conducted to further improve methanol-dependent biomass formation with xylose (Chapter 3.6), the specific growth rate of strain *C. glutamicum* Δ*ald* Δ*fadH* Δ*rpi* (pEKEx3-*xylAB*) (pVWEx1-*mdh-hxlAB*) (0.02 ± 0.00 h^{-1} (Figure 23A)) was already in range of the fastest growth rate achieved by the evolved *C. glutamicum* strain MX-11 (0.03 h^{-1}), and exceeded the growth rate of the unevolved strain MX-10 (0.0006 h^{-1}) more than 30-fold (Figure 23A)(Tuyishime et al., 2018). This might be accounted to two factors: First, additional *xylB* expression to *xylA* (Chapter 3.6), as it was shown to improve the growth rates of xylose utilizing *C. glutamicum* strains before (Meiswinkel et al., 2013) and secondly, the supply of 500 mM methanol (Chapter 3.6) in contrast to 125 mM used by Tuyishime et al., since increasing methanol concentrations were shown to benefit methanol-dependent growth of *C. glutamicum* (Figure 9B).

Methanol-dependent growth on xylose with *E. coli* was achieved in a two-step ALE approach as well (Chen et al., 2018). After deletion of the *rpiAB* genes, ALE was first conducted to improve growth on ribose and xylose through 20 passages, yielding *E. coli* strain CFC 65 (Chen et al., 2018). Heterologous expression of *mdh2* from *Cupriavidus necator* and *hps-phi* from *B. methanolicus* then allowed ALE towards methanol-dependent growth with xylose for improved growth after

35 passages (Chen et al., 2018). The resulting *E. coli* strain CFC133/pIB208 reached an OD_{600} of 4.0 with a specific growth rate of 0.17 ± 0.006 h^{-1} on 50 mM xylose and 250 mM methanol after 30 h of cultivation (Chen et al., 2018), which corresponds to 1.2 gCDW/l according to previously published biomass estimations for *E. coli* (Soini et al., 2008). No direct comparison to *E. coli* WT with equal amounts of xylose was made to confirm or disconfirm full complementation of the Δ*rpi* metabolic cut-off. However, the *E. coli* BL21 parental strain reached an OD_{600} of around 1.4 (0.42 gCDW/l) with 7 mM xylose (Chen et al., 2018), which can be estimated to a potential final biomass of 3 gCDW/l with 50 mM xylose. Therefore, only approximately 40% of potential biomass from xylose was reached by the evolved methanol-dependent *E. coli* strain CFC133/pIB208 (Chen et al., 2018), which corresponds to a slightly lower partly complementation of the Δ*rpi* cut-off compared to the unevolved methanol-dependent, xylose utilizing *C. glutamicum* Δ*rpi* strain presented here (Chapter 3.6) (42%).

Methanol-dependent growth of *C. glutamicum* Δ*ald* Δ*fadH* Δ*rpi* (pEKEx3-*xylAB*) (pVWEx1-*mdh-hxlAB*) with 20 mM gluconate reached final biomass of 0.59 ± 0.00 gCDW/l with a specific growth rate of 0.03 ± 0.00 h^{-1} after 48 h of cultivation (Figure 23B). According to previously published studies about gluconate utilization in *C. glutamicum* (Frunzke et al., 2008b), the maximal potential biomass from 20 mM gluconate can be estimated to 1.8 gCDW/l. Therefore, approximately 33% of potential biomass from gluconate was achieved after coupling gluconate to methanol utilization (Figure 23B), revealing partial complementation of the Δ*rpi* metabolic cut-off that offers potential for improvement through ALE.

To achieve methanol-dependent growth on gluconate with *E. coli,* the genes *rpiAB, edd,* and *maldh* were deleted to prevent methanol-independent gluconate utilization and reduce TCA cycle activity, respectively (Meyer et al., 2018). Lowered TCA cycle activity was previously reported for *B. methanolicus* during growth on methanol (Müller et al., 2015c) and was therefore applied as strategy in the methanol-essential *E. coli* strain (Meyer et al., 2018) Introduction of *mdh2* from *B. methanolicus* PB1 and *hps-phi* from *M. flagellatus* for heterologous expression resulted in *E. coli* strain MeSV2 (Meyer et al., 2018). Methanol-dependent growth on gluconate was optimized through a three-step ALE

experiment. First, *E. coli* MeSV2 was serially transferred in medium containing 5 mM gluconate, 20 mM pyruvate, 0.1 g/l yeast extract and 500 mM methanol for 5 passages (Meyer et al., 2018). Then pyruvate was removed from the medium for the next 11 passages, yielding strain *E. coli* MeSV2.1 that already showed full complementation of the Δ*rpi* metabolic cut-off through methanol utilization (Meyer et al., 2018). Finally, yeast extract was removed from the medium for 9 more passages to further optimize methanol-dependent growth on gluconate. The resulting strain MeSV2.2 is the only strain in synthetic methylotrophy up to this point that showed extra biomass formation solely from methanol, surpassing equimolar methanol and gluconate consumption to generate 31.4 % more biomass (OD$_{600}$: 1.34/ 0.4 gCDW/l) than *E. coli* WT with equal amounts of gluconate (OD$_{600}$: 1.06/0.32 gCDW/l) (Meyer et al., 2018).

Deletion of the *maldh* gene for reduced TCA cycle activity proved to be crucial for achieving full complementation of the Δ*rpi* cut-off through ALE in *E. coli*, since a previous version of the strain (MeSV1.1) without Δ*maldh* that was evolved through ALE in 12 passages only reached approximately 30% of the maximal potential biomass from 5 mM gluconate and 0.1 g/l yeast extract reached by *E. coli* WT (OD$_{600}$: 1.06/0.32 gCDW/l) in methanol-dependent growth on 5 mM gluconate and 500 mM methanol (OD$_{600}$: ~0.32/ 0.01 gCDW/l)(Meyer et al., 2018). A slightly higher level of Δ*rpi* complementation was achieved with methanol-dependent *C. glutamicum* growing on gluconate (33%) (Figure 23B) without further improvements through ALE (Chapter 3.6). Disruption of the TCA cycle and subsequent ALE as described by Meyer et al. might further elevate biomass formation of methanol-dependent *C. glutamicum* strains.

Enhanced methanol-dependent biomass formation through ALE of a Δ*rpe* metabolic cut-off with ribose as co-substrate was reported for the first time with *C. glutamicum* strain Evo 14 (Figure 11). Final biomass formation from 20 mM ribose and 500 mM methanol was improved 2.5-fold through ALE after 14 passages from 0.66 ± 0.03 gCDW/l after 120 h of cultivation with *C. glutamicum* strain Evo 1 (Figure 8) to 1.69 ± 0.10 gCDW/l of *C. glutamicum* Evo 14 after methanol-dependent growth for 28 h (Figure 14). Evo 14 also showed full methanol-dependent complementation of Δ*rpe* on 20 mM ribose in comparison to *C. glutamicum* WT (Figure 14). Maximal biomass formation of Evo 14 from

20 mM ribose and 500 mM methanol was 1.69 ± 0.10 gCDW/l, whereas *C. glutamicum* WT strain formed 1.63 ± 0.01 gCDW/l on 20 mM ribose as sole carbon source (Figure 14). The specific growth rate of methanol-dependent *C. glutamicum* strains with ribose and methanol (Chapters 3.1.3 and 3.3) was also improved 3-fold from Evo 1 (0.03 ± 0.00 h^{-1})(Figure 8) to Evo 14 (0.10 ± 0.10 h^{-1}) (Figure 14). Furthermore, the specific growth rate of Evo 14 was about 3-times faster than methanol-dependent growth of *C. glutamicum* on xylose reported before (0.03 h^{-1}) (Tuyishime et al., 2018), which was already matched by the unevolved *C. glutamicum* Evo 1 strain with ribose and methanol (0.03 ± 0.00 h^{-1}). Growth of *C. glutamicum* Evo 14 with ribose and methanol was also faster than methanol-essential growth of the previously published, evolved *E. coli* strain MeSV2.2 with gluconate as co-substrate (0.081 ± 0.002 h^{-1}) (Meyer et al., 2018).

All reported strains harbour key mutations that allowed improved biomass formation from methanol and a sugar co-substrate. Mutations found after ALE in methanol-dependent *C. glutamicum* strains (Chapter 3.4.1) and previously reported key mutations will be discussed in the following chapter.

4.4 Mutations involved in improved methanol-dependent growth

Recent work on engineering of a synthetic methylotroph organism has yielded methanol-dependent *E. coli* strains from two distinct approaches (CFC133/pIB208 and MeSV2.2) (Chen et al., 2018; Meyer et al., 2018), as well as two different *C. glutamicum* strains (MX-11 and Evo 14) (Tuyishime et al., 2018; This work). None of the evolved strains (Chapter 3.4.1) (Chen et al., 2018; Meyer et al., 2018; Tuyishime et al., 2018) revealed any mutations on the plasmids used for heterologous expression of methanol utilization enzymes after ALE. However, all strains harboured specific genomic key mutations that allowed improved methanol-dependent biomass formation from methanol and a sugar co-substrate (Table 5).

In general, the first group of mutations influenced the central carbon metabolism, to allow more efficient utilization of the sugar co-substrate. A mutation in the gene encoding transcriptional repressor GntR in evolved *E. coli* was speculated to have altered the gluconate uptake, for improved supply of co-substrate for methanol utilization (Meyer et al., 2018). An additional mutation found in *deoB* encoding phosphopentomutase was hypothesized to have prevented the utilization of Ru5-P for the synthesis of phosphoribosyl pyrophosphate (PRPP) to ensure substrate availability for formaldehyde fixation (Hammer-Jespersen and Munch-Petersem, 1970; Meyer et al., 2018). In *C. glutamicum*, the *altR* gene, coding for a multi-functional regulator in carbohydrate metabolism (Auchter et al., 2011; Laslo et al., 2012), was found to be mutated, leading to a 7.7-fold increased transcription of *xylB* needed for xylose utilization (Tuyishime et al., 2018). Furthermore, a mutation in *uriR*, encoding a transcriptional repressor for ribose utilization genes (Brinkrolf et al., 2008; Nentwich et al., 2009) was identified but not further considered, since xylose was chosen as co-substrate for methanol utilization (Tuyishime et al., 2018).

Discussion and Outlook

In contrast to previously published studies, none of the mutations found in the methanol-dependent *C. glutamicum* strains Evo 8 and Evo 14 (Chapter 3.4) were considered to influence the central carbon metabolism of *C. glutamicum* directly. The fact that no mutations were found in Evo 8 and Evo 14 to enhance co-substrate supply and that faster methanol-dependent growth of *C. glutamicum* Evo 14 on ribose, compared to *C. glutamicum* MX-11 on xylose was achieved (Chapter 4.3), as well as methanol-dependent biomass formation of unevolved *C. glutamicum* strains from ribose (Figure 8) was increased in comparison to xylose (Figure 23A), might indicate that overall ribose could be a more promising co-substrate for methanol-dependent growth in *C. glutamicum* than xylose.

Table 5: Key mutations found in evolved methanol-dependent organisms

Genes	Proteins	Mutations	Reference
E. coli			
gntR	Transcriptional repressor	Miss-sense mutation	(Meyer et al., 2018)
frmA	Formaldehyde dehydrogenase	Frameshifts/deletions/ insertions	(Meyer et al., 2018)
deoB	Phosphopentomutase	Frame shift	(Meyer et al., 2018)
nadR	NAD-synthesis regulator protein	Miss-sense mutation	(Meyer et al., 2018)
frmR	Transcriptional repressor	Frameshift	(Chen et al., 2018)
frmA	Formaldehyde dehydrogenase	Frameshift	(Chen et al., 2018)
frmB	S-formylglutathione hydrolase	Frameshift	(Chen et al., 2018)
cyaA	Adenylate cyclase	Early stop-codon	(Chen et al., 2018)
C. glutamicum			
altR	Regulator for carbon metabolism	Miss-sense mutation	(Tuyishime et al., 2018)
metY	O-acetyl-homoserine sulfhydrylase	Miss-sense mutation	(Tuyishime et al., 2018)
mtrA	Response regulator of MtrAB	Miss-sense mutation	(Tuyishime et al., 2018)
uriR	Transcriptional repressor	Miss-sense mutation	(Tuyishime et al., 2018)
ctaE	Cytochrome c oxidase subunit III	Miss-sense mutation	(Tuyishime et al., 2018)
cg3104	Putative ATPase for DNA repair	Deletions	This work
metK	S-adenosylmethionine synthetase	Miss-sense mutation	This work
rpe	Riboulose-5-phosphate epimerase	Transposon insertion	This work

Secondly, mutations in genes essential for formaldehyde oxidation, such as formaldehyde oxidase (*frmA*) (Meyer et al., 2018) or the whole *frmRAB* operon, including an additional transcriptional repressor (*frmR*) and S-formylglutathione hydrolase (*frmB*) (Chen et al., 2018) were revealed in *E. coli*. Those mutations prevented further formaldehyde degradation and made it available for fixation through assimilatory RuMP pathway reactions to form biomass (Chen et al., 2018; Meyer et al., 2018).

Differently from the work on evolution of *E. coli*, *C. glutamicum* Δ*ald* Δ*fadH* was chosen as the basis for engineering (Chapter 3.1), since the strain lacked the natural formaldehyde degradation pathway (Leßmeier et al., 2013) Because of that, no evolution towards a disrupted formaldehyde degradation pathway was observed (Table 4 and Table 5).

The third and most prominent group of mutations were related to TCA cycle activity and NAD^+/NADH balance. An early stop codon in *cyaA,* encoding adenylatcylcase in methanol-dependent *E. coli,* supposedly lowered the transcription of TCA cycle genes (Chen et al., 2018), as it was previously described for CRP mutant strains (Gosset et al., 2004), by lack of cAMP for cAMP-CRP regulation, resulting in reduced NADH generation (Chen et al., 2018). Another mutation argued to favour NAD^+ formation in methanol-dependent *E. coli* was found in the *nadR* gene coding for an NAD^+-synthesis regulator protein. The mutation led to a changed kinase domain of the protein, supposedly enhancing NAD^+ supply (Meyer et al., 2018; Osterman et al., 2003). The *altR* mutation found in methanol-dependent *C. glutamicum* was argued to have additionally lowered the transcription of *sucCD*, encoding succinyl-CoA synthetase that is active in the TCA cycle (Cho et al., 2010; Tuyishime et al., 2018). Furthermore, the *mtrA* gene encoding the response regulator protein for the MtrAB transduction system in *C. glutamicum* was found to be mutated, which was hypothesized to have influenced the regulation of NAD^+ synthetase (NadE) expression, an essential enzyme involved in redox state maintenance (Brocker et al., 2011; Tuyishime et al., 2018).

It has been pointed that ALE of synthetic methylotrophs revealed genetic mutations involved in either central carbon metabolism, formaldehyde oxidation or energy metabolism/TCA cycle activity. However, none of the mutations detected in evolved *C. glutamicum* strains Evo 8 and Evo 14 were directly related to those processes (Table 5). Instead, ALE-derived mutations discovered in Evo 8 and Evo 14 could be related to SAM biosynthesis (*metK*)(Chapter 3.4.1), PCN (cg3104)(Chapter 3.5.3) and riboflavin metabolism (IS upstream of *ribGCAH*)(Chapter 3.4.2). Further SNPs found in the non-coding region 20 bp downstream of the *dxs* (cg2083) gene (Chapter 3.4.1) or in the *res* (cg1929) gene of the chromosomally integrated prophage CGP3 (Frunzke et al., 2008a; Kalinowski et al., 2003) (Chapter 3.4.1) were not investigated but proved to be non-essential for improved methanol-dependent growth of the evolved *C. glutamicum* strains (Chapter 3.5.2).

The next Chapter will explore the impact of the discovered key mutations on the *C. glutamicum* metabolism and discuss how they might have led to improved methanol-dependent biomass formation of the evolved strain Evo 14.

4.5 ALE-derived mutations revealed evolved methanol-dependent *C. glutamicum* strains

4.5.1 Impact of the amino acid substitution S288N in MetK on methanol-dependent growth of *C. glutamicum* Evo 14

In the evolved methanol-dependent *C. glutamicum* strains Evo 8 and Evo 14, a point mutation in the *metK* gene was found that resulted in an amino acid substitution from serine to asparagine at position 288 of the translated protein (S288N) (Table 4).

The *metK* gene encodes S-adenosylmethionine synthetase in *C. glutamicum* (Grossmann et al., 2000; Han et al., 2016) and *E. coli* (Markham et al., 1984), an enzyme catalysing the formation of S-adenosylmethionine (SAM) from methionine and ATP (Sekowska et al., 2000). SAM is the principal biological methyl donor (Fontecave et al., 2004) and the second most used enzyme substrate, right after ATP (Cantoni, 1975). It is needed e.g. for the methylation of DNA (Cantoni, 1975; Chiang et al., 1996), quorum sensing (Wijayasinghe et al., 2014), the synthesis of menaquinone in the respiratory chain of *C. glutamicum* (Bott and Niebisch, 2003) or cell division (Wang et al., 2005). Moreover, previous studies revealed that SAM is essential for growth in *E. coli,* since the *metK* gene could only be deleted in the genome in presence of a plasmid carrying a functional copy of the gene (Wei and Newman, 2002) or by heterologous expression of a SAM transporter and additional SAM supplementation (El-Hajj et al., 2013).

Here, introduction of the *metK*_S288N mutation to *C. glutamicum* strain Evo 1 Δcg3104 resulted in a strain that was able to reach similar growth characteristics as previously observed in strain Evo 14 on ribose and methanol (Figure 18C and Figure 14) and *C. glutamicum* WT on ribose (Figure 14). Furthermore, a reversion to the *metK* WT sequence in *C. glutamicum* Evo 14 led to 70% reduction in methanol-dependent biomass formation on ribose (Figure 21), revealing the importance of *metK* for growth with methanol.

Discussion and Outlook

Unlike *S. cerevisiae* that harbours two copies of MetK encoding genes in the genome (*sam1* and *sam2*) (Cherest et al., 1978), only one copy of the *metK* gene was identified for *C. glutamicum*, without other similar genes being present in the genome (Grossmann et al., 2000). Therefore, since a functional MetK enzyme for SAM biosynthesis is essential for growth (Wei and Newman, 2002) and the evolved *C. glutamicum* strains Evo 8 and Evo 14 exhibited improved, rather than impaired growth characteristics compared to the Evo 1 parental strain not bearing the *metK_S*288N mutation (Figure 12)(Chapter 3.3), it can be concluded that the mutation did not result in a non-functional MetK protein.

According to the universal protein database (UniProt Consortium, 2018) the amino acid exchange S288N was located next to the methionine-binding lysine residue at position 289 of the enzyme, which might have had an impact on the substrate specificity (Harris and Craik, 1998). Similarly, a mutation in *gyrA* resulting in an amino acid substitution of S to N near the active center of the encoded DNA gyrase enzyme in evolved *Chlamydia pneumoniae* strains led to increased resistance against the gyrase-targeting antimicrobial agent quinolone, due to changed enzyme binding properties (Heddle and Maxwell, 2002; Rupp et al., 2005).

Because of the importance of SAM in cellular activities, SAM synthetases of pathogenic bacteria have been targeted with methionine analogues as specific inhibitors for the development of chemotherapeutic agents in the past (Lombardini et al., 1970; Wijayasinghe et al., 2014; Zano et al., 2013). Some analogues of methionine, such as its methyl- or ethyl-esters were found to be accepted as substrate by the *E. coli* MetK enzyme (Zano et al., 2013) and supported growth of *metK*-deficient *E. coli* strains expressing a SAM transporter (Zhao et al., 2015). Other analogues like N-acetyl-methionine, S-(methanethiol) homocysteine, O-methyl-serine or L-2-amino-4-methylthio-cis-but-3-enoic acid (L-cisAMTB), were identified as inhibitors for MetK (Kim et al., 1992; Lombardini et al., 1970; Sufrin et al., 1993). Another potential MetK inhibitor structurally similar to the MetK-inhibiting O-methyl-serine or the natural MetK substrate methionine is O-methyl-homoserine (OMH)(Figure 26) (Grob et al., 2017).

OMH was identified to have antimicrobial properties (Roblin et al., 1945) and its formation was observed in *Corynebacterium acetophilum* through a side reaction catalysed by O-acetyl-homoserine sulfhydrolase (MetY) in presence of homoserine and methanol (Murooka et al., 1977).
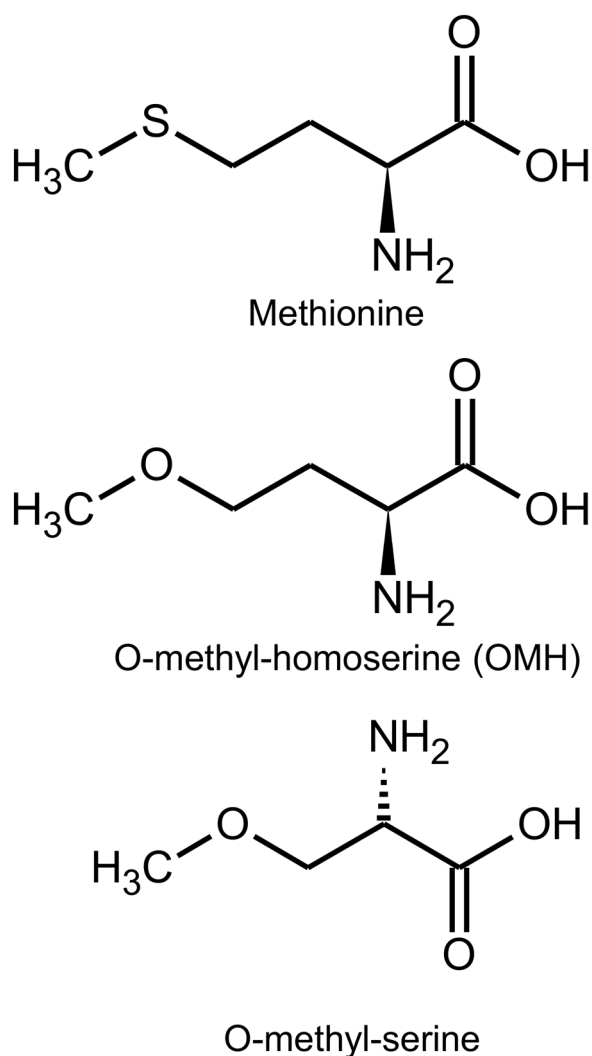
Figure 26: Chemical structures of methionine, O-methyl-homoserine (OMH) and O-methyl-serine.

MetY is part of the methionine biosynthesis of *C. glutamicum* and catalyzes the direct sulfhydrylation of O-acetyl-homoserine to the methionine precursor homocysteine, alternatively to the equally functional transsulfuration pathway, catalyzed by cystathionine γ-synthase (MetB) and cystathionine β-lyase (MetC) (Hwang et al., 2002; Rückert et al., 2003)(Figure 27).

Figure 27: S-adenosylmethionine biosynthesis pathway in *C. glutamicum* and hypothetical inhibition by O-methyl-homoserine (OMH).

Direct sulfhydrylation and transsulfuration pathways for methionine biosynthesis in *C. glutamicum* are depicted. Inhibition of S-adenosylmethionine synthetase (MetK) by O-methyl-homoserine is shown in red. MetK and MetY are highlighted in bold letters. Abbreviations: MetX: Homoserine acetyltransferase; MetB: Cstathionine γ-synthase; MetC: Cystathionine β-lysase; MetE/MetH: Homocysteine methylase; MetY: O-acetyl-homoserine sulfhydrylase; CoA: coenzyme A; H₄F: tetrahydrofolate.

It was hypothesized before that emerging OMH in methanol-utilizing *C. glutamicum* inhibits growth, when it was found that a SNP in the *metY* gene, resulting in an amino acid exchange A165T close to the substrate-cofactor binding site of the translated protein, significantly improved methanol tolerance (Leßmeier and Wendisch, 2015). Moreover, a mutated version of the *metY* gene was also found in the evolved methanol-dependent *C. glutamicum* strain MX-11 that showed improved methanol-dependent growth with xylose (Tuyishime et al., 2018)(Table 5). However, it remained unclear how OMH influences growth of *C. glutamicum* in presence of methanol. Here we hypothesize that OMH inhibits SAM formation of MetK by acting as a methionine analogue (Figure 27).

Discussion and Outlook

The amino acid exchange S288N, next to the methionine binding lysine at position 289, in the mutated MetK version of *C. glutamicum* strains Evo 8 and Evo 14 presumably led to a loss of effect of the MetK-inhibiting methionine analogue OMH, due to increased methionine specificity of the enzyme and therefore improved methanol-dependent growth (Figure 12). Moreover, the fact that both *C. glutamicum* strains Evo 1 Δcg3104 *metK*_S288N (Figure 18C) and Evo 1 Δcg3104 Δ*metY* (Figure 22) reached similar levels of methanol-dependent growth as observed in strain Evo 14 (Figure 14), reinforces the hypothesis that diminished OMH inhibition of MetK or the elimination of OMH production are related to improved methanol-dependent growth of *C. glutamicum.* Reversion of the ALE-derived *metK* mutation in Evo 14 possibly reinstated the MetK inhibiting effect of OMH and drastically reduced the biomass formation with methanol (Figure 21). Inhibition of MetK by OMH might have been a reason for relatively low methanol-dependent biomass formation from methanol and ribose before ALE was conducted (Figure 8).

Previous studies investigating the control of methionine biosynthesis in *E. coli* used mutant strains that showed resistance to the methionine analogues norleucine, ethionine or α-methylmethionine (Chattopadhyay et al., 1991). Genomic characterization of the methionine analogue resistant *E. coli* strains revealed that all of them harboured a mutated version of the *metK* gene, although the mutations were not further specified (Chattopadhyay et al., 1991). Hence, mutation of *metK* might be an alternative way of evolution to vanquish toxicity of the methionine analogue OMH in methanol-utilizing *C. glutamicum* strains, as opposed to the *metY* gene mutations reported before (Leßmeier and Wendisch, 2015; Tuyishime et al., 2018). Nevertheless, further enzymatic activity assays (Zano et al., 2013) are needed to confirm the inhibitory effect of OMH to SAM formation from MetK.

Since the transfer of the *metK*_S288N mutation to Evo 1 only elevated biomass formation when cg3104 was additionally deleted (Figure 18), OMH toxicity could not be the only growth limiting factor in methanol-dependent growth.

4.5.2 Deletion of cg3104 increased the plasmid copy number

In the present study, it was shown that ALE of *C. glutamicum* towards methanol-dependent growth resulted in a deletion within the open reading frame (ORF) of cg3104 in strains Evo 8 and Evo 14 (Table 4 and Table 5). However, introducing a cg3104 deletion in the Evo 1 parental strain did not result in increased methanol-dependent biomass formation with ribose in comparison to the unchanged Evo 1 strain (Figure 18B), presumably due to prevalent OMH toxicity (Chapter 4.5.1). Nevertheless, strains Evo 14 and Evo 1 Δcg3104, showed a PCN increase of about 60% confirmed by qPCR (Figure 19), as well as 60 % higher activity of the pEKEx3 plasmid expressed enzymes HxlAB (Figure **20**). Calculated PCN relative to the chromosome were low for all examined strains, ranging from 1.33 ± 0.02 (Evo 1) to 2.17 ± 0.05 (Evo 1 Δcg3104), when copy numbers ranging from 8 to 30 per chromosome would have been expected for pEKEx3 as pBL1 derived plasmid (Stansen et al., 2005; Tauch, 2005). The generally low relative amounts of plasmid compared to the genome may be explained by a loss of plasmids during DNA isolation or the occurrence of plasmidless cells in overnight cultures for DNA isolation (Friehs, 2012).

Plasmid copy numbers in bacterial cells can be increased through varied factors, such as mutations on the plasmid, environmental changes or mutations of trans-acting elements on the chromosome (Friehs, 2012). For example, *E. coli* cells grown in presence of ethanol generally exhibited increased DNA synthesis and PCN (Basu and Poddar, 1997, 1994) that was founded on increased *in vitro* polymerase III activity in presence of ethanol (Kornberg and Gefter, 1972). Here, methanol-dependent growth could have caused a similar effect on the evolved *C. glutamicum* strains Evo 8 and Evo 14.

Since characterization of the gene product of cg3104 is not available, it is difficult to predict how its deletion increased the PCN in the evolved methanol-dependent *C. glutamicum* strains. The gene cg3104 has been annotated as ATPase involved in DNA repair (Kalinowski et al., 2003) and BLAST analysis (Altschul et al., 1990) of the amino acid sequence only revealed proteins with high similarity (>70%) in *Corynebacteria* that were annotated accordingly. However, analysis of the amino acid sequence and a search for protein motifs in the KEGG database (Kanehisa and Goto, 2000), revealed the presence of a P-loop (amino acids 17-

76) within an ATPase domain (amino acids 19-296) at the N-terminus of the protein sequence, typically found in all kinds of GTP- and ATPases (Leipe et al., 2002) and a putative subunit C of exonuclease SbcCD (amino acids 973-1060) at the C-terminus (Kanehisa and Goto, 2000).

The SbcCD protein has been well characterized in *E. coli* (Connelly et al., 1997) and consists of the subunits SbcC and SbcD that are both needed for ATP-dependent DNA exonuclease activity (Connelly and Leach, 1996). It cleaves secondary hairpin structures that can occur in palindromic sequences during DNA replication, to ensure genomic stability in *E. coli* (Connelly et al., 2002, 1999; Leach, 1994). Furthermore, it is capable of digesting linear double-stranded DNA to half its original length in a 3'→ 5' direction (Connelly et al., 1999) and has endonuclease activity on single-stranded DNA (Connelly et al., 1999; Connelly and Leach, 1996). A pUC18 plasmid with 24 repeats of TGG-CCA was revealed to have an increased propagation in *E. coli* strains lacking SbcCD, due to a loss of hairpin cleavage during replication (Pan and Leach, 2000). Similarly, the loss of cg3104 exonuclease activity on replicating plasmids might have been relevant for the increased PCN of Evo 14 (Chapter 3.5.3).

Improved plasmid replication, due to a lack of SbcCD was reported for pUC18 that harbours a pMB1 origin of replication (Yanisch-Perron et al., 1985) and replicates through theta replication (Del Solar et al., 1998). Here, pEKEx3 was used for the expression of *mdh* and *hxlAB*, since it showed the best activity for those enzymes (Figure 6 and Figure 7). The pBL1 origin of replication of pEKEx3 (Stansen et al., 2005; Tauch, 2005) mediates rolling circle replication in *C. glutamicum* (Fernandez-Gonzalez et al., 1994). Rolling circle replication is wide-spread in Gram-positive bacteria (Khan, 1997) and usually mediates the replication of compact plasmids, less than 10 kb in size (Khan, 2005). However, hairpins are a typical structure during rolling circle replication (Khan, 2005, 1997) and intermediate single-stranded DNA was found in *C. glutamicum* harbouring a pBL1 plasmid (Deb and Nath, 1999; Fernandez-Gonzalez et al., 1994). The plasmid pEKEx3-*mdh-hxlAB* (10.697 bp) used in this study exceeded 10 kb, providing a lot of potential sequences for hairpin formation of single-stranded DNA during its replication. In fact, sequence analysis of the genes *mdh* and *hxlAB* using the ViennaRNA web-tool to predict secondary structures of ssDNA (Gruber

et al., 2008; Lorenz et al., 2011) revealed the formation of several potential hairpin structures during replication of the heterologous genes. In case of cg3104 encoding for subunit C of a SbcCD protein, an intact ORF might lead to a functional exonuclease that could interfere with plasmid replication, as it was reported for *E. coli* before (Pan and Leach, 2000).

Deletions found within cg3104 of the evolved *C. glutamicum* strains Evo 8 and Evo 14 (amino acids 1061-1065) were located behind the putative SbcCD subunit C (amino acids 973-1060) and introduced a frame-shift for the translation of the remaining amino acid sequence (1066-1111) that might have interfered with the function of the protein. Consequential loss of putative SbcCD protein function might have prevented the degradation of hairpin structures or ssDNA in the evolved strains, leading to an increase in PCN (Figure 28). Moreover, cg3104 encoding the C-subunit of a putative SbcCD protein might be supported by the activation of cg3104 transcription by the DNA cross-linking agent mitomycin C, as predicted by the CoryneRegnet database for *C. glutamicum* (Baumbach et al., 2011). Activation of SbcC expression in medium supplemented with mitomycin C was previously reported for *B. subtilis* and *E. coli* (Darmon et al., 2007).
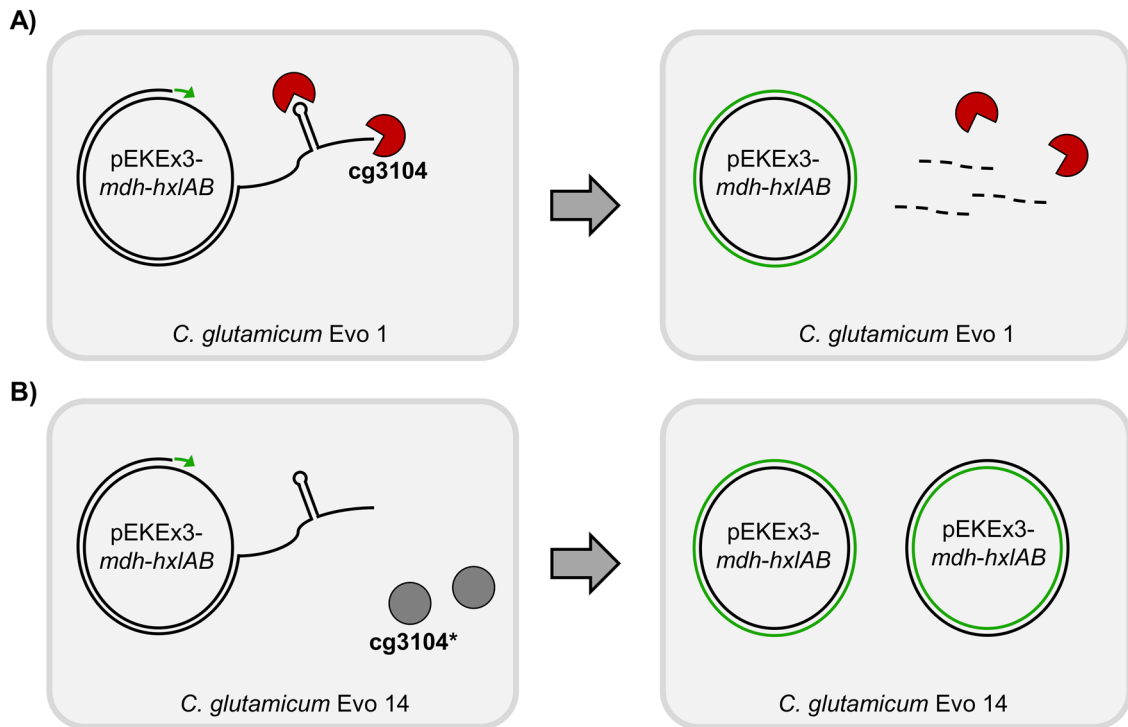
Figure 28: Schematic depiction of the proposed influence of cg3104 on pEKEx3-*mdh-hxlAB* replication in *C. glutamicum* strains Evo 1 and Evo 14.

A) Single stranded DNA (ssDNA) during rolling circle replication of pEKEx3-*mdh-hxlAB* in *C. glutamicum* strain Evo 1 can form a loop structure that gets detected and subsequently digested by the cg3104 gene product, resulting impaired plasmid replication due to ssDNA degradation. B) Plasmid replication in *C. glutamicum* strain Evo 14 is not disturbed by the cg3104 gene product, due to a disruption of the ORF resulting in an inactive enzyme (cg3104*). Newly synthesized DNA strands after replication are depicted in green.

Nevertheless, further research needs to be conducted towards the characterization of the cg3014 gene product to confirm this hypothesis. To recent knowledge, a SbcCD system was found for *Corynebacterium pseudotuberculosis* (Baumbach et al., 2011), but has not yet been described for *C. glutamicum*.

4.5.3 Insertion sequence in *C. glutamicum* Evo 14 improved riboflavin availability

After deletion of the *rpe* gene in *C. glutamicum* Δ*ald* Δ*fadH* (Chapter 3.1.1), complementation of the deletion through overexpression of endogenous *rpe* restored growth with ribose as sole carbon source (Figure 4). However, the complemented strain did not reach the same maximal biomass as *C. glutamicum* WT carrying the pVWEx1 empty vector (Figure 4), which was initially attributed to metabolic burden due to plasmid expression (Bentley et al., 1990; Wu et al., 2016). However, cultivations with glucose as sole carbon source and riboflavin supplementation after ALE revealed a surprising riboflavin deficiency in *C. glutamicum* strains Evo 1 and Evo 8, resulting in weak growth on glucose that could be recovered by riboflavin supplementation (Figure 17A and B). In contrast, strain Evo 14 was capable of exponential growth on glucose, without addition of riboflavin (Figure 17C).

For the biosynthesis of riboflavin, guanosine-triphosphate (GTP) and Ru5-P are required as precursors, generating riboflavin in several enzymatic reactions (Bacher et al., 2001, 2000). Riboflavin then acts as a precursor for the essential flavins flavin mononucleotide (FMN) and flavin adenine nucleotide (FAD) (Bacher et al., 2001; García-Angulo, 2017). Both, FMN and FAD serve as co-factors for a great variety of different enzymes, such as oxidoreductases, transferases, lyases, isomerases and ligases, making them essential in cellular metabolic processes (MacHeroux et al., 2011; Mansoorabadi et al., 2007; Vitreschak et al., 2002). FAD is furthermore needed for the formation of the succinate dehydrogenase complex (complex II) that is part of the TCA cycle and respiratory chain of aerobic bacteria (McNeil and Fineran, 2013; Niebisch et al., 2005).

The gene *rpe* (cg1801), followed by *ribG* (cg1800; putative bifunctional riboflavin-specific deaminase/reductase) is part of a bigger operon structure sharing the same transcription start site (TSS), additionally including *ribC* (cg1799; putative riboflavin synthase), *ribA* (cg1798; putative GTP cyclohydrolase II/3,4-dihydroxy-2-butanone-4-phosphatesynthase) and *ribH* (cg1797; riboflavin synthase, beta chain) downstream of *ribG* (Pfeifer-Sancar et al., 2013) (Figure 29). Additional TSS for *rpe* independent transcription of the genes *ribA* and *ribH* are located upstream of *ribA* (Pfeifer-Sancar et al., 2013) (Figure 29).
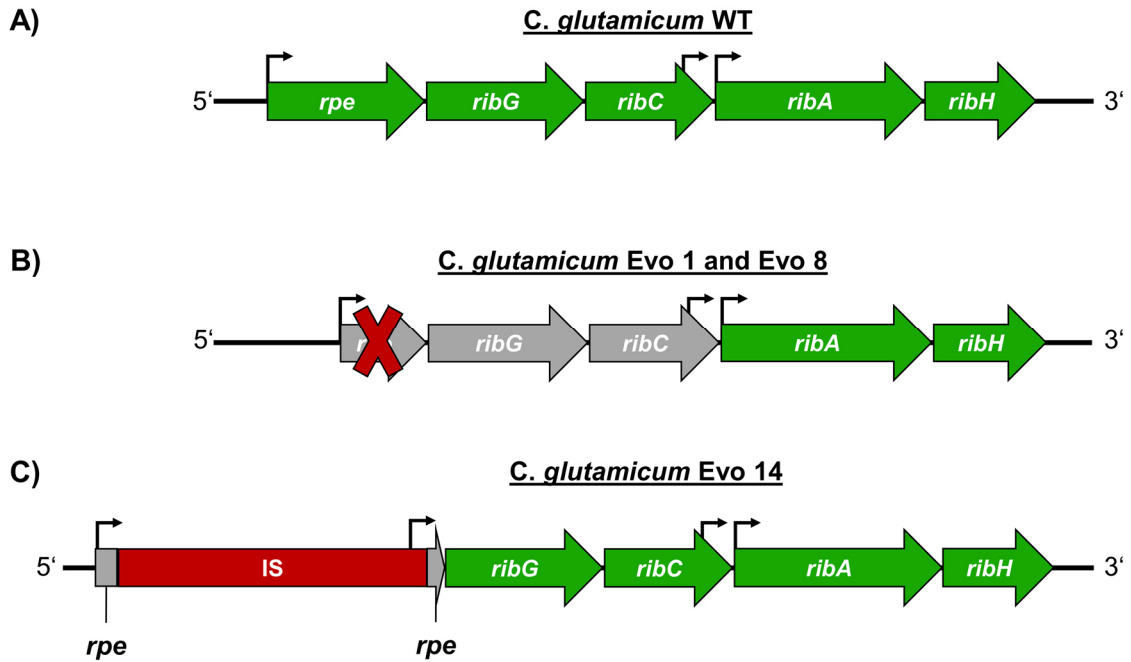
Figure 29: Organisation of the *ribGCAH* operon in *C. glutamicum* WT and methanol-dependent strains Evo 1 and Evo 14.

Genomic organisation of the *ribGCAH* genes in A) C. glutamicum wildtype (WT) B) Methanol-dependent *C. glutamicum* strains Evo 1 and Evo 8 and C) Evolved methanol-dependent *C. glutamicum* strain Evo 14. DNA orientation is indicated through 3' and 5' ends. Genes not affected in expression are depicted in green. Presumably negatively affected genes *ribG* and *ribC* after *rpe* deletion are shown in grey. The revealed insertion sequence (IS) in *C. glutamicum* strain Evo 14 is depicted in red. Arrows indicate transcription start sites. Abbreviations: *rpe* (ribulose-5-phosphate epimerase), *ribG* (putative bifunctional riboflavin-specific deaminase/reductase), *ribC* (putative riboflavin synthase), *ribA* (putative GTP cyclohydrolase II/3,4-dihydroxy-2-butanone-4-phosphatesynthase), *ribH* (riboflavin synthase, beta chain).

The vector for deletion of the *rpe* gene was deliberately designed to not disturb the transcription of the following riboflavin synthesis genes, as the TSS and the first 18 bp of the *rpe* gene remained untouched after deletion (Chapter 3.4.2). However, *rpe* deletion surprisingly resulted in a riboflavin deficiency (Chapter 3.5.1), presumably caused by a disturbed expression of the *rpe* downstream genes *ribG* and *ribC* that share the same TSS (Figure 29)(Pfeifer-Sancar et al., 2013). The *ribGCAH* operon was revealed to be expressed as a leaderless transcript, missing a 5' untranslated region (UTR) with a clear RBS (Albersmeier et al., 2017; Pátek et al., 2003; Pfeifer-Sancar et al., 2013). Genes without 5'UTR have their transcriptional start point close to the ATG start codon

for translation (Pátek, 2005), but since they lack a RBS, the recognition and binding mechanisms of the translational machinery is still not fully understood to this day (Beck and Moll, 2018).

Together, *rpe-ribGCAH* form a sub-operon that is part of a larger operon structure that includes 16 genes from cg1792 to cg1806 (Pfeifer-Sancar et al., 2013). Previous work revealed that *ribA* is essential for riboflavin synthesis in *C. glutamicum* since Δ*ribA* strains exhibited growth deficiencies that could be cured by external riboflavin supplementation (Takemoto et al., 2014). External riboflavin can be taken up by *C. glutamicum* through the RibM transporter (Vogl et al., 2007). Moreover, expression of the riboflavin operon was shown to be upregulated by overexpression of the *sigH* gene (Taniguchi and Wendisch, 2015)*,* encoding sigma factor SigH that is generally associated with stress responses (pH, heat shock, oxidative stress) (Kim et al., 2005).

Genome sequencing revealed the integration of a transposable element in methanol-dependent *C. glutamicum* strain Evo 14 at the former *rpe* locus, upstream of *ribG* (Figure 15) which provided alternative TSS and RBS motifs for the expression of *ribG* and *ribC* in the *ribGCAH* operon (Figure 16 and Figure 29) (Albersmeier et al., 2017; Pfeifer-Sancar et al., 2013), curing the riboflavin deficiency (Figure 17C). Integration of the IS in strain Evo 14 was possibly promoted by mutation of the *res* gene of the integrated prophage CGP3 (Chapter 3.4.1), as resolvases are often related to relocation and recombination of transposable elements (Mahillon and Chandler, 1998; Olorunniji and Stark, 2010).

The reinstated riboflavin biosynthesis in *C. glutamicum* Evo 14 was an essential modification for increased methanol-dependent biomass formation from ribose to finally reach WT levels of growth (Figure 14), since it was the only genetic modification distinguishing the evolved *C. glutamicum* strains Evo 8 and Evo 14 (Chapter 3.4). Riboflavin deficiency might have been a reason for relatively low methanol-dependent biomass formation of *C. glutamicum* before ALE (Figure 8), as well as an incomplete ribose consumption of methanol-dependent strains Evo 1 and Evo 8 grown on methanol and ribose (Figure 13), possibly due to a shortage of co-factors FMN and FAD for enzymatic reactions. *C. glutamicum*

Evo 14 was the only strain capable of fully utilizing ribose during methanol-dependent growth, after riboflavin biosynthesis was restored (Figure 13). Riboflavin limitation could also justify the only partial complementation of Δ*rpe* through simultaneous supply of ribose and xylose together with heterologous expression of xylose metabolizing enzymes (Figure 5), unlike reported for *E. coli*, where full Δ*rpe* complementation was achieved through co-supply of ribose and xylose (Chen et al., 2018).

Past work in *E. coli* revealed that a Δ*rpe* strain started methanol independent growth after a lag-phase of 29 h, making the strain unsuitable for an evolution experiment (Chen et al., 2018). The riboflavin deficiency in addition to *rpe* deletion in this work might have had the positive effect for ALE towards methanol-dependent growth that *C. glutamicum* Evo 1 was utterly dependent on methanol supplementation, regardless of cultivation time (Figure 8). Furthermore, starting ALE with a riboflavin synthesis-deficient strain could have caused a reduction of TCA cycle activity, due to a lack of FAD for the succinate dehydrogenase complex. As discussed in chapters 4.3 and 4.4 reduction of TCA cycle activity was a successfully applied engineering strategy for methanol-dependent growth in *E. coli* and proved to be crucial for extra biomass formation solely from methanol (Meyer et al., 2018).

4.5.4 Improved methanol-dependent growth of *C. glutamicum* Evo 14

In the present study, 3 significant chromosomal changes were found in ALE-derived *C. glutamicum* strain Evo 14, which were important for improved methanol-dependent biomass formation:

1. A point mutation in *metK*, leading to amino acid exchange S288N in the translated protein that possibly resulted in resistance from inhibition by OMH, a side product of MetY that emerges from methanol and O-acetyl-homoserine (Chapter 4.5.1) (Figure 27 and Figure 30).

2. Disruption of the ORF cg3104 that increased the pEKEx3-*mdh-hxlAB* PCN, presumably by removal of a SbcCD-type DNA exonuclease, degrading plasmid DNA during rolling circle replication (Chapter 4.5.2) (Figure 30).

3. Integration of an IS element into the former locus of the deleted *rpe* gene (Chapter 4.5.3) that provided alternative TSS and RBS motifs for the *rpe* downstream genes *ribG* and *ribC* in the *ribGCAH* operon (Figure 16), curing riboflavin deficiency caused by *rpe* deletion and increasing the availability for essential flavin co-factors FMN and FAD (Chapter 4.5.3) (Figure 30).

Figure 30 summarizes the proposed hypotheses for the improved biomass formation from ribose and methanol of Evo 14. A combination of all three genomic mutations was needed, before full complementation of Δ*rpe* through methanol utilization could be achieved (Figure 11 and Figure 14). Separately, neither deletion of cg3104 (Figure 18B), nor an introduction of *metK*_S288N (Figure 18A) to *C. glutamicum* Evo 1 supplemented with riboflavin led to a significant growth change (Chapter 3.5.2). With OMH presumably inhibiting SAM formation, improved methanol utilization and formaldehyde fixation from increased expression of heterologously expressed enzymes Mdh and HxlAB, caused by higher PCN through cg3104 deletion, could not improve growth in strain Evo 1 Δcg3104 (Figure 18B). On the other hand, cells not inhibited by OMH, due to a transfer of the *metK*_S288N mutation, were still limited in biomass formation by

poor methanol utilization (Figure 18A). Riboflavin supplementation to provide flavin co-factors was the third necessity since *C. glutamicum* strain Evo 8 already harboured genomic mutations in the genes cg3104 and *metK,* but still exhibited a riboflavin deficiency (Figure 17) and was therefore impaired in methanol-dependent growth compared to strain Evo 14 (Figure 12).
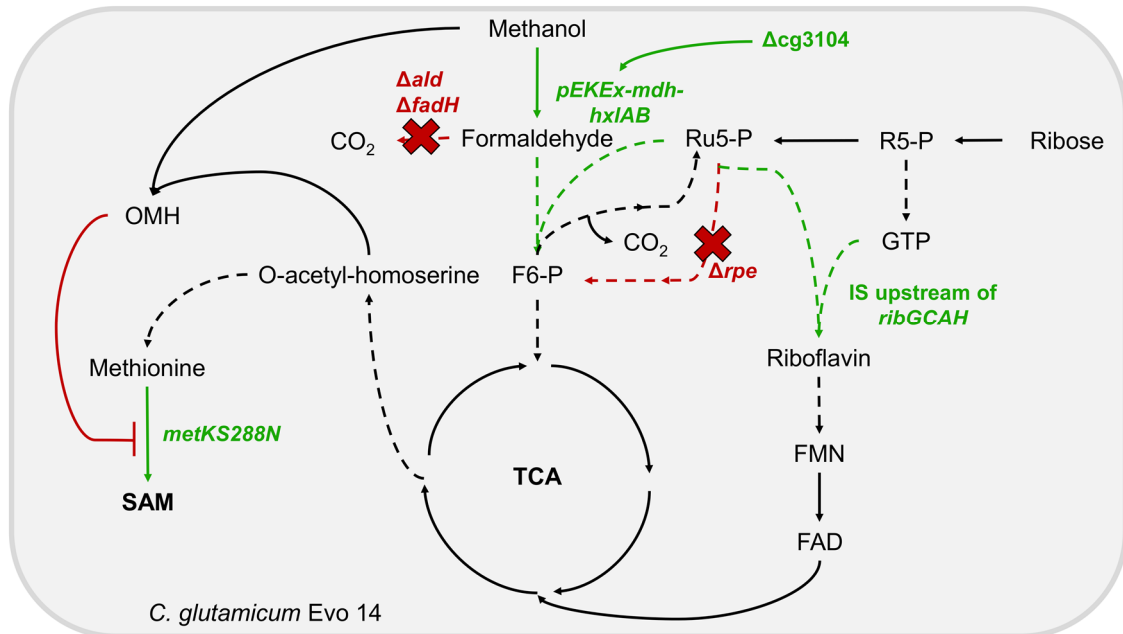
Figure 30: Summary of proposed mechanisms leading to increased methanol-dependent biomass formation with ribose in *C. glutamicum* Evo 14.

Improved pathways with according gene mutations are shown in green. Pathways deleted before evolution, as well as reduced inhibition by OMH are depicted in red. Dotted arrows indicate multiple reactions. Abbreviations: *ald* (acetaldehyde dehydrogenase), *fadH* (mycothiol-dependent formaldehyde dehydrogenase), *rpe* (ribulose-5-phosphate epimerase), *ribG* (riboflavin-specific deaminase/reductase), *ribC* (riboflavin synthase) (IS (insertion sequence), TCA (tricarboxylic acid cycle), Ru5-P (ribulose-5-phosphate), R5-P (ribose-5-phosphate), F6-P (fructose-6-phosphate), OMH (O-methyl-homoserine), SAM (S-adenosylmethionine), GTP (guanosine-triphosphate), FMN (flavin mononucleotide), FAD (flavin adenine dinucleotide), IS (insertion sequence).

4.6 Methanol oxidation as limiting factor for growth

Determined *in vitro* activities from *C. glutamicum* cell crude extracts for heterologously expressed Mdh from *B. methanolicus* MGA3 (2.44 ± 0.34 mU/mg) (Figure 6) were in range of those previously reported for crude extracts of *E. coli* (1.40 mU/mg) (Müller et al., 2015b) and *C. glutamicum* (3.70 ± 0.90 mU/mg (Leßmeier et al., 2015); 3.30 ± 1.20 mU/mg (Witthoff et al., 2015)). However, observed *in vitro* activities in crude extracts were generally low compared to those determined from purified enzyme (129 ± 10 mU/mg) (Ochsner et al., 2014a). Despite its low activity, heterologous expression of *mdh* was necessary to support methanol-dependent growth of *C. glutamicum* (Figure 10), although endogenous alcohol dehydrogenase (*adhA*) of *C. glutamicum* was reported to accept methanol as substrate (Witthoff et al., 2013).

In general, the NAD-dependent methanol oxidation to formaldehyde by Mdh of *B. methanolicus* at mesophilic temperatures is a thermodynamically unfavourable reaction that only becomes feasible at temperatures of 45-55°C (Price et al., 2016; Whitaker et al., 2015). Additionally, characterization of the Mdh enzyme revealed low catalytic efficiency and a K_m for methanol of approximately 350 mM (Krog et al., 2013b; Ochsner et al., 2014a). To compensate low Mdh activity, *B. methanolicus* harbours three homolog *mdh* genes (*mdh*, *mdh2*, *mdh3*), two on the chromosome and one on the naturally occurring plasmid pBM19 (Heggeset et al., 2012; Müller et al., 2015a), as well as an additional *act* gene encoding a Mdh activator protein (Arfman et al., 1991) that stimulates Mdh activity (Krog et al., 2013b; Ochsner et al., 2014a). Furthermore, *B. methanolicus* grown on methanol shows high *mdh* expression (Jakobsen et al., 2006) resulting in Mdh constituting up to 30% of total cell protein (Arfman et al., 1989; Brautaset et al., 2007). However, since Act did not improve Mdh activity in *C. glutamicum* (Leßmeier et al., 2015), it was not additionally expressed in the present study. Poor Mdh activity and the high K_m of the enzyme might have been reasons why methanol-dependent growth was improved with increasing methanol concentrations (Figure 9B). Increased PCN observed after the deletion of cg3104 (Figure 19) have likely led to increased *mdh* expression, resulting in improved

methanol oxidation and faster growth, as well as higher biomass formation of the evolved *C. glutamicum* strains Evo 8 and Evo 14 (Figure 12).

In addition to *mdh* overexpression, one reported strategy to promote the equilibrium of the Mdh-catalyzed reaction towards continuous methanol oxidation is to efficiently remove formaldehyde in assimilation reactions as soon as it emerges (Price et al., 2016; Whitaker et al., 2015; Woolston et al., 2018a). In methylotrophic *B. methanolicus,* this happens through upregulated expression of the RuMP pathway genes *hps* and *phi* (Jakobsen et al., 2006; Müller et al., 2015c).

The combined HxlAB activity after expression from pEKEx3-*mdh-hxlAB* before ALE (197 ± 18 mU/mg)(Figure 7) was relatively low compared to previous work aiming at synthetic methylotrophy in *C. glutamicum* (530 ± 120 mU/mg) (Leßmeier et al., 2015). This might be because *hxlAB* were expressed in a synthetic operon together with *mdh* in this work, whereas the enzymes in previous work were expressed singularly on pEKEx3-*hxlAB* (Leßmeier et al., 2015). Additional Mdh in the reaction mixture might have reduced supplemented formaldehyde to methanol, as it is the thermodynamically favoured direction of the Mdh catalysed reaction (Price et al., 2016), and consequently removed formaldehyde for the fixation reaction of HxlA. Furthermore, synthetic operons often require a fine-tuned gene expression to ensure optimal function of the singular enzymes (Engstrom and Pfleger, 2017). Therefore, the *mdh* gene might have interfered with optimal gene expression of *hxlAB* from pEKEx3-*mdh-hxlAB*, leading to reduced enzyme activities in comparison to previous work using pEKEx3-*hxlAB* for heterologous expression (Leßmeier et al., 2015).

Nevertheless, improvement of HxlAB activities from 197 ± 18 mU/mg before ALE to 268 ± 21 mU/mg in *C. glutamicum* strain Evo 14 after ALE (Figure 20), due to increased PCN (Figure 19) was sufficient to elevate methanol-dependent biomass formation to full complementation of the Δ*rpe* metabolic cut-off (Figure 14).

4.7 What comes next: Ways to improve methanol oxidation and formaldehyde fixation towards synthetic methylotrophy

Full synthetic methylotrophy has not been achieved to this day (Chen et al., 2018; Meyer et al., 2018; Tuyishime et al., 2018). However, methanol-dependent growth of *E. coli* (Chen et al., 2018; Meyer et al., 2018) and *C. glutamicum* (Tuyishime et al., 2018) (Chapter 3.1.3 – Chapter 3.6) offered essential insights on synthetic methylotrophy for future engineering approaches to optimize methanol oxidation and formaldehyde fixation for the creation of the first full synthetic methylotroph organism.

ALE-derived disruption of the cg314 gene resulted in increased pEKEx3-*mdh-hxlAB* PCN of evolved methanol-dependent *C. glutamicum* strain Evo 14, which was shown to be beneficial for methanol-dependent growth (Chapter 3.5.2), supposedly due to higher expression of methanol utilizing enzymes *mdh* and *hxlAB*. One way of improving heterologous expression of proteins is the optimization and addition of a synthetic RBS to increase the translation initiation rate (TIR) (Salis et al., 2009). The ribosome binding sites for *mdh*, *hxlA* and *hxlB* used here consisted of the consensus motif derived from previous investigation of transcriptomics and promoter structures of *C. glutamicum* (Albersmeier et al., 2017; Pfeifer-Sancar et al., 2013) but have not been analyzed in terms of TIR before cloning. According to predictions of the Salis lab RBS calculator (Salis et al., 2009), TIRs of all heterologously expressed enzymes could be improved at least 4-fold by addition of a synthetic RBS (Espah Borujeni et al., 2014; Salis et al., 2009). The TIR of *mdh* was predicted to be improved 6.5-fold (from 141797 arbitrary units (au) to 913774 au), whereas the TIRs of *hxlA* and *hxlB* were predicted to be improved 31-fold (5659 au to 177244 au) and 4-fold (223415 au to 897552 au), respectively (Espah Borujeni et al., 2014; Salis et al., 2009). Especially the 31-fold increased TIR of *hxlA* might lead to great improvements in methanol utilization, since it was shown before that an increased number of the formaldehyde fixing enzyme Hps led to improved methanol utilization in *E. coli* (Price et al., 2016).

Discussion and Outlook

To further improve methanol utilization in synthetic methylotrophy, it is of great interest to overcome limitations from poor enzymatic properties of known natural NAD-dependent methanol dehydrogenases (Meyer et al., 2018; Müller et al., 2015b; Woolston et al., 2018a). Initial attempts were made to create fluorescence-based formaldehyde biosensors, using the *E. coli* FrmR repressor that naturally regulates the transcription of *frmA* (formaldehyde oxidase), therefore using *frmA* promoter to control the expression of a fluorescent reporter gene (Rohlhill et al., 2017; Woolston et al., 2018b). With this approach, increasing fluorescence dependent on cellular formaldehyde concentrations was achieved in *E. coli* and different Mdh variants were screened for their methanol oxidation capability, revealing the highest methanol oxidation in *E. coli* through heterologously expressed *mdh* from *Geothermus stearmophilus* (Woolston et al., 2018b). Biosensors also provide the possibility to evolve desired enzymes in an iterative process of random mutagenesis and subsequent high throughput screening using fluorescence activated cell sorting (FACS), to sort out and analyse cells showing the highest fluorescence signal (Schallmey et al., 2014; Williams et al., 2016). Applying this approach to evolve Mdh enzymes might lead to improved versions with more suitable properties in the future (Figure 31C).

Instead of using iterative cycles of random mutagenesis and FACS selection, phage-assisted continuous evolution (PACE) is another system that allows the rapid evolution of desired proteins (Esvelt et al., 2011). Generally, in PACE the target gene is distributed between bacterial host cells in continuous cultivations by modified M13 phages whose infection functionality is dependent on the target proteins activities (Dickinson et al., 2014; Esvelt et al., 2011). Due to the fast phage life cycle, an average of 38 phage generations harbouring mutated versions of the desired protein, can be generated in 24 h (Esvelt et al., 2011). PACE has been successfully applied to evolve T7 RNA polymerase in *E. coli* towards the recognition of different promoter sequences (Esvelt et al., 2011), for 30-fold increased drug resistance of hepatitis C virus proteases and subsequent characterization of the emerged mutations (Dickinson et al., 2014), or for changed substrate specificity of tobacco etch virus protease towards a different cleaving target sequence (Packer et al., 2017). Finally, recent work applied PACE in a non-continuous way (PANCE) to improve V_{max} of Mdh2 from *B. methanolicus* 3.5-

fold, which also led to twice as much *in vivo* assimilation of methanol carbon into central metabolites in *E. coli* (Roth et al., 2019). Further PACE or PANCE approaches show a high potential for the rapid evolution of enzymatic properties and might be useful to further improve *C. glutamicum* methanol utilization in the future (Figure 31C).

Further ways of improving methanol oxidation, as mentioned in the previous chapter, is the efficient assimilation of formaldehyde into central carbon metabolites (Price et al., 2016; Whitaker et al., 2015; Woolston et al., 2018a) and the change of NAD^+/NADH ratios in the cell (Chen et al., 2018; Meyer et al., 2018)(Figure 31A). Mutations affecting TCA cycle activity, as well as NAD^+/NADH metabolism found in evolved methanol-dependent *E. coli* and *C. glutamicum* strains (Chapter 4.4), were all considered to positively influence methanol oxidation by the increased availability of NAD^+ for the NAD^+ dependent methanol oxidation reaction (Chen et al., 2018; Meyer et al., 2018; Tuyishime et al., 2018). Furthermore, TCA cycle activity is downregulated in *B. methanolicus* growing on methanol as sole carbon source, revealing its unimportance in natural methylotrophy (Müller et al., 2015a, 2015c). A viable option to engineer. *C. glutamicum* towards reduced TCA cycle activity for reduced NADH production to benefit methanol oxidation could be the deletion of the *odhA* gene (2-oxoglutarate dehydrogenase), as it was applied for overproduction of L-glutamate in *C. glutamicum* (Asakura et al., 2007). Possible accumulated 2-oxoglutarate/L-glutamate could further be used for methanol-based production of ornithine, proline, putrescine or GABA (Jensen et al., 2015; Jensen and Wendisch, 2013; Jorge et al., 2016). Alternatively, TCA activity could be altered by changing the start codon of *odhA* from ATG to TTG, which resulted in 5-fold reduced OdhA enzyme activity in a putrescine producing *C. glutamicum* strain (Nguyen et al., 2015).

To achieve increased formaldehyde fixation, a self-assembling supramolecular enzyme complex of Mdh3 from *B. methanolicus* and a Hps-Phi fusion from *M. gastri* was engineered to benefit substrate channelling of formaldehyde towards F6-P formation by Hps and Phi (Price et al., 2016). Application of this strategy in *E. coli* led to a 9-fold improvement of the methanol consumption rate in comparison to a strain expressing the non-assembled enzymes (Price et al.,

2016). The introduction of lactate dehydrogenase (Ldh) as NADH sink increased methanol oxidation more than two-fold *in vitro*, underlining the significant role of NAD^+ availability for the oxidation reaction (Price et al., 2016). The addition of an NADH sink in form of POS5 from *S. cerevisiae* also revealed a 1.3-fold increased methanol consumption in *E. coli* strains engineered for L-lysine production from glucose and methanol (Wang et al., 2019). Additionally, increased formaldehyde consumption by an improved supply of Ru5-P for RuMP pathway reactions through inhibition of glycolytic reactions with iodoacetate and simultaneous overexpression of endogenous *glpX* (fructose-1,6-bisphosphatase), led to a 2-fold increase of methanol utilization in *E. coli* (Woolston et al., 2018a). Both, substrate channelling and the introduction of NADH consuming reactions, show potential to further improve the oxidation of methanol and subsequent assimilation of formaldehyde into the central carbon metabolism in synthetic methylotrophs (Figure 31A).

In methylotrophic yeasts, such as *Pichia pastoris*, methanol utilization takes place in peroxisomes, separate compartments that ensure physical proximity of methanol oxidation and subsequent formaldehyde fixation and shield the rest of the cell from formaldehyde toxicity (van der Klei et al., 2006; Yurimoto et al., 2011). To mimic this kind of environment for methanol utilization reactions in synthetic methylotroph prokaryotes, synthetic scaffolds made of noncoding RNA (Delebecque et al., 2012; Polka et al., 2016) or synthetic microcompartments to encapsulate the participating enzymes and substrates (Chessher et al., 2015; Frank et al., 2013; Siu et al., 2015) might be a viable option to further optimize methanol utilization (Figure 31A). Microcompartments have already been successfully formed in *C. glutamicum* through heterologous expression of shell proteins of the propanediol utilization (Pdu) compartment from *Citrobacter freundii* (Huber et al., 2017). Furthermore, the targeted localization of yellow fluorescent protein (YFP) into the synthetic microcompartments was shown to be successful (Huber et al., 2017). Since it is possible to form microcompartments in *C. glutamicum*, investigation of microcompartment assembly for methanol-utilizing enzymes, as well as efficient import of Ru5-P for formaldehyde fixation and export of F6-P, can further establish efficient methanol utilization.

Discussion and Outlook

To circumvent the limitations of methanol oxidation and to focus on the evolution of formaldehyde fixing reactions, different substrates such as sarcosine or vanillate might be applied to yield formaldehyde during utilization(He et al., 2018; Merkens et al., 2005)(Figure 31B). Vanillate gets demethylated to protocatechuate by *vanAB* (vanillate demethylase subunits A and B) in *C. glutamicum* yielding formaldehyde (Merkens et al., 2005), which was already used to verify the function of *fadH* (formaldehyde dehydrogenase) in deletion and complementation mutants (Leßmeier et al., 2013). Overexpression of *vanAB* in addition to RuMP pathway enzymes *hxlAB* in *C. glutamicum* Δ*ald* Δ*fadH* Δ*rpe*/Δ*rpi*, together with ribose/gluconate as co-substrate should lead to biomass formation, derived from the vanillate-emerging formaldehyde. To prevent growth on vanillate alone, the genes *pcaGH* (protocatechuate 3,4-dioxygenase) essential for protocatechuate metabolism (Brinkrolf et al., 2006) should be additionally deleted, to create a dependency on formaldehyde fixation for ALE. Previous work has followed a similar approach in *E. coli*, using sarcosine as alternative formaldehyde source for RuMP pathway assimilation (He et al., 2018). Sarcosine oxidation by sarcosine oxidase (SOX) from *Bacillus sp*. strain B-0618 yields glycine and formaldehyde (Chen et al., 2008), which was exploited for biomass formation from formaldehyde with xylose in an engineered glycine auxotroph (Δ*glyA* = serine hydroxymethyltransferase, Δ*gcl* = glyoxylate carboligase) and RuMP pathway enzymes (*hps*, *phi*) and SOX expressing *E. coli* strain with additional deletions of *frmRAB*, *zwf* (glucose-6-phosphate dehydrogenase) and *tktAB* (transketolase) (He et al., 2018). Deletion of *tkt* created a metabolic cut-off that forced carbon flux through RuMP pathway reactions and led to a growth dependency on sarcosine oxidation and subsequent formaldehyde fixation. This resulted in a strain that showed 85% of biomass precursors produced from formaldehyde and xylose through RuMP pathway reactions (He et al., 2018). However, no attempt of ALE was made in the reported work, leaving the opportunity to further improve formaldehyde fixation while circumventing methanol oxidation, which might be a valuable approach in the future (Figure 31B).

Discussion and Outlook

Another major challenge for synthetic methylotrophy is continuous Ru5-P regeneration for formaldehyde fixation to allow growth on methanol as sole carbon source (Whitaker et al., 2015). To increase PPP activity for Ru5-P regeneration, one option might be to delete genes encoding the transcriptional regulators GntK1/2 that repress the expression of PPP enzymes in absence of gluconate in *C. glutamicum* (Frunzke et al., 2008b; Toyoda and Inui, 2016). Another approach might be the overexpression of PPP enzymes from plasmids, independently from cellular regulation mechanisms. Additional genomic integration of *rpe*, *tkt*, *fba*, *glpX* and *pfk* and their expression from synthetic promoters, together with a deletion of *pgi* and *frmA* in *E. coli* already showed successful regeneration of Ru5-P by revealing pyruvate labelled at all carbon positions from ^{13}C-methanol (Bennett et al., 2018). Several copies of PPP enzymes could be integrated into the *C. glutamicum* genome to benefit Ru5-P regeneration. A similar approach was followed to improve L-lysine production in the L-lysine overproducing strain *C. glutamicum* GRLys1, when two additional copies of several key enzymes for L-lysine production were integrated into the genome for additional expression (Pérez-García et al., 2016; Unthan et al., 2015).
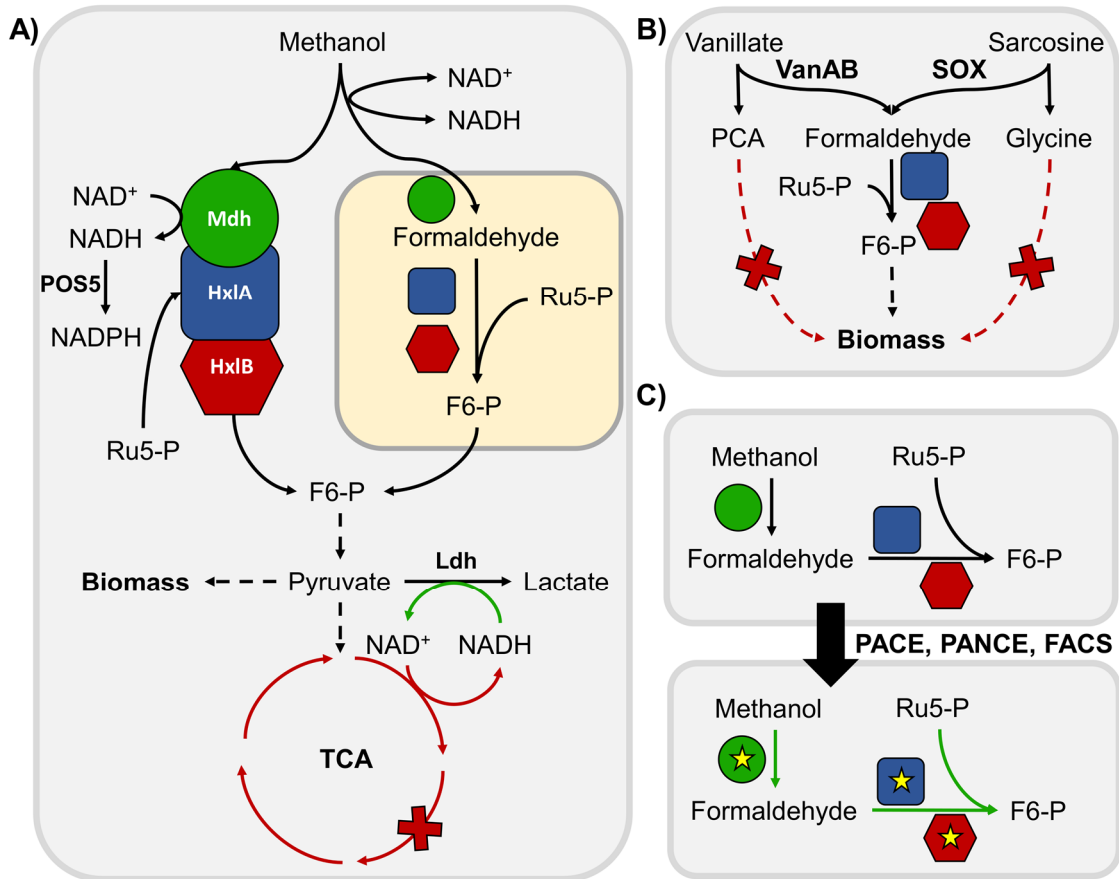
Figure 31: Overview of different approaches to improve methanol oxidation and formaldehyde fixation in synthetic methylotrophy.

A) Clustering of methanol-utilizing RuMP pathway enzymes Mdh (methanol dehydrogenase) (green circle), HxlA (3-hexulose-6-phosphate synthase) (blue square) and HxlB (6-phospho-3-hexuloisomerase)(red hexagon) or methanol utilization in synthetic compartments. Disruption of the TCA cycle and additional "NADH sink" reactions catalysed by Ldh (lactate dehydrogenase) and POS5 (peroxide sensitive NADH kinase) increase NAD+ availability for methanol oxidation. B) Application of vanillate and sarcosine as alternative formaldehyde sources to circumvent methanol oxidation. Utilization of vanillate by VanAB (vanillate demethylase subunits A and B) yields formaldehyde and PCA (protocatechuic acid), sarcosine oxidation by SOX (sarcosine oxidase) yields formaldehyde and glycine. Deletions in PCA and glycine metabolism to prevent biomass formation create formaldehyde dependency for the evolution of RuMP pathway enzymes. C) Enzyme evolution through PACE (phage-assisted continuous evolution), PANCE (phage-assisted non-continuous evolution) and FACS (fluorescence activated cell sorting) potentially results in methanol-utilizing enzymes with improved properties (yellow star). Dotted arrows represent multiple reactions, green arrows indicate increased activity, red arrows indicate reduced activity. Red crosses depict genomic deletions. Additional abbreviations: Ru5-P (ribulose-5-phosphate), F6-P (fructose-6-phosphate).

4.8 Expanding the C1 substrate spectrum of *C. glutamicum*

Current effort points to the establishment of methanol as carbon source in *C. glutamicum*. This achievement would bring several advantages for the biotechnological industry (Chapter 1.1). In the future, a considerable challenge is to expand the *C. glutamicum* substrate spectrum of C1 carbon sources for the utilization of formate, methane or CO_2.

4.8.1 <u>Formate</u>

To build upon an established synthetic methylotroph metabolism in the future, formate could be reduced to formaldehyde for further assimilation in RuMP pathway reactions (Bar-Even, 2016). For formate reduction, acetyl-CoA synthase from *E. coli* in combination with acetaldehyde dehydrogenase from *Listeria monocytogenes* have been proposed to catalyse the reactions that generate formyl-CoA from formate, eventually yielding formaldehyde (Siegel et al., 2015). Heterologous expression of those two enzymes might allow formate assimilation for biomass formation in synthetic methylotroph *C. glutamicum* in the future. Recent work focused on exploiting the reductive glycine pathway of *E. coli* for formate and CO_2 fixation through heterologous expression of formate-tetrahydrofolate ligase (*ftfL*), 5,10-methenyl-tetrahydrofolate cyclohydrolase (*fchA*) and 5,10-methylene-tetrahydrofolate cyclohydrolase (*mtdA*) from *M. extorquens* and successfully managed to couple growth to formate consumption (Bang et al., 2018; Döring et al., 2018; Yishai et al., 2018). Adaption of this approach to *C. glutamicum* would not require previously established synthetic methylotrophy since formate fixation is realized independently from RuMP pathway reactions, through H_4F and GCS intermediates, to eventually end up in glycine (Döring et al., 2018; Yishai et al., 2018). However, there is no GCS known to be present in *C. glutamicum*, which would require the additional heterologous expression of aminomethyltransferase (*gcvT*), glycine decarboxylase (*gcvP*) and H protein of the GCS (*gcvH*) from *E. coli* to potentially allow formate and CO_2 fixation (Yishai et al., 2018).

4.8.2 Methane

To achieve methane utilization, a single-step oxidation of methane to methanol is needed before metabolization in a synthetic methylotroph organism (Haynes and Gonzalez, 2014). The oxidation reaction of methane to methanol is energetically unfavourable (Whitaker et al., 2015) but some *Methylococcus* and *Methylomonas* species express methane monooxygenases (MMOs) catalyzing the reaction (Haynes and Gonzalez, 2014). Heterologous expression of MMO in synthetic methylotroph *C. glutamicum* might open methane utilization for biomass and product formation, although calculated total energy and carbon efficiencies for the hypothetical product n-butanol were low with only 51% and 67% respectively, due to the high energy demand of methane oxidation (Haynes and Gonzalez, 2014; Whitaker et al., 2015).

4.8.3 CO_2

Since methanol has a high degree of reduction, it was proposed before that excess of electrons from its utilization might be beneficial to drive CO_2 reduction to formaldehyde by formate- and formaldehyde dehydrogenases (Whitaker et al., 2015). Following this approach, co-utilization of methanol and CO_2 might be achieved through heterologous expression of CO_2 reducing enzymes in synthetic methylotroph *C. glutamicum.* A similar approach was already realized in the natural methylotroph *M. extorquens,* by heterologous expression of CBB cycle enzymes phosphoribulokinase (*prk*) and RuBisCO from *Paracoccus denitrificans* DSM 413 to allow co-utilization of CO_2 and methanol (von Borzyskowski et al., 2018). Functional CO_2 fixation was confirmed by ^{13}C tracer analysis, revealing multiply labelled hexose phosphates from labelled CO_2 (glucose-6-phosphate, glucose-1-phosphate and F6-P), indicating that the CBB cycle functionally turned multiple times (von Borzyskowski et al., 2018).

Previous work in *E. coli* reported successful CO_2 fixation for sugar synthesis by decoupling energy production and carbon fixation through deletion of phosphoglycerate mutase genes (*gpmA* and *gpmM*), heterologous expression of CBB cycle enzymes *prkA* from *Synechococcus elongatus* PCC 7942 and RuBisCO from *Rhodospirillum rubrum* ATCC 11170 and subsequent ALE

(Antonovsky et al., 2016). Since Ru5-P is needed as central metabolite for PrkA and ensuing RuBisCO reactions to assimilate CO_2 (Antonovsky et al., 2016) and synthetic methylotroph *C. glutamicum* will necessarily have elevated Ru5-P regeneration to allow growth on methanol, heterologous expression of CBB cycle enzymes might lead to significant CO_2 fixation that may possibly be further optimized by ALE.

5. <u>Concluding remarks</u>

Past work on synthetic methylotrophy in *C. glutamicum* has revealed incorporation of methanol-carbon into central metabolites and methanol dependent biomass formation with xylose. Here, the main goal was to achieve methanol-dependent biomass formation of *C. glutamicum* through a metabolic cut-off in the central carbon metabolism and subsequent improvement through ALE, as well as investigation of beneficial mutations in evolved strains.

Methanol-dependent growth of *C. glutamicum* was achieved with the 3 different co-substrates (ribose, xylose and gluconate) for the first time, by creation of two different metabolic cut-off strains. Moreover, ALE led to improved methanol-dependent growth with ribose until the artificially created metabolic cut-off was fully complemented by methanol utilization and biomass formation of *C. glutamicum* WT with equal ribose amounts was reached. Investigation of chromosomal mutations in evolved methanol-dependent *C. glutamicum* strains revealed 3 significant changes (*metK*, cg3104, *ribGCAH*) that need further investigation to confirm the proposed hypotheses. Furthermore, methanol-dependent production of the non-natural product cadaverine was achieved here for the first time and isotopic labelling experiments revealed approximately 4-times as much total incorporation of methanol-derived carbon into cadaverine compared to previous studies.

The results presented here will serve as basis for future engineering approaches towards synthetic methylotrophy in *C. glutamicum* for growth and production of valuable compounds solely from the non-food C1-carbon source methanol.

6. <u>Literature</u>

Albersmeier, A., Pfeifer-Sancar, K., Rückert, C., Kalinowski, J., 2017. Genome-wide determination of transcription start sites reveals new insights into promoter structures in the actinomycete *Corynebacterium glutamicum*. J. Biotechnol. 257, 99–109. https://doi.org/10.1016/j.jbiotec.2017.04.008

Altschul, S.F., Gish, W., Miller, W., Myers, E.W., Lipmann, D.J., 1990. Basic Local Alignment Search Tool. J. Mol. Biol. 215, 403–410. https://doi.org/10.1016/S0022-2836(05)80360-2

Anthony, C., 1983. The biochemistry of methylotrophs, London: Academic. https://doi.org/10.1016/0300-9629(83)90116-0

Antonovsky, N., Gleizer, S., Noor, E., Zohar, Y., Herz, E., Barenholz, U., Zelcbuch, L., Amram, S., Wides, A., Tepper, N., Davidi, D., Bar-On, Y., Bareia, T., Wernick, D.G., Shani, I., Malitsky, S., Jona, G., Bar-Even, A., Milo, R., 2016. Sugar Synthesis from CO_2 in Escherichia coli. Cell 166, 115–125. https://doi.org/10.1016/j.cell.2016.05.064

Aresta, M., Dibenedetto, A., 2007. Utilisation of CO_2 as a chemical feedstock: opportunities and challenges, in: Dalton Transactions. pp. 2975–2992. https://doi.org/10.1039/b700658f

Arfman, N., Van Beeumen, J., De Vries, G.E., Harder, W., Dijkhuizen, L., 1991. Purification and characterization of an activator protein for methanol dehydrogenase from thermotolerant *Bacillus* spp. J. Biol. Chem. 266, 3955–3960.

Arfman, N., Watling, E.M., Clement, W., van Oosterwijk, R.J., de Vries, G.E., Harder, W., Attwood, M.M., Dijkhuizen, L., Dijkhuizenl, L., 1989. Methanol metabolism in thermotolerant methylotrophic *Bacillus* strains involving a novel catabolic NAD-dependent methanol dehydrogenase as a key enzyme. Arch. Microbiol. 152, 280–288.

Asakura, Y., Kimura, E., Usuda, Y., Kawahara, Y., Matsui, K., Osumi, T., Nakamatsu, T., 2007. Altered metabolic flux due to deletion of odhA causes L-glutamate overproduction in *Corynebacterium glutamicum*. Appl. Environ. Microbiol. 73, 1308–1319. https://doi.org/10.1128/AEM.01867-06

Auchter, M., Laslo, T., Fleischer, C., Schiller, L., Arndt, A., Gaigalat, L., Kalinowski, J., Eikmanns, B.J., 2011. Control of adhA and sucR expression by the SucR regulator in Corynebacterium glutamicum. J. Biotechnol. 152, 77–86. https://doi.org/10.1016/j.jbiotec.2011.02.003

Bacher, A., Eberhardt, S., Fischer, M., Kis, K., Richter, G., 2000. Biosynthesis of Vitamin B_2 (Riboflavin). Annu. Rev. Nutr. 20, 153–167. https://doi.org/10.1146/annurev.micro.58.030603.123615

Bacher, A., Herz, S., Richter, G., Fischer, M., Eberhardt, S., Kis, K., Illarionov, B., Eisenreich, W., 2001. Biosynthesis of riboflavin. Vitam. Horm. 61, 1–49. https://doi.org/10.1016/s0083-6729(01)61001-x

Literature

Bang, J., Yup, S., Lee, S.Y., 2018. Assimilation of formic acid and CO2 by engineered *Escherichia coli* equipped with reconstructed one-carbon assimilation pathways. PNAS 115, E9271–E9279. https://doi.org/10.1073/pnas.1810386115

Bar-Even, A., 2016. Formate Assimilation: The Metabolic Architecture of Natural and Synthetic Pathways. Biochemistry 55, 3851–3863. https://doi.org/10.1021/acs.biochem.6b00495

Bar-even, A., Noor, E., Milo, R., 2011. A survey of carbon fixation pathways through a quantitative lens. J. Exp. Bot. 63, 2325–2342. https://doi.org/10.1093/jxb/err417

Barbato, L., Centi, G., Iaquaniello, G., Mangiapane, A., Perathoner, S., 2014. Trading Renewable Energy by using CO_2: An Effective Option to Mitigate Climate Change and Increase the use of Renewable Energy Sources. Energy Technol. 2, 453–461. https://doi.org/10.1002/ente.201300182

Barrett, E., Stanton, C., Zelder, O., Fitzgerald, G., Ross, R.P., 2004. Heterologous expression of lactose- and galactose-utilizing pathways from lactic acid bacteria in *Corynebacterium glutamicum* for production of lysine in whey, in: Applied and Environmental Microbiology. pp. 2861–2866. https://doi.org/10.1128/AEM.70.5.2861-2866.2004

Basu, T., Poddar, R.K., 1997. Overexpression of inducible proteins in *Escherichia Coli* by treatment with ethanol. Biochem. Mol. Biol. Int. 41, 1093–1100.

Basu, T., Poddar, R.K., 1994. Effect of ethanol on *Escherichia coli* cells. Enhancement of DNA synthesis due to ethanol treatment. Folia Microbiol. Off. J. Inst. Microbiol. Acad. Sci. Czech Repub. 39, 3–6. https://doi.org/10.1007/BF02814520

Baumbach, J., Azevedo, V., Tauch, A., Rottger, R., Pauling, J., 2011. CoryneRegNet 6.0--Updated database content, new analysis methods and novel features focusing on community demands. Nucleic Acids Res. 40, D610–D614. https://doi.org/10.1093/nar/gkr883

Beck, H.J., Moll, I., 2018. Leaderless mRNAs in the Spotlight: Ancient but Not Outdated! Regul. with RNA Bact. Archaea 155–170. https://doi.org/10.1128/microbiolspec.rwr-0016-2017

Becker, J., Wittmann, C., 2015. Advanced Biotechnology: Metabolically Engineered Cells for the Bio-Based Production of Chemicals and Fuels, Materials, and Health-Care Products. Angew. Chemie Int. Ed. 54, 3328–3350. https://doi.org/10.1002/anie.201409033

Becker, J., Zelder, O., Häfner, S., Schröder, H., Wittmann, C., Häfner, S., Schröder, H., Wittmann, C., 2011. From zero to hero-Design-based systems metabolic engineering of *Corynebacterium glutamicum* for L-lysine production, in: Metabolic Engineering. pp. 159–168. https://doi.org/10.1016/j.ymben.2011.01.003

Bennett, R.K., Gonzalez, J.E., Whitaker, W.B., Antoniewicz, M.R., Papoutsakis, E.T., 2018. Expression of heterologous non-oxidative pentose phosphate pathway from Bacillus methanolicus and phosphoglucose isomerase deletion improves methanol assimilation and metabolite production by a synthetic Escherichia coli methylotroph. Metab. Eng. 45, 75–85. https://doi.org/10.1016/j.ymben.2017.11.016

Bentley, W.E., Mirjalili, N., Kompala, D.S., Andersen, D.C., Davis, R.H., 1990. Plasmid-encoded protein: The principal factor in the "metabolic burden" associated with recombinant bacteria. Biotechnol. Bioeng. 35, 668–681. https://doi.org/10.1002/bit.260350704

Bertani, G., 1951. Studies on lysogenesis. I. The mode of phage liberation by lysogenic *Escherichia coli*. J. Bacteriol. 62, 293–300.

Bertau, M., Effenberger, F.X., Keim, W., Menges, G., Offermanns, H., 2010. Methanol findet zu wenig beachtung als kraftstoff und chemierohstoff der zukunft. Chemie-Ingenieur-Technik 82, 2055–2058. https://doi.org/10.1002/cite.201000159

Bertau, M., Offermanns, H., Plass, L., Schmidt, F., 2014. Methanol: The Basic Chemical and Energy Feedstock of the Future, Methanol: The Basic Chemical and Energy Feedstock of the Future. https://doi.org/10.1007/978-3-642-39709-7

Blombach, B., Seibold, G.M., 2010. Carbohydrate metabolism in *Corynebacterium glutamicum* and applications for the metabolic engineering of L-lysine production strains. Appl. Microbiol. Biotechnol. 86, 1313–1322. https://doi.org/10.1007/s00253-010-2537-z

Blug, M., Leker, J., Plass, L., Günther, A., 2014. Methanol generation economics, in: Methanol: The Basic Chemical and Energy Feedstock of the Future. Springer, pp. 603–618.

Bolten, C.J., Kiefer, P., Letisse, F., Portais, J., Wittmann, C., 2007. Sampling for Metabolome Analysis of Microorganisms. Anal. Chem. 79, 3843–3849. https://doi.org/10.1021/ac0623888

Bott, M., Niebisch, A., 2003. The respiratory chain of *Corynebacterium glutamicum*. J. Biotechnol. 104, 129–153. https://doi.org/10.1016/S0168-1656(03)00144-5

Bouzon, M., Perret, A., Loreau, O., Perchat, N., Weissenbach, J., Delmas, V., Taran, F., Marlière, P., 2017. A Synthetic Alternative to Canonical One-Carbon Metabolism. ACS Synth. Biol. 6, 1520–1533. https://doi.org/10.1021/acssynbio.7b00029

Bradford, M.M., 1976. A Rapid and Sensitive Method for the Quantitation Microgram Quantities of Protein Utilizing the Principle of Protein-Dye Binding, in: Analytical Biochemistry. pp. 248–254.

Literature

Brautaset, T., Bennaars, A., Crabbe, E., Williams, M.D., Kaufmann, C., Flickinger, M.C., Dillingham, R.D., 2003. Role of the *Bacillus methanolicus* Citrate Synthase II Gene, *citY*, in Regulating the Secretion of Glutamate in L-Lysine-Secreting Mutants. Appl. Environ. Microbiol. 69, 3986–3995. https://doi.org/10.1128/aem.69.7.3986-3995.2003

Brautaset, T., Ellingsen, T.E., Flickinger, M.C., Jakobsen, Ø.M., Netzer, R., Degnes, K.F., Nærdal, I., Dillingham, R., Krog, A., 2010. *Bacillus methanolicus* pyruvate carboxylase and homoserine dehydrogenase I and II and their roles for L-lysine production from methanol at 50°C. Appl. Microbiol. Biotechnol. 87, 951–964. https://doi.org/10.1007/s00253-010-2559-6

Brautaset, T., Jakobsen, Ø.M., Flickinger, M.C., Valla, S., Ellingsen, T.E., Jakobsen, O.M., Flickinger, M.C., Valla, S., Ellingsen, T.E., Jakobsen, Ø.M., Flickinger, M.C., Valla, S., Ellingsen, T.E., 2004. Plasmid-Dependent Methylotrophy in Thermotolerant *Bacillus methanolicus*. J. Bacteriol. 186, 1229–1238. https://doi.org/10.1128/JB.186.5.1229-1238.2004

Brautaset, T., Jakobsen, Ø.M., Josefsen, K.D., Flickinger, M.C., Ellingsen, T.E., 2007. *Bacillus methanolicus*: A candidate for industrial production of amino acids from methanol at 50°C, in: Applied Microbiology and Biotechnology. pp. 22–34. https://doi.org/10.1007/s00253-006-0757-z

Brinkrolf, K., Brune, I., Tauch, A., 2006. Transcriptional regulation of catabolic pathways for aromatic compounds in *Corynebacterium glutamicum*. Genet. Mol. Res. 5, 773–789.

Brinkrolf, K., Plöger, S., Solle, S., Brune, I., Nentwich, S.S., Hüser, A.T., Kalinowski, J., Pühler, A., Tauch, A., 2008. The LacI/GaIR family transcriptional regulator UriR negatively controls uridine utilization of *Corynebecterium glutamicum* by binding to catabolite-responsive element (cre)-like sequences. Microbiology 154, 1068–1081. https://doi.org/10.1099/mic.0.2007/014001-0

Brocker, M., Mack, C., Bott, M., 2011. Target genes, consensus binding site, and role of phosphorylation for the response regulator MtrA of *Corynebacterium glutamicum*. J. Bacteriol. 193, 1237–1249. https://doi.org/10.1128/JB.01032-10

Buschke, N., Becker, J., Schäfer, R., Kiefer, P., Biedendieck, R., Wittmann, C., 2013. Systems metabolic engineering of xylose-utilizing *Corynebacterium glutamicum* for production of 1,5-diaminopentane. Biotechnol. J. 8, 557–570. https://doi.org/10.1002/biot.201200367

Cantoni, G.L., 1975. Biological methylation: selected aspects. Annu. Rev. Biochem. 44, 435–51. https://doi.org/10.1146/annurev.bi.44.070175.002251

Celaje, J.J.A., Lu, Z., Kedzie, E.A., Terrile, N.J., Lo, J.N., Williams, T.J., 2016. A prolific catalyst for dehydrogenation of neat formic acid. Nat. Commun. 7, 11308. https://doi.org/10.1038/ncomms11308

Chattopadhyay, M.K., Ghosh, A.K., Sengupta, S., 1991. Control of methionine biosynthesis in *Escherichia coli* K12: a closer study with analogue-resistant mutants. J. Gen. Microbiol. 137, 685–691.

Chen, C.-T., Chen, F.Y.-H., Bogorad, I.W., Wu, T.-Y., Zhang, R., Lee, A.S., Liao, J.C., 2018. Synthetic methanol auxotrophy of *Escherichia coli* for methanol-dependent growth and production. Metab. Eng. 49, 257–266. https://doi.org/10.1016/j.ymben.2018.08.010

Chen, N.H., Djoko, K.Y., Veyrier, F.J., McEwan, A.G., 2016. Formaldehyde stress responses in bacterial pathogens. Front. Microbiol. 7, 1–17. https://doi.org/10.3389/fmicb.2016.00257

Chen, Z., Mathews, F.S., Zhao, G., Schuman Jorns, M., Hassan-Abdallah, A., 2008. Arginine 49 Is a Bifunctional Residue Important in Catalysis and Biosynthesis of Monomeric Sarcosine Oxidase: A Context-Sensitive Model for the Electrostatic Impact of Arginine to Lysine Mutations † , ‡ . Biochemistry 47, 2913–2922. https://doi.org/10.1021/bi702351v

Cherest, H., Surdin-Kerjan, Y., Exinger, F., Lacroute, F., 1978. S-adenosyl methionine requiring mutants in *Saccharomyces cerevisiae*: Evidences for the existence of two methionine adenosyl transferases. MGG Mol. Gen. Genet. 163, 153–167. https://doi.org/10.1007/BF00267406

Chessher, A., Breitling, R., Takano, E., 2015. Bacterial Microcompartments: Biomaterials for Synthetic Biology-Based Compartmentalization Strategies. ACS Biomater. Sci. Eng. 1, 345–351. https://doi.org/10.1021/acsbiomaterials.5b00059

Chiang, P.K., Gordon, R.K., Tal, J., Zeng, G.C., Doctor, B.P., Pardhasaradhi, K., McCann, P.P., 1996. S-Adenosylmethionine methylation. FASEB J. 10, 471–480.

Chistoserdova, L., 2018. Applications of methylotrophs: can single carbon be harnessed for biotechnology? Curr. Opin. Biotechnol. 50, 189–194. https://doi.org/10.1016/j.copbio.2018.01.012

Chistoserdova, L., 2015. Methylotrophs in natural habitats: current insights through metagenomics. Appl. Microbiol. Biotechnol. 99, 5763–5779. https://doi.org/10.1007/s00253-015-6713-z

Chistoserdova, L., 2011. Modularity of methylotrophy, revisited. Environ. Microbiol. 13, 2603–2622. https://doi.org/10.1111/j.1462-2920.2011.02464.x

Chistoserdova, L., Kalyuzhnaya, M.G., Lidstrom, M.E., 2009. The Expanding World of Methylotrophic Metabolism. Annu. Rev. Microbiol. 63, 477–499. https://doi.org/10.1146/annurev.micro.091208.073600

Cho, H.Y., Lee, S.G., Hyeon, J.E., Han, S.O., 2010. Identification and characterization of a transcriptional regulator, SucR, that influences sucCD transcription in *Corynebacterium glutamicum*. Biochem. Biophys. Res. Commun. 401, 300–305. https://doi.org/10.1016/j.bbrc.2010.09.057

Choo, S., Um, Y., Han, S.O., Woo, H.M., 2016. Engineering of Corynebacterium glutamicum to utilize methyl acetate, a potential feedstock derived by carbonylation of methanol with CO. J. Biotechnol. 224, 47–50. https://doi.org/10.1016/j.jbiotec.2016.03.011

Claassens, N.J., Sánchez-Andrea, I., Sousa, D.Z., Bar-Even, A., 2018. Towards sustainable feedstocks: A guide to electron donors for microbial carbon fixation. Curr. Opin. Biotechnol. 50, 195–205. https://doi.org/10.1016/j.copbio.2018.01.019

Clay, K.L., Murphy, R.C., Watrins, W.D., 1975. Experimental methanol toxicity in the primate: Analysis of metabolic acidosis. Toxicol. Appl. Pharmacol. 34, 49–61. https://doi.org/10.1016/0041-008X(75)90174-X

Connelly, J.C., De Leau, E.S., Leach, D.R.F., 1999. DNA cleavage and degradation by the SbcCD protein complex from *Escherichia coli*. Nucleic Acids Res. 27, 1039–1046. https://doi.org/10.1093/nar/27.4.1039

Connelly, J.C., De Leau, E.S., Okely, E.A., Leach, D.R.F., 1997. Overexpression, purification, and characterization of the SbcCD protein from *Escherichia coli*. J. Biol. Chem. 272, 19819–19826. https://doi.org/10.1074/jbc.272.32.19819

Connelly, J.C., Kirkham, L.A., Leach, D.R.F., 2002. The SbcCD nuclease of Escherichia coli is a structural maintenance of chromosomes (SMC) family protein that cleaves hairpin DNA. Proc. Natl. Acad. Sci. 95, 7969–7974. https://doi.org/10.1073/pnas.95.14.7969

Connelly, J.C., Leach, D.R.F., 1996. The sbcC and sbcD genes of Escherichia coli encode a nuclease involved in palindrome inviability and genetic recombination. Genes to Cells 1, 285–291. https://doi.org/10.1046/j.1365-2443.1996.23024.x

Couderc, R., Baratti, J., 1980. Oxidation of methanol by the yeast, Pichia pastoris. Purification and properties of the alcohol oxidase. Agric. Biol. Chem. 44, 2279–2289. https://doi.org/10.1271/bbb1961.44.2279

Dalena, F., Senatore, A., Marino, A., Gordano, A., Basile, M., Basile, A., 2017. Methanol Production and Applications: An Overview, in: Methanol: Science and Engineering. Elsevier B.V., pp. 3–28. https://doi.org/10.1016/B978-0-444-63903-5.00001-7

Darmon, E., Lopez-Vernaza, M.A., Helness, A.C., Borking, A., Wilson, E., Thacker, Z., Wardrope, L., Leach, D.R.F., 2007. SbcCD regulation and localization in *Escherichia coli*. J. Bacteriol. 189, 6686–6694. https://doi.org/10.1128/JB.00489-07

Deb, J.K., Nath, N., 1999. Plasmids of corynebacteria. FEMS Microbiol. Lett. 175, 11–20. https://doi.org/10.1016/s0378-1097(99)00104-4

Del Solar, G., Giraldo, R., Ruiz-Echevarria, M.J., Espinosa, M., Diaz-Orejas, R., 1998. Replication and control of circular bacterial plasmids. Microbiol. Mol. Biol. Rev. 62, 434–464. https://doi.org/10.1016/S0025-3227(97)00030-3

Delebecque, C.J., Silver, P.A., Lindner, A.B., 2012. Designing and using RNA scaffolds to assemble proteins in vivo. Nat. Protoc. 7, 1797–1807. https://doi.org/10.1038/nprot.2012.102

Dickinson, B.C., Packer, M.S., Badran, A.H., Liu, D.R., 2014. A system for the c of proteases rapidly reveals drug-resistance mutations. Nat. Commun. 5, 5352. https://doi.org/10.1038/ncomms6352

Literature

Dijkhuizen, L., Arfman, N., Attwood, M.M., Brooke, A.G., Watling, E.M., Harder, W., 1988. Isolation and initial characterization of thermotolerant methylotrophic *Bacillus* strains. FEMS Microbiol. Lett. 52, 209–214. https://doi.org/10.1111/j.1574-6968.1988.tb02597.x

Dijkhuizen, L., Harder, W., 1984. Current views on the regulation of autotrophic carbon dioxide fixation via the calvin cycle in bacteria. Antonie van Leeuwenhoek, Int. J. Gen. Mol. Microbiol. 50, 473–487.

Dominguez, H., Rollin, C., Guyonvarch, A., Guerquin-Kern, J.L., Cocaign-Bousquet, M., Lindley, N.D., 1998. Carbon-flux distribution in the central metabolic pathways of *Corynebacterium glutamicum* during growth on fructose. Eur. J. Biochem. 254, 96–102. https://doi.org/10.1046/j.1432-1327.1998.2540096.x

Döring, V., Darii, E., Yishai, O., Bar-Even, A., Bouzon, M., 2018. Implementation of a Reductive Route of One-Carbon Assimilation in *Escherichia coli* through Directed Evolution. ACS Synth. Biol. 7, 2029–2036. https://doi.org/10.1021/acssynbio.8b00167

Eggeling, L., Bott, M., 2004. Experiments, in: Handbook of Corynebacterium Glutamicum. pp. 421–422. https://doi.org/10.1007/s10750-004-4543-6

Ehira, S., Shirai, T., Teramoto, H., Inui, M., Yukawa, H., 2008. Group 2 sigma factor sigB of *Corynebacterium glutamicum* positively regulates glucose metabolism under conditions of oxygen deprivation. Appl. Environ. Microbiol. 74, 5146–5152. https://doi.org/10.1128/AEM.00944-08

Eikmanns, B., 2005. Central Metabolism: Tricarboxylic Acid Cycle and Anaplerotic Reactions, in: Handbook of Corynebacterium Glutamicum. pp. 241–276. https://doi.org/10.1201/9781420039696.ch11

Eikmanns, B.J., Follettie, M.T., Griot, M.U., Sinskey, A.J., 1989. The phosphoenolpyruvate carboxylase gene of *Corynebacterium glutamicum*: Molecular cloning, nucleotide sequence, and expression. MGG Mol. Gen. Genet. 218, 330–339. https://doi.org/10.1007/BF00331286

Eikmanns, B.J., Thum-schmitz, N., Eggeling, L., Ludtke, K., Sahm, H., 1994. Nucleotide sequence, expression and transcriptional analysis of the *Corynebacterium glutamicum gltA* gene encoding citrate synthase. Microbiology 140, 1817–1828.

El-Hajj, Z.W., Reyes-Lamothe, R., Newman, E.B., 2013. Cell division, one-carbon metabolism and methionine synthesis in a *metK*-deficient *Escherichia coli* mutant, and a role for MmuM. Microbiol. (United Kingdom) 159, 2036–2048. https://doi.org/10.1099/mic.0.069682-0

Engstrom, M.D., Pfleger, B.F., 2017. Transcription control engineering and applications in synthetic biology. Synth. Syst. Biotechnol. 2, 176–191. https://doi.org/10.1016/j.synbio.2017.09.003

Erb, T.J., Berg, I.A., Brecht, V., Müller, M., Fuchs, G., Alber, B.E., 2007. Synthesis of C5 -dicarboxylic acids from C2 -units involving crotonyl-CoA carboxylase/reductase: The ethylmalonyl-CoA pathway. PNAS 104, 1–6.

Literature

Erb, T.J., Jones, P.R., Bar-Even, A., 2017. Synthetic metabolism: metabolic engineering meets enzyme design. Curr. Opin. Chem. Biol. 37, 56–62. https://doi.org/10.1016/j.cbpa.2016.12.023

Espah Borujeni, A., Channarasappa, A.S., Salis, H.M., 2014. Translation rate is controlled by coupled trade-offs between site accessibility, selective RNA unfolding and sliding at upstream standby sites. Nucleic Acids Res. 42, 2646–2659. https://doi.org/10.1093/nar/gkt1139

Esvelt, K.M., Carlson, J.C., Liu, D.R., 2011. A system for the continuous directed evolution of biomolecules. Nature 472, 499–503. https://doi.org/10.1038/nature09929

Fast, A.G., Papoutsakis, E.T., 2012. Stoichiometric and energetic analyses of non-photosynthetic CO_2-fixation pathways to support synthetic biology strategies for production of fuels and chemicals. Curr. Opin. Chem. Eng. 1, 380–395. https://doi.org/10.1016/j.coche.2012.07.005

Fei, Q., Guarnieri, M.T., Tao, L., Laurens, L.M.L., Dowe, N., Pienkos, P.T., 2014. Bioconversion of natural gas to liquid fuel: Opportunities and challenges. Biotechnol. Adv. 32, 596–614. https://doi.org/10.1016/j.biotechadv.2014.03.011

Fernandez-Gonzalez, C., Cadenas, R.F., Noirot-Gros, M.F., Martin, J.F., Gil, J.A., 1994. Characterization of a region of plasmid pBL1 of *Brevibacterium lactofermentum* involved in replication via the rolling circle model. J. Bacteriol. 176, 3154–3161. https://doi.org/10.1128/jb.176.11.3154-3161.1994

Fontecave, M., Atta, M., Mulliez, E., 2004. S-adenosylmethionine: Nothing goes to waste. Trends Biochem. Sci. 29, 243–249. https://doi.org/10.1016/j.tibs.2004.03.007

Frank, S., Lawrence, A.D., Prentice, M.B., Warren, M.J., 2013. Bacterial microcompartments moving into a synthetic biological world. J. Biotechnol. 163, 273–279. https://doi.org/10.1016/j.jbiotec.2012.09.002

Frenkel, C., Peters, J.S., Tieman, D.M., Tiznado, M.E., Handa, A.K., 1998. Pectin methylesterase regulates methanol and ethanol accumulation in ripening tomato (*Lycopersicon esculentum*) fruit. J. Biol. Chem. 273, 4293–4295. https://doi.org/10.1074/jbc.273.8.4293

Friehs, K., 2012. Plasmid Copy Number and Plasmid Stability, in: New Trends and Developments in Biochemical Engineering. Advances in Biochemical Engineering Vol. 86. pp. 47–82. https://doi.org/10.1007/b12440

Frunzke, J., Bramkamp, M., Schweitzer, J., Bott, M., 2008a. Population Heterogeneity in *Corynebacterium glutamicum* ATCC 13032 Caused by Prophage CGP3 □, in: Journal of Bacteriology. pp. 5111–5119.

Frunzke, J., Engels, V., Hasenbein, S., Gätgens, C., Bott, M., 2008b. Co-ordinated regulation of gluconate catabolism and glucose uptake in *Corynebacterium glutamicum* by two functionally equivalent transcriptional regulators, GntR1 and GntR2. Mol. Microbiol. 67, 305–322. https://doi.org/10.1111/j.1365-2958.2007.06020.x

Literature

García-Angulo, V.A., 2017. Overlapping riboflavin supply pathways in bacteria. Crit. Rev. Microbiol. 43, 196–209. https://doi.org/10.1080/1040841X.2016.1192578

Georgi, T., Rittmann, D., Wendisch, V.F., 2005. Lysine and glutamate production by *Corynebacterium glutamicum* on glucose , fructose and sucrose : Roles of malic enzyme and. Metab. Eng. 7, 291–301. https://doi.org/10.1016/j.ymben.2005.05.001

Gerstmeir, R., Wendisch, V.F., Schnicke, S., Ruan, H., Farwick, M., Reinscheid, D., Eikmanns, B.J., 2003. Acetate metabolism and its regulation in *Corynebacterium glutamicum*. J. Biotechnol. 104, 99–122. https://doi.org/10.1016/S0168-1656(03)00167-6

Gibson, D.G., Young, L., Chuang, R.-Y., Venter, J.C., Hutchison, C. a, Smith, H.O., 2009. "Enzymatic assembly of DNA molecules up to several hundred kilobases." Nat. Methods 6, 343–345.

Goeppert, A., Olah, G.A., Prakash, G.K.S., 2018. Toward a Sustainable Carbon Cycle : The Methanol Economy, in: Green Chemistry. Elsevier Inc., pp. 919–962. https://doi.org/https://doi.org/10.1016/B978-0-12-809270-5.00031-5

Gonzalez, C.F., Proudfoot, M., Brown, G., Korniyenko, Y., Mori, H., Savchenko, A. V., Yakunin, A.F., 2006. Molecular basis of formaldehyde detoxification: Characterization of two S-formylglutathione hydrolases from *Escherichia coli*, FrmB and YeiG. J. Biol. Chem. 281, 14514–14522. https://doi.org/10.1074/jbc.M600996200

Gordon, D., Abajian, C., Green, P., 1998. Consed: a graphical tool for sequence finishing. Genome Res. 8, 195–202.

Gosset, G., Zhang, Z., Nayyar, S., Cuevas, W.A., Saier, M.H., 2004. Transcriptome analysis of Crp-dependent catabolite control of gene expression in *Escherichia coli*. J. Bacteriol. 186, 3516–3524. https://doi.org/10.1128/JB.186.11.3516-3524.2004

Grob, N.M., Behe, M., von Guggenberg, E., Schibli, R., Mindt, T.L., 2017. Methoxinine - an alternative stable amino acid substitute for oxidation-sensitive methionine in radiolabelled peptide conjugates. J. Pept. Sci. 23, 38–44. https://doi.org/10.1002/psc.2948

Grossmann, K., Herbster, K., Mack, M., 2000. Rapid cloning of *metK* encoding methionine adenosyltransferase from *Corynebacterium glutamicum* by screening a genomic library on a high density colony-array., in: FEMS Microbiology Letters. pp. 99–103. https://doi.org/10.1111/j.1574-6968.2000.tb09409.x

Gruber, A.R., Lorenz, R., Bernhart, S.H., Neuböck, R., Hofacker, I.L., 2008. The Vienna RNA websuite. Nucleic Acids Res. 36, 70–74. https://doi.org/10.1093/nar/gkn188

Gumber, S., Gurumoorthy, A.V.P., 2017. Methanol Economy Versus Hydrogen Economy, in: Methanol: Science and Engineering. Elsevier B.V., pp. 661–674. https://doi.org/10.1016/B978-0-444-63903-5.00025-X

Gutheil, W.G., Holmquist, B., Vallee, B.L., 1992. Purification, characterization, and partial sequence of the glutathione-dependent formaldehyde dehydrogenase from *Escherichia coli*: a class III alcohol dehydrogenase. Biochemistry 31, 475–481. https://doi.org/10.1021/bi00117a025

Hadiati, A., Krahn, I., Lindner, S.N., Wendisch, V.F., 2014. Engineering of *Corynebacterium glutamicum* for growth and production of L-ornithine , L-lysine , and lycopene from hexuronic acids, in: Bioresources and Bioprocessing. pp. 1–10.

Hammer-Jespersen, K., Munch-Petersem, A., 1970. Phosphodeoxyribomutase from *Escherichia coli* Purification and Some Properties. Eur. J. Biochem. 17, 397–407. https://doi.org/10.1111/j.1432-1033.1970.tb01179.x

Han, G., Hu, X., Wang, X., 2016. Overexpression of methionine adenosyltransferase in *Corynebacterium glutamicum* for production of S-adenosyl-l-methionine. Biotechnol. Appl. Biochem. 63, 679–689. https://doi.org/10.1002/bab.1425

Hanahan, D., 1985. Techniques for transformation of *E. coli*. DNA cloning a Pract. approach 1, 109–135.

Harris, J.L., Craik, C.S., 1998. Engineering enzyme specificity. Curr. Opin. Chem. Biol. 2, 127–132. https://doi.org/10.1016/S1367-5931(98)80044-6

Haynes, C.A., Gonzalez, R., 2014. Rethinking biological activation of methane and conversion to liquid fuels. Nat. Chem. Biol. 10, 331–339. https://doi.org/10.1038/nchembio.1509

He, H., Edlich-Muth, C., Lindner, S.N., Bar-Even, A., 2018. Ribulose Monophosphate Shunt Provides Nearly All Biomass and Energy Required for Growth of *E. coli*. ACS Synth. Biol. 7, 1601–1611. https://doi.org/10.1021/acssynbio.8b00093

Heddle, J., Maxwell, A., 2002. Quinolone-Binding Pocket of DNA Gyrase: Role of GyrB. Antimicrob. Agents Chemother. 46, 1805–1815. https://doi.org/10.1128/AAC.46.6.1805

Heggeset, T.M.B., Krog, A., Balzer, S., Wentzel, A., Ellingsen, T.E., Brautaseta, T., 2012. Genome sequence of thermotolerant *Bacillus methanolicus*: Features and regulation related to methylotrophy and production of L-lysine and L-glutamate from methanol. Appl. Environ. Microbiol. 78, 5170–5181. https://doi.org/10.1128/AEM.00703-12

Heider, S. a E., Wolf, N., Hofemeier, A., Peters-Wendisch, P., Wendisch, V.F., 2014. Optimization of the IPP Precursor Supply for the Production of Lycopene, Decaprenoxanthin and Astaxanthin by *Corynebacterium glutamicum*., in: Frontiers in Bioengineering and Biotechnology. p. 28. https://doi.org/10.3389/fbioe.2014.00028

Herring, C.D., Blattner, F.R., 2004. Global transcriptional effects of a suppressor tRNA and the inactivation of the regulator *frmR*. J. Bacteriol. 186, 6714–6720. https://doi.org/10.1128/JB.186.20.6714-6720.2004

Literature

Huber, I., Brown, I.R., Warren, M.J., Frunzke, J., Ludwig, K.N., Palmer, D.J., 2017. Construction of Recombinant Pdu Metabolosome Shells for Small Molecule Production in *Corynebacterium glutamicum*. ACS Synth. Biol. 6, 2145–2156. https://doi.org/10.1021/acssynbio.7b00167

Hwang, B.-J., Yeom, H.-J., Kim, Y., Lee, H.-S., 2002. *Corynebacterium glutamicum* Utilizes both Transsulfuration and Direct Sulfhydrylation Pathways for Methionine Biosynthesis. J. Bacteriol. 184, 1277–1286. https://doi.org/10.1128/JB.184.5.1277-1286.2002

Iaquaniello, G., Centi, G., Salladini, A., Palo, E., 2017. Methanol Economy: Environment, Demand, and Marketing With a Focus on the Waste-to-Methanol Process, Methanol: Science and Engineering. Elsevier B.V. https://doi.org/10.1016/B978-0-444-63903-5.00022-4

Ikeda, M., 2005. Tryptophan Production, in: Handbook of Corynebacterium Glutamicum. pp. 491–512.

Inui, M., Suda, M., Okino, S., Nonaka, H., Puskás, L.G., Vertès, A.A., Yukawa, H., 2007. Transcriptional profiling of *Corynebacterium glutamicum* metabolism during organic acid production under oxygen deprivation conditions. Microbiology 153, 2491–2504. https://doi.org/10.1099/mic.0.2006/005587-0

Irla, M., Heggeset, T.M.B., Nærdal, I., Paul, L., Haugen, T., Le, S.B., Brautaset, T., Wendisch, V.F., 2016. Genome-Based Genetic Tool Development for *Bacillus methanolicus*: Theta- and Rolling Circle-Replicating Plasmids for Inducible Gene Expression and Application to Methanol-Based Cadaverine Production. Front. Microbiol. 7. https://doi.org/10.3389/fmicb.2016.01481

Irla, M., Nærdal, I., Brautaset, T., Wendisch, V.F., 2017. Methanol-based γ-aminobutyric acid (GABA) production by genetically engineered *Bacillus methanolicus* strains. Ind. Crops Prod. 106, 12–20. https://doi.org/10.1016/j.indcrop.2016.11.050

Irla, M., Neshat, A., Brautaset, T., Rückert, C., Kalinowski, J., Wendisch, V.F., 2015. Transcriptome analysis of thermophilic methylotrophic *Bacillus methanolicus* MGA3 using RNA-sequencing provides detailed insights into its previously uncharted transcriptional landscape. BMC Genomics 16, 73. https://doi.org/10.1186/s12864-015-1239-4

Irla, M., Neshat, A., Winkler, A., Albersmeier, A., Heggeset, T.M.B., Brautaset, T., Kalinowski, J., Wendisch, V.F., Rückert, C., 2014. Complete genome sequence of Bacillus methanolicus MGA3, a thermotolerant amino acid producing methylotroph. J. Biotechnol. 188, 110–111. https://doi.org/10.1016/j.jbiotec.2014.08.013

Jakobsen, O.M., Flickinger, M.C., Degnes, K.F., Brautaset, T., Valla, S., Ellingsen, T.E., Heggeset, T.M.B., Balzer, S., 2008. Overexpression of Wild-Type Aspartokinase Increases L-Lysine Production in the Thermotolerant Methylotrophic Bacterium *Bacillus methanolicus*. Appl. Environ. Microbiol. 75, 652–661. https://doi.org/10.1128/aem.01176-08

Literature

Jakobsen, O.M., Valla, S., Benichou, A., Flickinger, M.C., Brautaset, T., Ellingsen, T.E., 2006. Upregulated Transcription of Plasmid and Chromosomal Ribulose Monophosphate Pathway Genes Is Critical for Methanol Assimilation Rate and Methanol Tolerance in the Methylotrophic *Bacterium Bacillus methanolicus*. J. Bacteriol. 188, 3063–3072. https://doi.org/10.1128/jb.188.8.3063-3072.2006

Jensen, J.V.K., Eberhardt, D., Wendisch, V.F., 2015. Modular pathway engineering of *Corynebacterium glutamicum* for production of the glutamate-derived compounds ornithine, proline, putrescine, citrulline, and arginine, in: Journal of Biotechnology. Elsevier B.V., pp. 85–94. https://doi.org/10.1016/j.jbiotec.2015.09.017

Jensen, J.V.K., Wendisch, V.F., 2013. Ornithine cyclodeaminase-based proline production by *Corynebacterium glutamicum*. Microb. Cell Fact. 12, 1–10. https://doi.org/10.1186/1475-2859-12-63

Jorge, J.M.P., Leggewie, C., Wendisch, V.F., 2016. A new metabolic route for the production of gamma-aminobutyric acid by *Corynebacterium glutamicum* from glucose, in: Amino Acids. Springer Vienna, pp. 2519–2531. https://doi.org/10.1007/s00726-016-2272-6

Jungwirth, B., Sala, C., Kohl, T.A., Uplekar, S., Baumbach, J., Cole, S.T., Pühler, A., Tauch, A., 2013. High-resolution detection of DNA binding sites of the global transcriptional regulator GlxR in *Corynebacterium glutamicum*. Microbiol. (United Kingdom) 159, 12–22. https://doi.org/10.1099/mic.0.062059-0

Kalinowski, J., Bathe, B., Bartels, D., Bischoff, N., Bott, M., Burkovski, A., Dusch, N., Eggeling, L., Eikmanns, B.J., Gaigalat, L., Goesmann, A., Hartmann, M., Huthmacher, K., Krämer, R., Linke, B., McHardy, A.C., Meyer, F., Möckel, B., Pfefferle, W., Pühler, A., Rey, D.A., Rückert, C., Sahm, H., Wendisch, V.F., Wiegra, I., 2003. The complete *Corynebacterium glutamicum* ATCC 13032 genome sequence and its impact on the production of L -aspartate-derived amino acids and vitamins. J. Biotechnol. 104, 5–25. https://doi.org/10.1016/S0168-1656(03)00154-8

Kalinowski, J., Cremer, J., Bachmann, B., Eggeling, L., Sahm, H., Pühler, A., 1991. Genetic and biochemical analysis of the aspartokinase from *Corynebacterium glutamicum*. Mol. Microbiol. 5, 1197–1204.

Kanehisa, M., Goto, S., 2000. KEGG: Kyoto Encyclopedia of Genes and Genomes. Nucleic Acids Res. 28, 27–30. https://doi.org/10.1016/j.meegid.2016.07.022

Kato, N., Yurimoto, H., Thauer, R.K., 2006. The Physiological Role of the Ribulose Monophosphate Pathway in Bacteria and Archaea. Biosci. Biotechnol. Biochem. 70. https://doi.org/10.1271/bbb.70.10

Kawaguchi, H., Sasaki, M., Vertès, A.A., Inui, M., Yukawa, H., 2008. Engineering of an L-arabinose metabolic pathway in *Corynebacterium glutamicum*. Appl. Microbiol. Biotechnol. 77, 1053–1062. https://doi.org/10.1007/s00253-007-1244-x

Kawaguchi, H., Vertès, A.A., Okino, S., Inui, M., Yukawa, H., 2006. Engineering of a xylose metabolic pathway in *Corynebacterium glutamicum*. Appl. Environ. Microbiol. 72, 3418–28. https://doi.org/10.1128/AEM.72.5.3418-3428.2006

Keilhauer, C., Eggeling, L., Sahm, H., 1993. Isoleucine synthesis in *Corynebacterium glutamicum*: molecular analysis of the ilvB-ilvN-ilvC operon. J. Bacteriol. 175, 5595–603. https://doi.org/<p></p>

Kelle, R., Hermann, T., Bathe, B., 2005. L-Lysine Production, in: Handbook of Corynebacterium Glutamicum. pp. 467–490.

Khan, S.A., 2005. Plasmid rolling-circle replication: Highlights of two decades of research. Plasmid 53, 126–136. https://doi.org/10.1016/j.plasmid.2004.12.008

Khan, S.A., 1997. Rolling-circle replication of bacterial plasmids. Microbiol. Mol. Biol. Rev. 61, 442–55.

Kiekebusch, D., Thanbichler, M., 2014. Plasmid segregation by a moving ATPase gradient. Proc. Natl. Acad. Sci. 111, 4741–4742. https://doi.org/10.1073/pnas.1402867111

Kim, H.-J., Kim, T.-H., Kim, Y., Lee, H.-S., 2004. Identification and Characterization of *glxR*, a Gene Involved in Regulation of Glyoxylate Bypass in *Corynebacterium glutamicum*. J. Bacteriol. 186, 3453–3460. https://doi.org/10.1128/JB.186.11.3453-3460.2004

Kim, H.J., Balcezak, T.J., Nathin, S.J., McMullen, H.F., Hansen, D.E., 1992. The use of a spectrophotometric assay to study the interaction of S-adenosylmethionine synthetase with methionine analogues. Anal. Biochem. 207, 68–72. https://doi.org/10.1016/0003-2697(92)90501-W

Kim, T.H., Kim, H.J., Park, J.S., Kim, Y., Kim, P., Lee, H.S., 2005. Functional analysis of *sigH* expression in *Corynebacterium glutamicum*. Biochem. Biophys. Res. Commun. 331, 1542–1547. https://doi.org/10.1016/j.bbrc.2005.04.073

Kimura, E., 2005. Glutamate production, in: Handbook of Corynebacterium Glutamicum. pp. 439–466. https://doi.org/10.1007/s10750-004-4542-7

Kind, S., Neubauer, S., Wittmann, C., Becker, J., Zelder, O., Yamamoto, M., Völkert, M., Abendroth, G. von, 2014. From zero to hero – Production of bio-based nylon from renewable resources using engineered *Corynebacterium glutamicum*. Metab. Eng. 25, 113–123. https://doi.org/10.1016/j.ymben.2014.05.007

Kind, S., Wittmann, C., 2011. Bio-based production of the platform chemical 1,5-diaminopentane. Appl. Microbiol. Biotechnol. 91, 1287–1296. https://doi.org/10.1007/s00253-011-3457-2

Kinoshita, S., Udaka, S., Shimono, M., 1957. Studies on the amino acid fermentation Part I: Production of L-glutamicum acid by various microorganisms. J. Gen. Appl. Microbiol. 3.

Kirchner, O., Tauch, A., 2003. Tools for genetic engineering in the amino acid-producing bacterium *Corynebacterium glutamicum*. J. Biotechnol. 104, 287–299.

Kohl, T.A., Baumbach, J., Jungwirth, B., Pühler, A., Tauch, A., 2008. The GlxR regulon of the amino acid producer *Corynebacterium glutamicum*: In silico and in vitro detection of DNA binding sites of a global transcription regulator. J. Biotechnol. 135, 340–350. https://doi.org/10.1016/j.jbiotec.2008.05.011

Koopman, F.W., De Winde, J.H., Ruijssenaars, H.J., 2009. C1 compounds as auxiliary substrate for engineered *Pseudomonas putida* S12. Appl. Microbiol. Biotechnol. 83, 705–713. https://doi.org/10.1007/s00253-009-1922-y

Koren, S., Walenz, B.P., Berlin, K., Miller, J.R., Bergman, N.H., Phillippy, A.M., 2017. Canu: scalable and accurate long-read assembly via adaptive k -mer weighting and repeat separation. Genome Res. 27, 722–736. https://doi.org/10.1101/gr.215087.116

Kornberg, T., Gefter, M.L., 1972. Deoxyribonucleic Acid Synthesis in Cell-free Extracts. J. Biol. Chem. 274, 5369–5375.

Krog, A., Bjerkan, M., Ellingsen, E., 2013a. Functional Characterization of Key Enzymes involved in L -Glutamate Synthesis and Degradation in the Thermotolerant and Methylotrophic Bacterium *Bacillus methanolicus*. Appl. Environ. Microbiol. 79, 5321–5328. https://doi.org/10.1128/AEM.01382-13

Krog, A., Heggeset, T.M.B., Müller, J.E.N., Kupper, C.E., Schneider, O., Vorholt, J.A., Ellingsen, T.E., Brautaset, T., 2013b. Methylotrophic *Bacillus methanolicus* Encodes Two Chromosomal and One Plasmid Born NAD+ Dependent Methanol Dehydrogenase Paralogs with Different Catalytic and Biochemical Properties. PLoS One 8. https://doi.org/10.1371/journal.pone.0059188

Kruger, N.J., Von Schaewen, A., 2003. The oxidative pentose phosphate pathway: Structure and organisation. Curr. Opin. Plant Biol. 6, 236–246. https://doi.org/10.1016/S1369-5266(03)00039-6

Laslo, T., von Zaluskowski, P., Gabris, C., Lodd, E., Rückert, C., Dangel, P., Kalinowski, J., Auchter, M., Seibold, G., Eikmanns, B.J., 2012. Arabitol metabolism of *Corynebacterium glutamicum* and its regulation by AtlR. J. Bacteriol. 194, 941–955. https://doi.org/10.1128/JB.06064-11

Le, S.B., Heggeset, T.M.B., Haugen, T., Nærdal, I., Brautaset, T., 2017. 6-Phosphofructokinase and ribulose-5-phosphate 3-epimerase in methylotrophic *Bacillus methanolicus* ribulose monophosphate cycle. Appl. Microbiol. Biotechnol. 101, 4185–4200. https://doi.org/10.1007/s00253-017-8173-0

Leach, D.R.F., 1994. Long DNA palindromes, cruciform strcutures, genetic instability and secondary structure repair. Bioassays 16, 893–900.

Lee, H.-W., Lebeault, J.-M., 1998. Enhanced L-lysine production in threonine-limited continuous culture of *Corynebacterium glutamicum* by using gluconate as a secondary carbon source with glucose. Appl Microbiol Biotechnol 49, 9–15.

Literature

Leipe, D.D., Wolf, Y.I., Koonin, E. V., Aravind, L., 2002. Classification and evolution of P-loop GTPases and related ATPases. J. Mol. Biol. 317, 41–72. https://doi.org/10.1006/jmbi.2001.5378

Leßmeier, L., Hoefener, M., Wendisch, V.F., 2013. Formaldehyde degradation in Corynebacterium glutamicum involves acetaldehyde dehydrogenase and mycothiol-dependent formaldehyde dehydrogenase. Microbiol. (United Kingdom) 159, 2651–2662. https://doi.org/10.1099/mic.0.072413-0

Leßmeier, L., Pfeifenschneider, J., Carnicer, M., Heux, S., Portais, J.-C.C., Wendisch, V.F., 2015. Production of carbon-13-labeled cadaverine by engineered *Corynebacterium glutamicum* using carbon-13-labeled methanol as co-substrate. Appl. Microbiol. Biotechnol. 99, 10163–10176. https://doi.org/10.1007/s00253-015-6906-5

Leßmeier, L., Wendisch, V.F., 2015. Identification of two mutations increasing the methanol tolerance of *Corynebacterium glutamicum*. BMC Microbiol. 15, 216. https://doi.org/10.1186/s12866-015-0558-6

Liang, W.F., Cui, L.Y., Cui, J.Y., Yu, K.W., Yang, S., Wang, T.M., Guan, C.G., Zhang, C., Xing, X.H., 2017. Biosensor-assisted transcriptional regulator engineering for *Methylobacterium extorquens* AM1 to improve mevalonate synthesis by increasing the acetyl-CoA supply. Metab. Eng. 39, 159–168. https://doi.org/10.1016/j.ymben.2016.11.010

Lidstrom, M.E., 1990. Genetics of carbon metabolism in methylotrophic bacteria. FEMS Microbiol. Rev. 7, 431–436. https://doi.org/10.1111/j.1574-6968.1990.tb04949.x

Lidstrom, M.E., Stirling, D.I., 1990. METHYLOTROPHS: Genetics and Commercial Applications. Annu. Rev. Microbiol. 44, 27–58. https://doi.org/10.1146/annurev.mi.44.100190.000331

Liesivuori, J., Savolainen, A.H., 1991. Methanol and Formic Acid Toxicity: Biochemical Mechanisms. Pharmacol. Toxicol. 69, 157–163. https://doi.org/10.1111/j.1600-0773.1991.tb01290.x

Link, A.J., Phillips, D., 1997. Methods for Generating Precise Deletions and Insertions in the Genome of Wild-Type *Escherichia coli* : Application to Open Reading Frame Characterization. J. Bacteriol. 179, 6228–6237.

Linton, J.D., Niekus, H.G.D., 1987. The potential of one-carbon compounds as fermentation feedstocks. Antonie Van Leeuwenhoek 53, 55–63. https://doi.org/10.1007/BF00422635

Litsanov, B., Brocker, M., Bott, M., 2013. Glycerol as a substrate for aerobic succinate production in minimal medium with *Corynebacterium glutamicum*. Microb. Biotechnol. 6, 189–195. https://doi.org/10.1111/j.1751-7915.2012.00347.x

Litsanov, B., Brocker, M., Bott, M., 2012. Toward homosuccinate fermentation: Metabolic engineering of *Corynebacterium glutamicum* for anaerobic production of succinate from glucose and formate, in: Applied and Environmental Microbiology. pp. 3325–3337. https://doi.org/10.1128/AEM.07790-11

Literature

Lombardini, J.B., Coulter, A.W., Talalay, P., 1970. Analogues of methionine as substrates and inhibitors of the methionine adenosyltransferase reaction. Mol. Pharmacol. 6, 481–499.

Lorenz, R., Bernhart, S.H., Höner zu Siederdissen, C., Tafer, H., Flamm, C., Stadler, P.F., Hofacker, I.L., 2011. ViennaRNA Package 2.0. Algorithms Mol. Biol. 6.

MacHeroux, P., Kappes, B., Ealick, S.E., 2011. Flavogenomics - A genomic and structural view of flavin-dependent proteins. FEBS J. 278, 2625–2634. https://doi.org/10.1111/j.1742-4658.2011.08202.x

Macrotrends.net, 2019. Sugar Prices - 37 Year Historical Chart [WWW Document]. URL https://www.macrotrends.net/2537/sugar-prices-historical-chart-data (accessed 4.8.19).

Mahillon, J., Chandler, M., 1998. Insertion Sequences. Microbiol. Mol. Biol. Rev. 62, 725–774.

Maitah, M., Smutka, L., 2019. The Development of World Sugar Prices. Sugar Tech 21, 1–8. https://doi.org/10.1007/s12355-018-0618-y

Mansoorabadi, S.O., Thibodeaux, C.J., Liu, H., 2007. The Diverse Roles of Flavin Coenzymes - Nature's Most Versatile Thespians. J. Org. Chem. 72, 6329–6342.

Markert, B., Stolzenberger, J., Brautaset, T., Wendisch, V.F., 2014. Characterization of two transketolases encoded on the chromosome and the plasmid pBM19 of the facultative ribulose monophosphate cycle methylotroph *Bacillus methanolicus*. BMC Microbiol 14, 7. https://doi.org/10.1186/1471-2180-14-7

Markham, G.D., DeParasis, J., Gatmaitan, J., 1984. The sequence of *metK*, the structural gene for S-adenosylmethionine synthetase in *Escherichia coli*. J. Biol. Chem. 259, 14505–14507. https://doi.org/10.1097/01.ccm.0000408627.24229.88

Marx, C.J., Bringel, F., Chistoserdova, L., Moulin, L., Farhan Ul Haque, M., Fleischman, D.E., Gruffaz, C., Jourand, P., Knief, C., Lee, M.C., Muller, E.E.L.L., Nadalig, T., Peyraud, R., Roselli, S., Russ, L., Goodwin, L.A., Ivanova, N., Kyrpides, N., Lajus, A., Land, M.L., Médigue, C., Mikhailova, N., Nolan, M., Woyke, T., Stolyar, S., Vorholt, J.A., Vuilleumier, S., 2012. Complete genome sequences of six strains of the genus *Methylobacterium*. J. Bacteriol. 194, 4746–4748. https://doi.org/10.1128/JB.01009-12

Matano, C., Uhde, A., Youn, J., 2014. Engineering of *Corynebacterium glutamicum* for growth and L -lysine and lycopene production from N -acetyl-glucosamine, in: Applied Microbiology and Biotechnollogy. pp. 5633–5643. https://doi.org/10.1007/s00253-014-5676-9

Mattozzi, M. d., Ziesack, M., Voges, M.J., Silver, P.A., Way, J.C., 2013. Expression of the sub-pathways of the *Chloroflexus aurantiacus* 3-hydroxypropionate carbon fixation bicycle in *E. coli*: Toward horizontal transfer of autotrophic growth. Metab. Eng. 16, 130–139. https://doi.org/10.1016/j.ymben.2013.01.005

Literature

McNeil, M.B., Fineran, P.C., 2013. Prokaryotic assembly factors for the attachment of flavin to complex II. Biochim. Biophys. Acta - Bioenerg. 1827, 637–647. https://doi.org/10.1016/j.bbabio.2012.09.003

McTaggart, T.L., Beck, D.A.C., Setboonsarng, U., Shapiro, N., Woyke, T., Lidstrom, M.E., Kalyuzhnaya, M.G., Chistoserdova, L., Mcdowell, A., 2015. Genomics of Methylotrophy in Gram-Positive Methylamine-Utilizing Bacteria. Microorganisms 3, 94–112. https://doi.org/10.3390/microorganisms3010094

Meiswinkel, T.M., Gopinath, V., Lindner, S.N., Nampoothiri, K.M., Wendisch, V.F., 2013. Accelerated pentose utilization by *Corynebacterium glutamicum* for accelerated production of lysine , glutamate , ornithine and putrescine, in: Microbial Biotechnology. pp. 131–140. https://doi.org/10.1111/1751-7915.12001

Merkens, H., Beckers, G., Wirtz, A., Burkovski, A., 2005. Vanillate metabolism in *Corynebacterium glutamicum*. Curr. Microbiol. 51, 59–65. https://doi.org/10.1007/s00284-005-4531-8

Meyer, F., Keller, P., Hartl, J., Gröninger, O.G., Kiefer, P., Vorholt, J.A., Julia, A., 2018. Methanol-essential growth of *Escherichia coli*. Nat. Commun. 9, 1–26. https://doi.org/10.1038/s41467-018-03937-y

Millet, D.B., Jacob, D.J., Custer, T.G., de Gouw, J.A., Goldstein, A.H., Karl, T., Singh, H.B., Sive, B.C., Talbot, R.W., Warneke, C., Williams, J., 2008. New constraints on terrestrial and oceanic sources of atmospheric methanol. Atmos. Chem. Phys. 8, 6887–6905. https://doi.org/10.5194/acp-8-6887-2008

Mimitsuka, T., Sawai, H., Hatsu, M., Yamada, K., 2007. Metabolic Engineering of *Corynebacterium glutamicum* for Cadaverine Fermentation. Biosci. Biotechnol. Biochem. 71, 2130–2135. https://doi.org/10.1271/bbb.60699

Mindt, M., Risse, J.M., Gruß, H., Sewald, N., Eikmanns, B.J., Wendisch, V.F., 2018. One-step process for production of N-methylated amino acids from sugars and methylamine using recombinant *Corynebacterium glutamicum* as biocatalyst. Sci. Rep. 8, 1–11. https://doi.org/10.1038/s41598-018-31309-5

Müller, J.E.N., Heggeset, T.M.B., Wendisch, V.F., Vorholt, J.A., 2015a. Methylotrophy in the thermophilic *Bacillus methanolicus*, basic insights and application for commodity production from methanol. Appl. Microbiol. Biotechnol. 99, 535–551. https://doi.org/10.1007/s00253-014-6224-3

Müller, J.E.N., Meyer, F., Litsanov, B., Kiefer, P., Potthoff, E., Heux, S., Quax, W.J., Wendisch, V.F., Brautaset, T., Portais, J.-C.C., Vorholt, J.A., 2015b. Engineering *Escherichia coli* for methanol conversion. Metab. Eng. 28, 190–201. https://doi.org/10.1016/j.ymben.2014.12.008

Müller, J.E.N., Meyer, F., Litsanov, B., Kiefer, P., Vorholt, J.A., 2015c. Core pathways operating during methylotrophy of *Bacillus methanolicus* MGA3 and induction of a bacillithiol-dependent detoxification pathway upon formaldehyde stress. Mol. Microbiol. 98, 1089–1100. https://doi.org/10.1111/mmi.13200

Literature

Murooka, Y., Kakihara, K., Miwa, T., Seto, K., Harada, T., 1977. O-alkylhomoserine synthesis catalyzed by O-acetylhomoserine sulfhydrylase in microorganisms. J. Bacteriol. 130, 62–73.

Nærdal, I., Netzer, R., Irla, M., Krog, A., Marita, T., Heggeset, B., Wendisch, V.F., Brautaset, T., 2017. l -lysine production by *Bacillus methanolicus*: Genome-based mutational analysis and l -lysine secretion engineering. J. Biotechnol. 244, 25–33. https://doi.org/10.1016/j.jbiotec.2017.02.001

Naerdal, I., Pfeifenschneider, J., Brautaset, T., Wendisch, V.F., 2015. Methanol-based cadaverine production by genetically engineered *Bacillus methanolicus* strains. Microb Biotechnol 8, 342–350. https://doi.org/10.1111/1751-7915.12257

Nemecek-Marshal, M., MacDonald, R.C., Franzen, J.J., Wojciechowski, C.L., Fall, R., 1995. Methanol emission from plants. Plant Physiol. 108, 1359–1368.

Nentwich, S.S., Brinkrolf, K., Gaigalat, L., Hüser, A.T., Rey, D.A., Mohrbach, T., Marin, K., Pühler, A., Tauch, A., Kalinowski, J., 2009. Characterization of the LacI-type transcriptional repressor RbsR controlling ribose transport in *Corynebacterium glutamicum* ATCC 13032, in: Microbiology. pp. 150–164. https://doi.org/10.1099/mic.0.020388-0

Nguyen, A.Q.D.D., Schneider, J., Reddy, G.K., Wendisch, V.F., 2015. Fermentative production of the diamine Putrescine: System metabolic engineering of *Corynebacterium glutamicum*. Metabolites 5, 211–231. https://doi.org/10.3390/metabo5020211

Niebisch, A., Bott, M., Niebisch, A., 2005. Respiratory Energy Metabolism, in: Handbook of Corynebacterium Glutamicum. pp. 307–334. https://doi.org/10.1201/9781420039696.ch13

Noack, S., Voges, R., Gätgens, J., Wiechert, W., 2017. The linkage between nutrient supply, intracellular enzyme abundances and bacterial growth: New evidences from the central carbon metabolism of *Corynebacterium glutamicum*. J. Biotechnol. 258, 13–24. https://doi.org/10.1016/j.jbiotec.2017.06.407

Nybo, S.E., Khan, N.E., Woolston, B.M., Curtis, W.R., 2015. Metabolic engineering in chemolithoautotrophic hosts for the production of fuels and chemicals. Metab. Eng. 30, 105–120. https://doi.org/10.1016/j.ymben.2015.04.008

Ochsner, A.M., Müller, J.E.N., Mora, C.A., Vorholt, J.A., 2014a. In vitro activation of NAD-dependent alcohol dehydrogenases by Nudix hydrolases is more widespread than assumed. FEBS Lett. 588, 2993–2999. https://doi.org/10.1016/j.febslet.2014.06.008

Ochsner, A.M., Sonntag, F., Buchhaupt, M., Schrader, J., Vorholt, J.A., 2014b. *Methylobacterium extorquens*: methylotrophy and biotechnological applications. Appl. Microbiol. Biotechnol. 99, 517–534. https://doi.org/10.1007/s00253-014-6240-3

Literature

Olah, G.A., 2013. Towards oil independence through renewable methanol chemistry. Angew. Chemie - Int. Ed. 52, 104–107. https://doi.org/10.1002/anie.201204995

Olah, G.A., Goeppert, A., Prakash, G.K.S., 2009. Beyond Oil and Gas: The Methanol Economy: Second Edition. Beyond Oil Gas Methanol Econ. Second Ed. 1–334. https://doi.org/10.1002/9783527627806

Olorunniji, F.J., Stark, W.M., 2010. Catalysis of site-specific recombination by Tn3 resolvase. Biochem. Soc. Trans. 38, 417–21. https://doi.org/10.1042/BST0380417

Orita, I., Sakamoto, N., Kato, N., Yurimoto, H., Sakai, Y., 2007. Bifunctional enzyme fusion of 3-hexulose-6-phosphate synthase and 6-phospho-3-hexuloisomerase. Appl. Microbiol. Biotechnol. 76, 439–445. https://doi.org/10.1007/s00253-007-1023-8

Osterman, A.L., Tam, A., Polanuyer, B.M., Kurnasov, O. V., Sloutsky, R., Ananta, S., Gerdes, S.Y., 2003. Ribosylnicotinamide Kinase Domain of NadR Protein: Identification and Implications in NAD Biosynthesis. J. Bacteriol. 185, 698–698. https://doi.org/10.1128/jb.185.2.698.2003

Packer, M.S., Rees, H.A., Liu, D.R., 2017. Phage-assisted continuous evolution of proteases with altered substrate specificity. Nat. Commun. 8. https://doi.org/10.1038/s41467-017-01055-9

Pan, X., Leach, D.R.F., 2000. The roles of *mutS*, *sbcCD* and *recA* in the propagation of TGG repeats in *Escherichia coli*. Nucleic Acids Res. 28, 3178–3184.

Papoutsakis, E., Lim, H.C., Tsao, G.T., 1978. Role of Formaldehyde in the Utilization of C1 Compounds via the Ribulose Monophosphate Cycle. Biotechnol. Bioeng. 421–442.

Pátek, M., 2005. Regulation of Gene Expression, in: Handbook of Corynebacterium Glutamicum. pp. 81–98.

Pátek, M., Nešvera, J., Guyonvarch, A., Reyes, O., Leblon, G., 2003. Promoters of *Corynebacterium glutamicum*. J. Biotechnol. 104, 311–323. https://doi.org/10.1016/S0168-1656(03)00155-X

Pechtl, A., Rückert, C., Maus, I., Koeck, D.E., Trushina, N., Kornberger, P., Schwarz, W.H., Schlüter, A., Liebl, W., Zverlov, V. V., 2018. Complete Genome Sequence of the Novel Cellulolytic, Anaerobic, Thermophilic Bacterium *Herbivorax saccincola* Type Strain GGR1, Isolated from a Lab Scale Biogas Reactor as Established by Illumina and Nanopore MinION Sequencing. Genome Announc. 6, e01493-17. https://doi.org/10.1128/genomeA.01493-17

Pellegrini, L.A., Soave, G., Gamba, S., Langè, S., 2011. Economic analysis of a combined energy – methanol production plant. Appl. Energy 88, 4891–4897. https://doi.org/10.1016/j.apenergy.2011.06.028

Literature

Pérez-garcía, F., Jorge, J.M.P., Dreyszas, A., Risse, J.M., Wendisch, V.F., 2018. Efficient Production of the Dicarboxylic Acid Glutarate by *Corynebacterium glutamicum* via a Novel Synthetic Pathway, in: Frontiers in Microbiology. pp. 1–13. https://doi.org/10.3389/fmicb.2018.02589

Pérez-García, F., Peters-Wendisch, P., Wendisch, V.F., 2016. Engineering *Corynebacterium glutamicum* for fast production of l-lysine and l-pipecolic acid. Appl. Microbiol. Biotechnol. 100, 8075–8090. https://doi.org/10.1007/s00253-016-7682-6

Peters-Wendisch, P.G., Kreutzer, C., Kalinowski, J., Patek, M., Sahm, H., Eikmannsl, B.J., 1998. Pyruvate carboxylase from Corynebacterium glutamicum: characterization , expression and inactivation of the pyc gene. Microbiology 144, 915–927.

Peters-Wendisch, P.G., Schiel, B., Volker, F., Katsoulidis, E., Möckel, B., Sahm, H., Eikmanns, B.J., 2001. Pyruvate Carboxylase is a Major Bottleneck for Glutamate and Lysine Production by Corynebacterium glutamicum. J. Mol. Microbiol. Biotechnol. 3, 295–300.

Pfeifenschneider, J., Brautaset, T., Wendisch, V.F., 2017. Methanol as carbon substrate in the bio-economy: Metabolic engineering of aerobic methylotrophic. Biofuels, Bioprod. Biorefining 11, 719–731. https://doi.org/10.1002/bbb.1773

Pfeifer-Sancar, K., Mentz, A., Ruckert, C., Kalinowski, J., 2013. Comprehensive analysis of the *Corynebacterium glutamicum* transcriptome using an improved RNAseq technique. BMC Genomics 14, 888. https://doi.org/10.1186/1471-2164-14-888

Pirola, C., Bozzano, G., Manenti, F., 2017. Fossil or Renewable Sources for Methanol Production?, in: Methanol: Science and Engineering. Elsevier B.V., pp. 53–93. https://doi.org/10.1016/B978-0-444-63903-5.00003-0

Polka, J.K., Hays, S.G., Silver, P.A., 2016. Building Spatial Synthetic Biology with Compartments, Scaffolds, and Communities. Cold Spring Harb. Perspect. Biol. 8, a024018. https://doi.org/10.1101/cshperspect.a024018

Poust, S., Piety, J., Bar-Even, A., Louw, C., Baker, D., Keasling, J.D., Siegel, J.B., 2015. Mechanistic Analysis of an Engineered Enzyme that Catalyzes the Formose Reaction. ChemBioChem 16, 1950–1954. https://doi.org/10.1002/cbic.201500228

Price, J.V., Chen, L., Whitaker, W.B., Papoutsakis, E., Chen, W., 2016. Scaffoldless engineered enzyme assembly for enhanced methanol utilization. Proc. Natl. Acad. Sci. 113, 12691–12696. https://doi.org/10.1073/pnas.1601797113

Räuchle, K., Plass, L., Wernicke, H.-J., Bertau, M., 2016. Methanol for Renewable Energy Storage and Utilization. Energy Technol. 4, n/a-n/a. https://doi.org/10.1002/ente.201500322

Literature

Rittmann, D., Lindner, S.N., Wendisch, V.F., 2008. Engineering of a glycerol utilization pathway for amino acid production by *Corynebacterium glutamicum*. Appl. Environ. Microbiol. 74, 6216–6222. https://doi.org/10.1128/AEM.00963-08

Roblin, R.O., Lampen, J.O., English, J.P., Cole, Q.P., Vaughan, J.R., 1945. Studies in Chemotherapy. VIII. Methionine and Purine Antagonists and their Relation to the Sulfonamides 1. J. Am. Chem. Soc. 67, 290–294. https://doi.org/10.1021/ja01218a043

Rohlhill, J., Sandoval, N.R., Papoutsakis, E.T., 2017. Sort-Seq Approach to Engineering a Formaldehyde-Inducible Promoter for Dynamically Regulated *Escherichia coli* Growth on Methanol. ACS Synth. Biol. 6, 1584–1595. https://doi.org/10.1021/acssynbio.7b00114

Roth, T., Woolston, B., Stephanopoulos, G., Liu, D.R., 2019. Phage-assisted evolution of *Bacillus methanolicus* methanol dehydrogenase 2. ACS Synth. Biol. acssynbio.8b00481. https://doi.org/10.1021/acssynbio.8b00481

Rückert, C., Pühler, A., Kalinowski, J., 2003. Genome-wide analysis of the L-methionine biosynthetic pathway in *Corynebacterium glutamicum* by targeted gene deletion and homologous complementation. J. Biotechnol. 104, 213–228. https://doi.org/10.1016/S0168-1656(03)00158-5

Rupp, J., Gebert, A., Solbach, W., Maass, M., 2005. Serine-to-asparagine substitution in the GyrA gene leads to quinolone resistance in moxifloxacin-exposed *Chlamydia pneumoniae*. Antimicrob. Agents Chemother. 49, 406–407. https://doi.org/10.1128/AAC.49.1.406-407.2005

Salis, H.M., Mirsky, E.A., Voigt, C.A., 2009. Automated design of synthetic ribosome binding sites to control protein expression. Nat. Biotechnol. 27, 946–950. https://doi.org/10.1038/nbt.1568

Sambrook, J., Russell, D.W., 2001. Molecular cloning, vol. 1-3, Cold Spring Habour Laboratory Press, New York.

Sasaki, M., Teramoto, H., Inui, M., Yukawa, H., 2011. Identification of mannose uptake and catabolism genes in *Corynebacterium glutamicum* and genetic engineering for simultaneous utilization of mannose and glucose. Appl. Microbiol. Biotechnol. 89, 1905–1916. https://doi.org/10.1007/s00253-010-3002-8

Schafer, A., Kalinowski, J., Simon, R., Seep-Feldhaus, A.-H., Puhler, A., 1990. High-Frequency Conjugal Plasmid Transfer from Gram-Negative *Escherichia coli* to Various Gram-Positive Coryneform Bacteria. J. Bacteriol. 172, 1663–1666.

Schäfer, A., Tauch, A., Jäger, W., Kalinowski, J., Thierbach, G., Pühler, A., 1994. Small mobilizable multi-purpose cloning vectors derived from the *Escherichia coli* plasmids pK18 and pK19: selection of defined deletions in the chromosome of *Corynebacterium glutumicum*. Gene 145, 69–73.

Schallmey, M., Frunzke, J., Eggeling, L., Marienhagen, J., 2014. Looking for the pick of the bunch: High-throughput screening of producing microorganisms with biosensors. Curr. Opin. Biotechnol. 26, 148–154. https://doi.org/10.1016/j.copbio.2014.01.005

Schendel, F.J., Bremmon, C.E., Flickinger, M.C., Guettler, M., Hanson, R.S., 1990. L-Lysine Production at 50°C by Mutants of a Newly Isolated and Characterized Methylotrophic *Bacillus sp.* Appl. Environ. Microbiol. 56, 963–970.

Schneider, J., Niermann, K., Wendisch, V.F., 2011. Production of the amino acids l -glutamate , l -lysine , l -ornithine and l -arginine from arabinose by recombinant *Corynebacterium glutamicum*, in: Journal of Biotechnology. pp. 191–198. https://doi.org/10.1016/j.jbiotec.2010.07.009

Schrader, J., Schilling, M., Holtmann, D., Sell, D., Filho, M.V., Marx, A., Vorholt, J.A., 2009. Methanol-based industrial biotechnology: current status and future perspectives of methylotrophic bacteria. Trends Biotechnol. 27, 107–115. https://doi.org/10.1016/j.tibtech.2008.10.009

Schwander, T., Erb, T.J., 2016. Do it your (path)way –synthetische Wege zur CO_2-Fixierung. BIOspektrum 22, 590–592. https://doi.org/10.1007/s12268-016-0733-9

Schwander, T., Schada von Borzyskowski, L., Burgener, S., Cortina, N.S., Erb, T.J., 2016. A synthetic pathway for the fixation of carbon dioxide in vitro. Science (80-.). 354, 900–904. https://doi.org/10.1126/science.aah5237

Sekowska, A., Kung, H., Danchin, A., 2000. Sulfur metabolism in *Escherichia coli* and related bacteria: Facts and Fiction. J. Mol. Microbiol. Biotechnol. 2, 145–177.

Siebert, D., Wendisch, V.F., 2015. Metabolic pathway engineering for production of 1,2-propanediol and 1-propanol by *Corynebacterium glutamicum*., in: Biotechnology for Biofuels. Biotechnology for Biofuels, p. 91. https://doi.org/10.1186/s13068-015-0269-0

Siegel, J.B., Smith, A.L., Poust, S., Wargacki, A.J., Bar-Even, A., Louw, C., Shen, B.W., Eiben, C.B., Tran, H.M., Noor, E., Gallaher, J.L., Bale, J., Yoshikuni, Y., Gelb, M.H., Keasling, J.D., Stoddard, B.L., Lidstrom, M.E., Baker, D., 2015. Computational protein design enables a novel one-carbon assimilation pathway. Proc. Natl. Acad. Sci. U.S.A. 112, 3704–3709. https://doi.org/10.1073/pnas.1500545112

Simon, R., Priefer, U., Pühler, A., Puhl, A., 1983. A Broad Host Range Mobilization System for In Vivo Genetic Engineering: Transposon Mutagenesis in Gram Negative Bacteria. Bio/Technology 1, 784–791. https://doi.org/10.1038/nbt1183-784

Siu, K.H., Chen, R.P., Sun, Q., Chen, L., Tsai, S.L., Chen, W., 2015. Synthetic scaffolds for pathway enhancement. Curr. Opin. Biotechnol. 36, 98–106. https://doi.org/10.1016/j.copbio.2015.08.009

Literature

Škulj, M., Okršlar, V., Jalen, Š., Jevševar, S., Slanc, P., Štrukelj, B., Menart, V., 2008. Improved determination of plasmid copy number using quantitative real-time PCR for monitoring fermentation processes. Microb. Cell Fact. 7, 1–12. https://doi.org/10.1186/1475-2859-7-6

Šmejkalová, H., Erb, T.J., Fuchs, G., 2010. Methanol assimilation in Methylobacterium extorquens AM1: Demonstration of all enzymes and their regulation. PLoS One 5. https://doi.org/10.1371/journal.pone.0013001

Soini, J., Ukkonen, K., Neubauer, P., 2008. High cell density media for Escherichia coli are generally designed for aerobic cultivations - Consequences for large-scale bioprocesses and shake flask cultures. Microb. Cell Fact. 7, 1–11. https://doi.org/10.1186/1475-2859-7-26

Sonntag, F., Buchhaupt, M., Schrader, J., 2014. Thioesterases for ethylmalonyl-CoA pathway derived dicarboxylic acid production in *Methylobacterium extorquens* AM1. Appl. Microbiol. Biotechnol. 98, 4533–4544. https://doi.org/10.1007/s00253-013-5456-y

Sonntag, F., Kroner, C., Lubuta, P., Peyraud, R., Horst, A., Buchhaupt, M., Schrader, J., 2015. Engineering Methylobacterium extorquens for de novo synthesis of the sesquiterpenoid α-humulene from methanol. Metab. Eng. 32, 82–94. https://doi.org/10.1016/j.ymben.2015.09.004

Stansen, C., Uy, D., Delaunay, S., Eggeling, L., Goergen, J., Wendisch, V.F., 2005. Characterization of a *Corynebacterium glutamicum* Lactate Utilization Operon Induced during Temperature-Triggered Glutamate Production †, in: Applied and Environmental Microbiology. pp. 5920–5928.

Stolzenberger, J., Lindner, S.N., Persicke, M., Brautaset, T., Wendisch, V.F., 2013a. Characterization of fructose 1,6-bisphosphatase and sedoheptulose 1,7-bisphosphatase from the facultative ribulose monophosphate cycle methylotroph *Bacillus methanolicus*. J. Bacteriol. 195, 5112–5122. https://doi.org/10.1128/JB.00672-13

Stolzenberger, J., Lindner, S.N., Wendisch, V.F., 2013b. The methylotrophic *Bacillus methanolicus* MGA3 possesses two distinct fructose 1,6-bisphosphate aldolases. Microbiol. (United Kingdom) 159, 1770–1781. https://doi.org/10.1099/mic.0.067314-0

Sufrin, J.R., Lombardini, J.B., Alks, V., 1993. Differential kinetic properties of l-2-amino-4-methylthio-cis-but-3-enoic acid, a methionine analog inhibitor of S-adenosylmethionine synthetase. Biochim. Biophys. Acta (BBA)/Protein Struct. Mol. 1202, 87–91. https://doi.org/10.1016/0167-4838(93)90067-2

Tai, Y.-S., Zhang, K., 2015. Enzyme pathways: C1 metabolism redesigned. Nat. Chem. Biol. 11, 384–386. https://doi.org/10.1038/nchembio.1819

Takemoto, N., Tanaka, Y., Inui, M., Yukawa, H., 2014. The physiological role of riboflavin transporter and involvement of FMN-riboswitch in its gene expression in *Corynebacterium glutamicum*. Appl. Microbiol. Biotechnol. 98, 4159–4168. https://doi.org/10.1007/s00253-014-5570-5

Tani, Y., Kato, N., Yamada, H., 1978. Utilization of Methanol by Yeasts. Adv. Appl. Microbiol. 24, 165–186.

Taniguchi, H., Wendisch, V.F., 2015. Exploring the role of sigma factor gene expression on production by *Corynebacterium glutamicum*: Sigma factor H and FMN as example. Front. Microbiol. 6, 1–12. https://doi.org/10.3389/fmicb.2015.00740

Tateno, T., Fukuda, H., Kondo, A., 2007. Production of L -Lysine from starch by Corynebacterium glutamicum displaying α-amylase on its cell surface. Appl. Microbiol. Biotechnol. 74, 1213–1220. https://doi.org/10.1007/s00253-006-0766-y

Tauch, A., 2005. Native Plasmids of Amino Acid–Producing *Corynebacteria*, in: Handbook of Corynebacterium Glutamicum. CRC Press, pp. 57–75. https://doi.org/10.1201/9781420039696.ch4

Tephly, T.R., 1991. The toxicity of methanol. Life Sci. 48, 1031–1041. https://doi.org/10.1016/0024-3205(91)90504-5

Toyoda, K., Inui, M., 2016. Regulons of global transcription factors in Corynebacterium glutamicum. Appl. Microbiol. Biotechnol. 100, 45–60. https://doi.org/10.1007/s00253-015-7074-3

Tsuchidate, T., Fukuda, H., Tanaka, T., Okada, Y., Kondo, A., Tateno, T., 2008. Direct production of cadaverine from soluble starch using Corynebacterium glutamicum coexpressing α-amylase and lysine decarboxylase. Appl. Microbiol. Biotechnol. 82, 115–121. https://doi.org/10.1007/s00253-008-1751-4

Tsuge, Y., Tateno, T., Sasaki, K., Hasunuma, T., Tanaka, T., Kondo, A., 2013. Direct production of organic acids from starch by cell surface-engineered *Corynebacterium glutamicum* in anaerobic conditions. AMB Express 3, 1–7.

Tuyishime, P., Wang, Y., Fan, L., Zhang, Q., Li, Q., Zheng, P., Sun, J., Ma, Y., 2018. Engineering *Corynebacterium glutamicum* for methanol-dependent growth and glutamate production. Metab. Eng. 49, 220–231. https://doi.org/10.1016/j.ymben.2018.07.011

Uhde, A., Youn, J., Maeda, T., Clermont, L., Matano, C., Krämer, R., Wendisch, V.F., Seibold, G.M., Marin, K., 2013. Glucosamine as carbon source for amino acid-producing *Corynebacterium glutamicum*, in: Applied Microbiology and Biotechnollogy. pp. 1679–1687. https://doi.org/10.1007/s00253-012-4313-8

UniProt Consortium, T., 2018. UniProt: the universal protein knowledgebase. Nucleic Acids Res. 46, 2699. https://doi.org/10.1093/nar/gky092

Unthan, S., Baumgart, M., Radek, A., Herbst, M., Siebert, D., Brühl, N., Bartsch, A., Bott, M., Wiechert, W., Marin, K., Hans, S., Krämer, R., Seibold, G., Frunzke, J., Kalinowski, J., Rückert, C., Wendisch, V.F., Noack, S., 2015. Chassis organism from *Corynebacterium glutamicum* - a top-down approach to identify and delete irrelevant gene clusters. Biotechnol. J. 10, 290–301. https://doi.org/10.1002/biot.201400041

van der Klei, I.J., Yurimoto, H., Sakai, Y., Veenhuis, M., 2006. The significance of peroxisomes in methanol metabolism in methylotrophic yeast. Biochim. Biophys. Acta - Mol. Cell Res. 1763, 1453–1462. https://doi.org/10.1016/j.bbamcr.2006.07.016

Veldmann, K.H., Minges, H., Sewald, N., Lee, J., Wendisch, V.F., 2019. Metabolic engineering of *Corynebacterium glutamicum* for the fermentative production of halogenated tryptophan, in: Journal of Biotechnology. Elsevier, pp. 7–16. https://doi.org/10.1016/j.jbiotec.2018.12.008

Vitreschak, A.G., Rodionov, D.A., Mironov, A.A., Gelfand, M.S., 2002. Regulation of riboflavin biosynthesis and transport genes in bacteria by transcriptional and translational attenuation. Nucleic Acids Res. 30, 3141–51. https://doi.org/10.1093/nar/gkf433

Vogl, C., Grill, S., Schilling, O., Stülke, J., Mack, M., Stolz, J., 2007. Characterization of riboflavin (vitamin B2) transport proteins from *Bacillus subtilis* and *Corynebacterium glutamicum*. J. Bacteriol. 189, 7367–7375. https://doi.org/10.1128/JB.00590-07

von Borzyskowski, L.S., Carrillo, M., Leupold, S., Glatter, T., Kiefer, P., Weishaupt, R., Heinemann, M., Erb, T.J., 2018. An engineered Calvin-Benson-Bassham cycle for carbon dioxide fixation in *Methylobacterium extorquens* AM1. Metab. Eng. 47, 423–433. https://doi.org/10.1016/j.ymben.2018.04.003

Vorholt, J.A., 2002. Cofactor-dependent pathways of formaldehyde oxidation in methylotrophic bacteria. Arch. Microbiol. 178, 239–249. https://doi.org/10.1007/s00203-002-0450-2

Vuilleumier, S., Chistoserdova, L., Lee, M.C., Bringel, F., Lajus, A., Yang, Z., Gourion, B., Barbe, V., Chang, J., Cruveiller, S., Dossat, C., Gillett, W., Gruffaz, C., Haugen, E., Hourcade, E., Levy, R., Mangenot, S., Muller, E., Nadalig, T., Pagni, M., Penny, C., Peyraud, R., Robinson, D.G., Roche, D., Rouy, Z., Saenempechek, C., Salvignol, G., Vallenet, D., Zaining, W., Marx, C.J., Vorholt, J.A., Olson, M. V., Kaul, R., Weissenbach, J., Médigue, C., Lidstrom, M.E., 2009. *Methylobacterium* genome sequences: A reference blueprint to investigate microbial metabolism of C1 compounds from natural and industrial sources. PLoS One 4. https://doi.org/10.1371/journal.pone.0005584

Walker, B.J., Abeel, T., Shea, T., Priest, M., Abouelliel, A., Sakthikumar, S., Cuomo, C.A., Zeng, Q., Wortman, J., Young, S.K., Earl, A.M., 2014. Pilon: An Integrated Tool for Comprehensive Microbial Variant Detection and Genome Assembly Improvement. PLoS One 9, e112963. https://doi.org/10.1371/journal.pone.0112963

Wang, S., Arends, S.J.R., Weiss, D.S., Newman, E.B., 2005. A deficiency in S-adenosylmethionine synthetase interrupts assembly of the septal ring in *Escherichia coli* K-12. Mol. Microbiol. 58, 791–799. https://doi.org/10.1111/j.1365-2958.2005.04864.x

Literature

Wang, X., Wang, X., Lu, X., Ma, C., Chen, K., Ouyang, P., 2019. Methanol fermentation increases the production of NAD(P)H - dependent chemicals in synthetic methylotrophic *Escherichia coli*. Biotechnol. Biofuels 12, 1–11. https://doi.org/10.1186/s13068-019-1356-4

Warneke, C., Karl, T., Judmaier, H., Hansel, A., Jordan, A., Lindinger, W., Crutzen, P.J., 1999. Acetone, methanol, and other partially oxidized volatile organic emissions from dead plant matter by abiological processes: Significance for atmospheric HO(X) chemistry. Global Biogeochem. Cycles 13, 9–17. https://doi.org/10.1029/98GB02428

Wei, Y., Newman, E.B., 2002. Studies on the role of the metK gene product of *Escherichia coli* K-12. Mol. Microbiol. 43, 1651–6. https://doi.org/2856 [pii]

Wendisch, V.F., Brito, L.F., Gil Lopez, M., Hennig, G., Pfeifenschneider, J., Sgobba, E., Veldmann, K.H., 2016a. The flexible feedstock concept in Industrial Biotechnology: Metabolic engineering of *Escherichia coli*, *Corynebacterium glutamicum*, *Pseudomonas*, *Bacillus* and yeast strains for access to alternative carbon sources. J. Biotechnol. 234, 139–157. https://doi.org/10.1016/j.jbiotec.2016.07.022

Wendisch, V.F., Jorge, J.M.P., Perez Garcia, F., Sgobba, E., 2016b. Updates on industrial production of amino acids using *Corynebacterium glutamicum*, in: World Journal of Microbiology and Biotechnology. https://doi.org/10.1007/s11274-016-2060-1

Whitaker, W.B., Jones, J.A., Bennett, R.K., Gonzalez, J.E., Vernacchio, V.R., Collins, S.M., Palmer, M.A., Schmidt, S., Antoniewicz, M.R., Koffas, M.A., Papoutsakis, E.T., 2017. Engineering the biological conversion of methanol to specialty chemicals in *Escherichia coli*. Metab. Eng. 39, 49–59. https://doi.org/10.1016/j.ymben.2016.10.015

Whitaker, W.B., Sandoval, N.R., Bennett, R.K., Fast, A.G., Papoutsakis, E.T., 2015. Synthetic methylotrophy: engineering the production of biofuels and chemicals based on the biology of aerobic methanol utilization. Curr. Opin. Biotechnol. 33, 165–175. https://doi.org/10.1016/j.copbio.2015.01.007

Wijayasinghe, Y.S., Blumenthal, R.M., Viola, R.E., 2014. Producing Proficient Methyl Donors from Alternative Substrates of S-Adenosylmethionine Synthetase. Biochemistry 53, 1521–1526. https://doi.org/10.1021/bi401556p

Williams, T.C., Pretorius, I.S., Paulsen, I.T., 2016. Synthetic Evolution of Metabolic Productivity Using Biosensors. Trends Biotechnol. 34, 371–381. https://doi.org/10.1016/j.tibtech.2016.02.002

Witthoff, S., Eggeling, L., Bott, M., Polen, T., 2012. Corynebacterium glutamicum harbours a molybdenum cofactor-dependent formate dehydrogenase which alleviates growth inhibition in the presence of formate, in: Microbiology (United Kingdom). pp. 2428–2439. https://doi.org/10.1099/mic.0.059196-0

Witthoff, S., Mühlroth, A., Marienhagen, J., Bott, M., 2013. C1 metabolism in *Corynebacterium glutamicum*: An endogenous pathway for oxidation of methanol to carbon dioxide. Appl. Environ. Microbiol. 79, 6974–6983. https://doi.org/10.1128/AEM.02705-13

Literature

Witthoff, S., Schmitz, K., Niedenführ, S., Nöh, K., Noack, S., Bott, M., Marienhagen, J., 2015. Metabolic engineering of *Corynebacterium glutamicum* for methanol metabolism. Appl. Environ. Microbiol. 81, 2215–2225. https://doi.org/10.1128/AEM.03110-14

Wittmann, C., Becker, J., 2007. The L-Lysine story: From Metabolic Pathways to Industrial Production, in: Amino Acid Biosynthesis - Pathways, Regulation and Metabolic Engineering. pp. 189–96. https://doi.org/10.1007/7171

Woolston, B.M., King, J.R., Reiter, M., Van Hove, B., Stephanopoulos, G., 2018a. Improving formaldehyde consumption drives methanol assimilation in engineered *E. coli*. Nat. Commun. 9. https://doi.org/10.1038/s41467-018-04795-4

Woolston, B.M., Roth, T., Kohale, I., Liu, D.R., Stephanopoulos, G., 2018b. Development of a formaldehyde biosensor with application to synthetic methylotrophy. Biotechnol. Bioeng. 115, 206–215. https://doi.org/10.1002/bit.26455

Wu, G., Yan, Q., Jones, J.A., Tang, Y.J., Fong, S.S., Koffas, M.A.G., 2016. Metabolic Burden: Cornerstones in Synthetic Biology and Metabolic Engineering Applications. Trends Biotechnol. 34, 652–664. https://doi.org/10.1016/j.tibtech.2016.02.010

Yanisch-Perron, C., Vieira, J., Messing, J., 1985. Improved Ml3 phage cloning vectors and host strains: nucleotide sequences of the M13mp18 and pUC19 vectors. Gene 33, 103–119.

Yasueda, H., Kawahara, Y., Sugimoto, S.I., 1999. *Bacillus subtilis yckG* and *yckF* encode two key enzymes of the ribulose monophosphate pathway used by methylotrophs, and *yckH* is required for their expression. J. Bacteriol. 181, 7154–7160.

Yishai, O., Bouzon, M., Döring, V., Bar-Even, A., 2018. In Vivo Assimilation of One-Carbon via a Synthetic Reductive Glycine Pathway in *Escherichia coli*. ACS Synth. Biol. 7, 2023–2028. https://doi.org/10.1021/acssynbio.8b00131

Yokota, A., Lindley, N.D., 2004. Central Metabolism: Sugar Uptake and Conversion, in: Handbook of Corynebacterium Glutamicum. pp. 213–242.

Youn, J., Jolkver, E., Kra, R., Marin, K., Wendisch, V.F., 2008. Identification and Characterization of the Dicarboxylate Uptake System DccT in *Corynebacterium glutamicum* □, in: Journal of Bacteriology. pp. 6458–6466. https://doi.org/10.1128/JB.00780-08

Yurimoto, H., Oku, M., Sakai, Y., 2011. Yeast methylotrophy: Metabolism, gene regulation and peroxisome homeostasis. Int. J. Microbiol. 2011, 1–8. https://doi.org/10.1155/2011/101298

Zahoor, A., Lindner, S.N., Wendisch, V.F., 2012. Metabolic engineering of *Corynebacterium glutamicum* aimed at alternative carbon sources and new products, in: Computational and Structural Biotechnology. Research Network of Computational and Structural Biotechnology, pp. 1–11. https://doi.org/10.5936/csbj.201210004

Literature

Zano, S.P., Bhansali, P., Luniwal, A., Viola, R.E., 2013. Alternative substrates selective for S-adenosylmethionine synthetases from pathogenic bacteria. Arch. Biochem. Biophys. 536, 64–71. https://doi.org/10.1016/j.abb.2013.05.008

Zhang, W., Song, M., Yang, Q., Dai, Z., Zhang, S., Xin, F., Dong, W., Ma, J., Jiang, M., 2018a. Current advance in bioconversion of methanol to chemicals. Biotechnol. Biofuels 11, 1–11. https://doi.org/10.1186/s13068-018-1265-y

Zhang, W., Zhang, T., Song, M., Dai, Z., Zhang, S., Xin, F., Dong, W., Ma, J., Jiang, M., 2018b. Metabolic Engineering of *Escherichia coli* for High Yield Production of Succinic Acid Driven by Methanol. ACS Synth. Biol. 7, 2803–2811. https://doi.org/10.1021/acssynbio.8b00109

Zhang, W., Zhang, T., Wu, S., Wu, M., Xin, F., Dong, W., Ma, J., Zhang, M., Jiang, M., 2017. Guidance for engineering of synthetic methylotrophy based on methanol metabolism in methylotrophy. RSC Adv. 7, 4083–4091. https://doi.org/10.1039/C6RA27038G

Zhao, M., Wijayasinghe, Y.S., Bhansali, P., Viola, R.E., Blumenthal, R.M., 2015. A surprising range of modified-methionyl S-adenosylmethionine analogues support bacterial growth. Microbiol. (United Kingdom) 161, 674–682. https://doi.org/10.1099/mic.0.000034

Zhao, N., Qian, L., Luo, G., Zheng, S., 2018. Synthetic biology approaches to access renewable carbon source utilization in *Corynebacterium glutamicum*. Appl. Microbiol. Biotechnollogy 102, 9517–9529. https://doi.org/10.1007/s00253-018-9358-x

7. <u>Acknowledgements</u>